

Development of analytical methodology for analysis of oxylipins in brain tissue and plasma

Alexander Napylov

A Thesis

In

the Department

of

Chemistry and Biochemistry

Presented in Partial Fulfillment of the Requirements

For the Degree of Master of Science (Chemistry) at

Concordia University

Montreal, Quebec, Canada

February 2019

© Alexander Napylov, 2019

CONCORDIA UNIVERSITY
School of Graduate Studies

This is to certify that the thesis prepared

By: Alexander Napylov

Entitled: Development of analytical methodology for measurement of
oxylipins in brain tissue and plasma

and submitted in partial fulfillment of the requirements for the degree of

Master of Science (Chemistry)

Complies with the regulations of the University and meets the accepted standards
with respect to originality and quality.

Signed by the final Examining Committee:

Dr. Louis Cuccia _____ Chair

Dr. Cameron Skinner _____ Examiner

Dr. Brandon Findlay _____ Examiner

Dr. Dajana Vuckovic _____ Supervisor

Approved by _____

Date: February 15, 2019 _____ Dean of faculty

ABSTRACT

Development of analytical methodology for measurement of oxylipins in brain tissue and plasma

Alexander Napylov, M. Sc.

Concordia University, 2019

Oxylipins are bioactive oxygenated products of long chain (18-22 carbons) polyunsaturated fatty acids. They play an important role in different physiological processes acting as local hormones, so they may be used as biomarkers of these processes. In addition, the pathways and exact biological functions of many members of this family are not clear and need further investigation. To enable such investigations, it is important to have reliable and accurate analytical methods for oxylipin measurements in biospecimens such as blood and tissue.

The analysis of oxylipins in biological matrices is challenging due to their low concentrations and the existence of many oxylipin isomers. So, the first objective of this thesis was to develop a sensitive LC-HRMS method for the quantitative analysis of oxylipins, that provides separation of isomers and works in a scan mode in order to enable comprehensive oxylipin profiling and further investigation of unknown oxylipins in real samples. To achieve this goal, different LC stationary phases were assessed to obtain maximum separation of oxylipin isomers and a C-18 UHPLC column was determined as the best choice for this separation. Also, different mobile phase additives were assessed, and it was found that 0.02% (v/v) acetic acid in mobile phase gives maximum sensitivity by increasing ionization efficiency. After LC optimization, three pairs of oxylipins among 65-standard mixture were still unresolved chromatographically. MS/MS fragmentation of these oxylipins was developed to resolve these three pairs. Thus, the final LC-MS method allows for a measurement of 62 oxylipins and seven deuterated standards in 40 min and with LLOQ 0.1-0.8 ng/ml.

Another challenge for oxylipin analysis in plasma and brain is the complexity of the biological matrix that can affect the sensitivity and accurate quantitation of the method due to possible matrix effects. Thus, the second objective of this thesis was to develop and optimize sample preparation methodology to decrease a possible matrix effect and achieve the best limits of detection in biological matrices. Solid-phase extraction (SPE) was chosen for method development.

During development, the following parameters were optimized: SPE sorbent type, elution solvent composition, elution solvent volume and sample treatment before loading. Due to the low abundance of oxylipins in biological matrices sample preparation requires preconcentration step following the extraction. This step was found to be critical for method reproducibility and was systematically optimized to decrease possible losses of analytes during this step. The final developed and optimized sample preparation method in combination with LC-MS was then applied to plasma and brain tissue samples. The average recovery was 70-97% and the matrix effect was 27-105%. High inter-individual variabilities and a wide range (0.26-681 ng/ml) of oxylipin concentrations in human plasma samples were found. Some high concentrations of oxylipins such as 408 ± 35 ng/ml for 9-HETE were reported at first time. To accommodate this wide linear dynamic range, two injections were required, one with dilution for the accurate measurement of high abundance oxylipins and one with pre-concentration factor to enable the measurement of low abundance oxylipins. In general, the developed method allowed to detect 38 oxylipins in pooled plasma and accurately quantitated 25 of them.

In rat brain tissue samples, the concentration range of oxylipins was narrower than in plasma 0.14-13.1 pg/mg of wet tissue and in general, 43 oxylipins were detected, among which 41 were accurately quantitated. The main issue with post-mortem analysis of oxylipins in brain tissue is the possibility of post-mortem formation of oxylipins, which can result in a 50-500x increase in oxylipin concentrations. Also, *in vitro* methods for the analysis of oxylipins in brain tissue do not allow multiple measurements to be performed with the same experimental animal over a period of time. This poses a critical limitation during the investigation of biochemical pathways in response to particular stimulus. *In vivo* solid-phase microextraction (SPME) could help solve these problems. *In vivo* SPME was performed in moving awake rats (n=15) in collaboration with the Centre for Addiction and Mental Health (CAMH) and the resulting extracts were analysed by LC-MS. Twenty (20) oxylipins were identified using authentic standards. In addition, 32 unknown peaks corresponding to expected oxylipin m/z were detected. Among these, 18 were unique to *in vivo* SPME while the rest were also detected in post-mortem SPE samples. Six (6) out of 32 unknowns were subsequently identified as oxylipins. Further characterization and identification of other unknowns will be performed in future. To the best of our knowledge, this is the largest oxylipin panel ever detected *in vivo* from the brain tissue of living animals and provides an important new tool in neuroscience.

Acknowledgements

I would like to express my deepest gratitude to my supervisor Dr. Dajana Vuckovic for all knowledge skills and experience that I obtained during my studies. These 2.5 years really changed my mind and my life, and I became a different person.

I would like to thank all my lab colleagues Dmitri Sitnikov, Cian Monnin, Marianna Russo, Irina Slobodchikova, Ankita Gupta, Rosalynde Sonnenberg and Shama Naz for help, collaboration and support.

As well I would like to thank my committee members Dr. Cameron Skinner and Dr. Brandon Findlay for the insights they shared.

And of course, many thanks to my family for support and for believing in me: my parents Sergey and Ludmilla, my brothers Vladimir and Anatoly and their families and my lovely wife Liza. My lovely Liza, thank you for your patience, understanding and support, I love you and I dedicate this thesis to you!

Contribution of authors

Chapter 2

This chapter entitled “Ultra-high performance liquid chromatography – high resolution mass spectrometry method for detection and quantitation of oxylipins in plasma” authored by Alexander Napylov and Dajana Vuckovic is the first draft of manuscript in preparation that will be submitted for publication in spring 2019.

A.N. performed all LC-MS experiments, plasma SPE and PP and analyses of obtained data. A.N. and D.V developed LC-MS and SPE methods. D.V supervised all work. A.N and D.V interpreted results and co-wrote the first draft of the manuscript, that is included in this thesis. All authors will review and contribute to the final version of the manuscript prior to the manuscript submission.

Chapter 3

This chapter entitled “*In vivo* solid-phase microextraction for sampling of oxylipins from the brain of awake, moving rats” authored by Alexander Napylov, Nathaly Reyes Garces, German Gomez-Rios, Mariola Olkowicz, Sofia Lendor, Cian Monnin, Barbara Bojko, Clement Hamani, Janusz Pawliszyn, Dajana Vuckovic is the first draft of manuscript in preparation that will be submitted for publication in spring 2019

AN performed all LC-MS experiments and analyses of obtained data. NRG, GGR, MO, SL, DV and CM performed *in vivo* SPME experiment. CH was responsible for all animal studies and collection of brain tissue. GGR designed the *in vivo* SPME sampler. AN and DV performed desorption of *in vivo* SPME samples, interpreted results and co-wrote the first draft of the manuscript, that is included in this thesis. BB, CH, JP and DV designed the study, helped in interpretation of all results and supervised all work in their respective laboratories and the project. All authors will review and contribute to the final version of the manuscript prior to the manuscript submission.

Acknowledgements: We thank Mustansir Diwan for the technical assistance

Table of Contents

1	Introduction.....	1
1.1	Eicosanoids	1
1.1.1	Mobilization of AA	3
1.1.2	Cyclooxygenase pathway (COX).....	4
1.1.3	Lipoxygenase pathway (LOX).....	10
1.1.4	Cytochrome P450 pathway (CYP).....	14
1.1.5	Nonenzymatic pathway	16
1.2	Analysis of eicosanoids in brain tissue.....	17
1.2.1	Brain tissue homogenization.....	20
1.2.2	Liquid-liquid extraction (LLE)	20
1.2.3	Solid-phase extraction (SPE)	21
1.2.4	<i>In vivo</i> solid-phase microextraction (SPME).....	24
1.2.5	Liquid chromatography (LC)	28
1.2.6	Mass spectrometry (MS)	30
1.2.7	Summary of the LC-MS methods for oxylipin measurement in brain.....	31
1.3	Research objectives	35
2	Ultra-high performance liquid chromatography – high resolution mass spectrometry method for detection and quantitation of oxylipins in plasma.	36
2.1	Abstract.....	36
2.2	Introduction.....	37
2.3	Materials and methods.....	39
2.3.1	Chemicals	39
2.3.2	Oxylipin standards.....	39
2.3.3	Optimized C-18 SPE procedure for standards in solvent	39
2.3.4	C-18 SPE with TCA precipitation.....	40
2.3.5	C-18 SPE without prior protein precipitation step	40
2.3.6	IPA protein precipitation	40
2.3.7	Final LC-MS method.....	41

2.3.8	Data analysis	42
2.3.9	Calibration curves	42
2.3.10	Method evaluation – recovery and matrix effects.....	43
2.4	Results and discussion.....	43
2.4.1	SPE method development.....	43
2.4.2	Protein precipitation of plasma samples before SPE	49
2.4.3	Evaluation of recovery and matrix effect of the developed SPE method in plasma	50
2.4.4	LC-MS method development.....	53
2.4.5	Individual plasma samples: inter-individual variability and comparison to HMDB and other studies.....	57
2.4.6	Calibration curves for plasma oxylipins.....	60
2.5	Conclusions.....	62
3	<i>In vivo</i> solid-phase microextraction for sampling of oxylipins from the brain of awake, moving rats.....	63
3.1	Introduction.....	63
3.2	Results and discussion.....	65
3.2.1	Oxylipin profiling using <i>in vivo</i> SPME.....	65
3.2.2	Comparison of <i>in vivo</i> SPME to post-mortem SPE extraction of pooled brain homogenate	67
3.2.3	Characterization of unknown oxylipins observed using <i>in vivo</i> SPME	72
3.3	Experimental	74
4	Conclusions and future work	75
4.1	Conclusions.....	75
4.2	Future work.....	79
	References.....	80
	Appendix A: Supplementary information for Chapters 2 and 3	88

List of figures

Figure 1.1 Structure of arachidonic acid. Structure obtained from LIPID MAPS ⁶	1
Figure 1.2 Major eicosanoid biosynthetic pathways.	2
Figure 1.3 Specific reaction catalyzed by phospholipase A2 at the sn-2 position of the glycerol backbone is shown.....	3
Figure 1.4 Pathways for prostaglandin synthesis and function.....	5
Figure 1.5 Biochemical pathway of the metabolism of arachidonic acid into the biologically active leukotrienes.	10
Figure 1.6 Common metabolic transformations of leukotriene C4 (LTC4) to the biologically active sulfidopeptide leukotrienes, LTD4 and LTE4.....	13
Figure 1.7 Structures of cytochrome P450 metabolites.....	15
Figure 1.8 Mechanism of formation of the F2-IsoPs from the free radical-catalyzed peroxidation of arachidonate.....	17
Figure 1.9 General SPE workflow.....	22
Figure 1.10 Recoveries of internal standards (IS) for the tested SPE protocols.....	23
Figure 1.11 Commercial prototype SPME fiber assembly based on a hypodermic needle for <i>in vivo</i> applications (A) and schematic of conventional SPME fiber with typical coating length of 10-15 mm (B) and high-spatial-resolution fiber with discontinuous coating (C).....	25
Figure 1.12 Workflow of <i>in vivo</i> extraction of analyte from brain tissue using SPME fibers.....	25
Figure 2.1 Final optimized SPE method workflow.....	46
Figure 2.2 Extraction recovery of oxylipin standards using the optimized SPE method.....	48
Figure 2.3 Evaluation of extraction recovery of oxylipins from human plasma.....	51
Figure 2.4 Comparison of matrix effect in plasma.....	52
Figure 2.5 Comparison of (a)recovery and (b)matrix effect of deuterated oxylipins in plasma...	53
Figure 2.6 Chromatographic separation of oxylipin isomers.....	56
Figure 2.7 Comparison of calibration curves for (a) 8-iso-15(R)-PGF2 α and (b) 5-oxoETE.....	62
Figure 3.1 Hierarchical clustering by class (baseline, drug and vehicle) using Euclidian distance of the oxylipins measured by <i>in vivo</i> SPME in a minimum of 50% of all study samples above LOQ.....	66
Figure 3.2 Relative change in the concentration of the selected oxylipins (PGD2, PGE2, 14-HDoHE and EPA).....	68
Figure 3.3 Inter-individual variability in the measured concentrations of the selected oxylipins (PGD2, PGE2, 14-HDoHE and EPA).....	69
Figure 3.4 Comparison of the distribution (% by amount) of oxylipins detected by <i>in vivo</i> SPME and post-mortem SPE extraction of oxylipins in brain.....	70

Figure 3.5 Hierarchical clustering and correlation analysis of oxylipins measured in this study (a) known and quantified oxylipins with levels >LOQ in more than 50% of samples using measured oxylipin concentration (ng/mL) and (b) unknown and subsequently identified oxylipins with levels >LOQ in more than 5 samples using peak areas. 71

List of tables

<i>Table 1.1</i> Concentrations and functions of some eicosanoids in the brain	18
<i>Table 1.2</i> Summary of the LC-MS methods for oxylipin measurement in brain	33
<i>Table 2.1</i> Comparison of TCA protein precipitation versus direct loading on oxylipin recovery in human plasma.....	50
<i>Table 2.2</i> Individual variability of oxylipin concentrations in human plasma	58
<i>Table 2.3</i> Oxylipins that can be detected and quantitated accurately in plasma	60
<i>Table 3.1</i> Summary of all unknown oxylipins detected using <i>in vivo</i> SPME	73

List of equations

<i>Equation 1.1</i> Amount of analyte extracted by SPME ⁵¹	26
<i>Equation 1.2</i> Distribution coefficient ⁵¹	26
<i>Equation 1.3</i> Amount of analyte extracted by SPME when sample volume is large ⁵¹	26
<i>Equation 1.4</i> Amount of analyte extracted by SPME at pre-equilibrium conditions ⁵¹	26

List of abbreviations

11,12-EET	11,12-epoxyeicosatrienoic acids
12-HpETE	12-hydroperoxy-eicosatetraenoic acid
12-oxoETE	12-oxo-eicosatetraenoic acid
12S-HETE	12-hydroxyeicosatetraenoic acid
14,15-EET	14,15-epoxyeicosatrienoic acids
15-HETE	15-hydroxyeicosatetraenoic acid
15-HpETE	15-hydroperoxy-eicosatetraenoic acid
15-oxoETE	15-oxo-eicosatetraenoic acid
16-HETE	16-hydroxyeicosatetraenoic acid
17-HETE	17-hydroxyeicosatetraenoic acid
18-HETE	18-hydroxyeicosatetraenoic acid
19-HETE	19-hydroxyeicosatetraenoic acid
2-PIC	Picolylamine
20-HETE	20-hydroxyeicosatetraenoic acid
5,6-EET	5,6-epoxyeicosatrienoic acids
5-HEDH	5-hydroxyeicosatetraenoic acid dehydrogenase
5-HETE	5-hydroxyeicosatetraenoic acid
5-HpETE	5-hydroperoxy-eicosatetraenoic acid
5-oxoETE	5-oxo-icosatetraenoic acid
8,9-EET	8,9-epoxyeicosatrienoic acids
8-HETE	8-hydroxyeicosatetraenoic acid
8-HpETE	8-hydroperoxy-eicosatetraenoic acid
AA	Arachidonic acid
ACN	Acetonitrile
AD	Alzheimer's disease
AmAc	Ammonium acetate
NH ₄ OH	Ammonium hydroxide
BALF	Bronchoalveolar lavage fluid
BHT	Butylated hydroxyl toluene
C1P	Ceramide 1-phosphate
cAMP	Cyclic adenosine monophosphate
CID	Collision induced dissociation
CNS	Central nervous system
CO ₂	Carbon dioxide
COX	Cyclooxygenase
cPGES	Cytosolic PGE synthase
cPLA ₂	Cytosolic phospholipase A ₂
CYP	Cytochrome P450
DDA	Data-dependent acquisition
DC	Dendritic cells
DHA	Docosahexaenoic acid
DHET or DiHETrE	Dihydroxy-eicosatrienoic acid
DiHETEs	Dihydroxyeicosatetraenoic acids

DTPA	Diethylenetriaminepenta-acetic acid
EDTA	Ethylenediaminetetra-acetic acid
EETs or EpETrEs	Epoxyeicosatrienoic acids
entPGE ₂	Enantiomer PGE ₂
EPA	Eicosapentaenoic acid
EPOX	Epoxygenase
ER	Endoplasmic reticulum
ESI	Electrospray ionization
EtOH	Ethanol
EtAc	Ethyl acetate
eV	Electron volt
EXC ₄	Eoxin C ₄
EXD ₄	Eoxin D ₄
EXE ₄	Eoxin E ₄
FA	Formic acid
FLAP	Five lipoxygenases activation protein
GC-MS	Gas chromatography - mass spectrometry
GC-MS/MS	Gas chromatography - tandem mass spectrometry
GSH	Glutathione
HAc	Acetic acid
HDoHE	Hydroxydocosahexaenoic acid
HEPE _s	Hydroxyeicosapentaenoic acids
HETE _s	Hydroxyeicosatetraenoic acids
HETP	Height equivalent theoretical plates
HLB	Hydrophilic-Lipophilic Balanced sorbent
H-PGDS	Hematopoietic-prostaglandin D synthase
HPLC	High performance liquid chromatography
HMDB	Human Metabolome Data Base
HRMS	High resolution mass spectrometry
HXA ₃	Hepoxilin A ₃
HXB ₃	Hepoxilin B ₃
HX _s	Hepoxilins
IL-1 β	Interleukin-1 beta
IS or ISTD	Internal standards
IPA	Isopropanol
IsoPs	Isoprostanes
kDa	Kilodalton
LC	Liquid chromatography
LC-MS	Liquid chromatography – mass spectrometry
LC-MS/MS	Liquid chromatography – tandem mass spectrometry
LIT	Linear ion trap
LLE	Liquid-liquid extraction
LLOQ	Lower limit of quantitation
LOX	Lipoxygenase
L-PGDS	Lipocaline-type-prostaglandin D synthase

LPS	Lipopolysaccharide
LTA ₄	Leukotriene A ₄
LTAH	LTA ₄ hydrolase
LTB ₄	Leukotriene B ₄
LTC ₄	Leukotriene C ₄
LTCS	LTC ₄ synthase
LTD ₄	Leukotriene D ₄
LTE ₄	Leukotriene E ₄
LTs	Leukotrienes
LXA ₄	Lipoxins A ₄
LXB ₄	Lipoxins B ₄
LXs	Lipoxins
MeOH	Methanol
MD	Microdialysis
mPGES-1	Microsomal PGE synthase-1
mPGES-2	Microsomal PGE synthase-2
MRM	Multiple reaction monitoring
NADPH/NADP	Nicotinamide adenine dinucleotide phosphate
PDMS	Polydimethylsiloxane
PDs	Protectins
PEG	Polyethylene glycol
PFP	Pentofluorophenyl
PGD ₂	Prostaglandin D ₂
PGDS	Prostaglandin D synthase
PGE ₂	Prostaglandin E ₂
PGF _{2α}	Prostaglandin F _{2α}
PGG ₂	Prostaglandin G ₂
PGH ₂	Prostaglandin H ₂
PGHS-1 or PGHS-2	PG endoperoxide H synthase-1 or -2
PGI ₂	Prostaglandin I ₂ or prostacyclin
PGIS	Prostaglandin I ₂ or prostacyclin synthase
PGJ ₂	Prostaglandin J ₂
PGs	Prostaglandins
PIP2	Phosphatidylinositol-4,5-bisphosphate
PLA ₂	Phospholipase A ₂
POX	Peroxidase
PPAR _α	Peroxisome Proliferator-Activated Receptor alpha
PPAR _β	Peroxisome Proliferator-Activated Receptor beta
PPAR _γ	Peroxisome Proliferator-Activated Receptor gamma
PPAR _δ	Peroxisome Proliferator-Activated Receptor delta
PPY	Polypyrrole
PUFA	Polyunsaturated fatty acids
QqLIT	Hybrid quadrupole-linear ion trap
QQQ	Triple quadrupole
QTOF	Quadrupole-Time-of-Flight

Rvs	Resolvins
sEH	Epoxide hydrolase
SFC	Supercritical fluid chromatography
SPE	Solid phase extraction
sPLA ₂	Secreted phospholipase A ₂
SPME	Solid-phase microextraction
SRM	Selected reaction monitoring
TCA	Trichloroacetic acid
Th2 cells	T helper-2 cells
TrXA ₃	Trioxilin A ₃
TrXB ₃	Trioxilin B ₃
TxA ₂	Thromboxane A ₂
TXAS	Thromboxane A synthase
TxB ₂	Thromboxane B ₂
Txs	Thromboxanes
UHPLC or UPLC	Ultra-high performance liquid chromatography
UV	Ultraviolet
v/v	Volume/volume

1 Introduction

1.1 Eicosanoids

The term “Eicosanoids” was introduced in 1979¹ to denote the family of biologically active oxygenated carbon-20 unsaturated fatty acids where arachidonic acid (AA) (Figure 1.1) occupied a central position as precursor.² In contemporary terms the term “Eicosanoids” is a part of more wide term “Oxylipins” that encompasses bioactive oxygenated products of long chain (18-22 carbons) polyunsaturated fatty acids.³ However, some authors claim that oxylipins are oxygenated fatty acids derivatives from plant tissues whereas corresponding series of metabolites in animals tissues belong to the eicosanoids.^{4,5} This thesis will focus on eicosanoids derived from arachidonic acid.

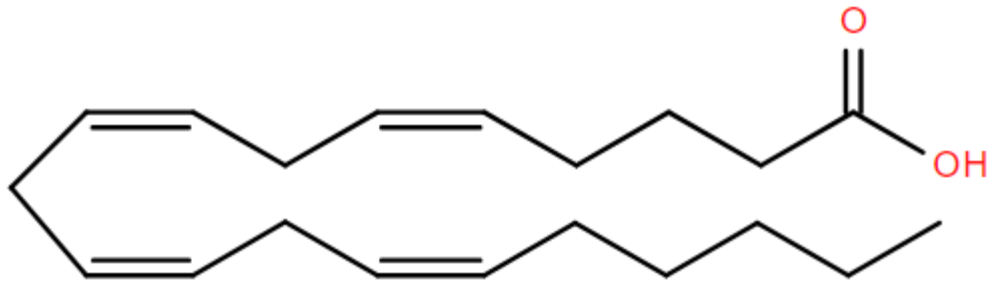


Figure 1.1 Structure of arachidonic acid. Structure obtained from LIPID MAPS⁶.

Eicosanoids are divided into four groups according to the AA oxidation pathway: *Cyclooxygenase pathway (COX)* - Prostanoids (Prostaglandins (PGs) and Thromboxanes (Tx)); *Lipoxygenase pathway (LOX)* - Leukotrienes (LTs), Hepoxilins (HXs), Lipoxins (LXs), Hydroxyeicosatetraenoic acids (HETEs), Dihydroxyeicosatetraenoic acids (DiHETEs); *Cytochrome P450 (or Epoxygenase) pathway (CYP or EPOX)* - Epoxyeicosatrienoic acids (EETs or EpETrEs), Hydroxyeicosatetraenoic acids (HETEs); *Nonenzymatic pathway* - Isoprostanes (IsoPs), Hydroxyeicosatetraenoic acids (HETEs). Each pathway is named by the enzyme that catalyses this step. Enzymatic pathways are known collectively as “arachidonate cascade” (Figure 1.2).^{7,8}

In general, each eicosanoid enzymatic pathway has three stages: 1) Activation of Phospholipase A₂ (PLA₂) which releases AA from membrane phospholipids; 2) Enzymatic oxidation of AA by one of the specific enzymes and formation of eicosanoids; 3) Exit of eicosanoids from the cell presumably via carrier-mediated transport and acting through G-protein-coupled receptors close to the site of their synthesis. Eicosanoids have a short lifetime and after acting they are rapidly inactivated, e.g. half-life of PGH₂ is around 5 minutes in aqueous solution and seconds in plasma; half-life of TxA₂ in plasma is around 30 seconds.⁹ Inactivation of different eicosanoids can be performed by different pathways but in general it leads to a decrease of their biological activity and an increase in their water solubility (e.g. by further oxidation) to facilitate excretion in the urine.^{7,8}

1.1.1 Mobilization of AA

Mobilization of AA is a common first step in all eicosanoid pathways. AA is stored at the sn-2 position on the glycerol backbone of membrane phospholipids and usually only small quantities of the free acid form of AA exist in the cells. To be used for biosynthesis of eicosanoids, AA is released from the cell membrane by a specific enzyme – phospholipase A₂ (PLA₂) (Figure 1.3).¹⁰

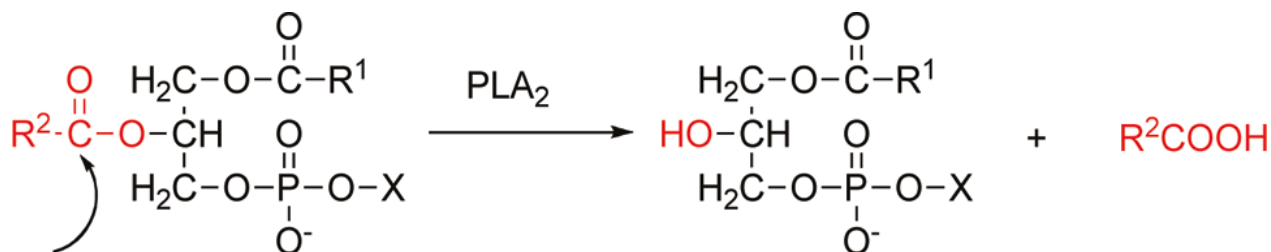


Figure 1.3 Specific reaction catalyzed by phospholipase A₂ at the sn-2 position of the glycerol backbone is shown. X, any of a number of polar head groups; R₁ and R₂, fatty acid chain (alkyl or alkenyl groups). Reprinted with permission from reference 11, Copyright 2011, American Chemical Society.

PLA₂ is a superfamily of enzymes that contains at least 16 groups that play important roles in different biological processes. They can be divided into six types: cytosolic PLA₂ (cPLA₂), secreted PLA₂ (sPLA₂), calcium-independent PLA₂, platelet-activating factor acetylhydrolase, lysosomal PLA₂, and adipose-specific PLA₂.^{10,11} The most relevant in AA release are Ca²⁺-dependent cPLA_{2α} (Group IVA)¹¹ and sPLA_{2s} (Group IIA and V).¹² Group IVA cPLA_{2α}, Group IIA and Group V sPLA_{2s} have common structures that contains highly conserved Ca²⁺ binding sites and a catalytic site.¹⁰ As the secreted enzyme, sPLA_{2s}, acts on membrane lipids extracellularly, its

levels are regulated transcriptionally in response to cell activation. cPLA_{2α} hydrolyzes lipids on intracellular bilayer membranes including membranes of cellular organelles. It can usually be found in resting cells and is directly involved in the immediate AA release.^{7,11} Activation of phospholipases A₂ starts from the interaction of various stimuli (e.g. Interleukin-1 beta (IL-1β), thrombin) with their receptors on the cell surface that leads to an increase of concentration of cytosolic Ca²⁺ in the cell.⁷ Ca²⁺ interacts with the Ca²⁺ binding site of the Group IVA cPLA_{2α} that leads to its translocation to intracellular membranes.¹³ Also, it was shown that Group IVA cPLA_{2α} can be activated in a Ca²⁺ independent manner by binding to the phosphatidylinositol-4,5-bisphosphate (PIP₂) and ceramide 1-phosphate (C1P) as well as by phosphorylation and membrane interactions. Groups of sPLA_{2s} also showed high dependence of activity from Ca²⁺ concentration.^{10,11}

1.1.2 Cyclooxygenase pathway (COX)

Prostanoids are a group of eicosanoids that consist of prostaglandins (PGs) and Thromboxanes (Tx_s) and are formed by action of COXs (Figure 1.4). PGs are hydroxylated, unsaturated carboxylic acids that contain a cyclopentane ring, a hydroxyl group at C-15 and a trans double bond between C-14 and C-13. These eicosanoids are probably the best studied group of all arachidonic acid metabolites.^{7,14} The letter that follows after the PG abbreviation (e.g. PG-X) is determined by the nature and position of oxygen-containing substituents in the cyclopentane ring that emanate from C-8 and C-12 (each letter reflects a certain set of substituents and there is no any logical dependence between letter and substituents). The numerical subscript shows the number of carbon-carbon double bonds in the side chains and the Greek subscripts show orientation of hydroxyl group in the cyclopentane ring. For example, prostaglandin F_{2α} (PGF_{2α}) has hydroxyl groups at C-8 and C-12 carbons orientated to the same side of the cyclopentane ring and two double bonds between C-5/C-6 and C-13/ C-14. Tx_s have a similar structure but instead of a cyclopentane ring, they have a six-member oxane ring. For Tx_s letters after abbreviation are used to distinguish between different Tx's derivatives and the numerical subscript shows number of carbon-carbon double bonds in the side chains.⁷

In prostanoids formation, released AA is metabolized to prostaglandin H₂ (PGH₂) – common initial compound of all prostanoids by COX 1 or 2 (also known as Prostaglandin H synthase).⁷ COXs are products of two distinct genes but they typically report a 60% sequence identity. They both are homodimers with subunit molecular masses of about 72 kilodaltons (kDa).

COXs molecules contain two distinct but complementary active sites: cyclooxygenase (COX) and peroxidase (POX) sites.¹⁵

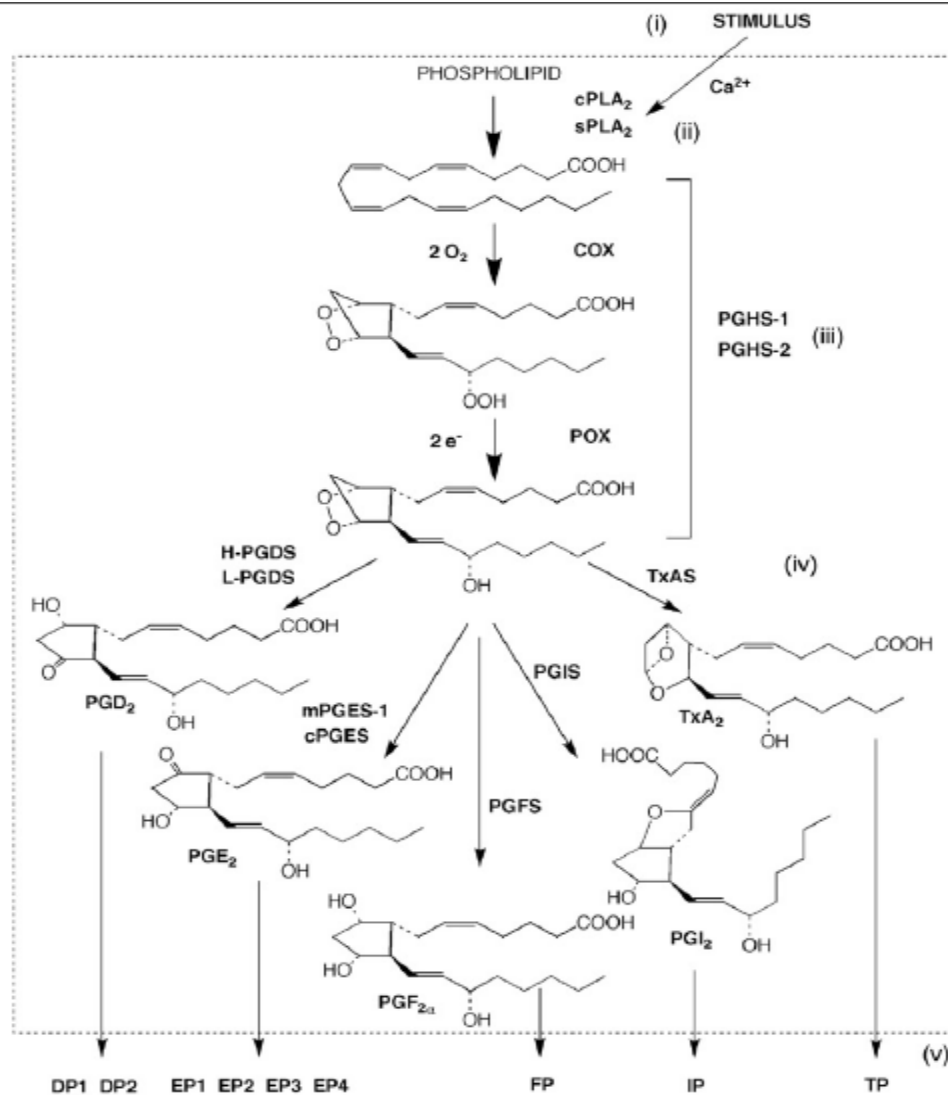


Figure 1.4 Pathways for prostaglandin synthesis and function. Shown are the structures and biosynthetic relationships among the most common prostanoids formed from arachidonic acid (AA). Following stimulation (i), a cascade of reactions is initiated by an increase in Ca^{2+} levels. (ii) $cPLA_2$ (cytosolic phospholipase A2) and/or $sPLA_2$, (non-pancreatic secretory phospholipase A2) cleave phospholipids to generate AA. (iii) AA is subsequently converted by the COX (cyclooxygenase) and POX (peroxidase) activities of PGHS-1 or PGHS-2 (PG endoperoxide H synthase-1 or -2) to form PGH₂. Subsequently, (iv) prostaglandins (PGs) are synthesized from PGH₂ in a cell-specific manner and then (v) exit cells and act via G-protein coupled receptors specific for particular prostanoid products. The dashed outline represents the cell membrane. The '2-series' PGs are formed from AA, whereas a homologous set of '3-series' PG products can be formed from EPA (eicosapentaenoic acid). Reprinted from reference 16, copyright 2008, with permission from Elsevier.

The COX site catalyzes formation of prostaglandin G₂ (PGG₂) incorporating two molecules of O₂ at the 11- and 15- carbon of AA. PGG₂ contains a five-member ring with an endoperoxide bridge across C-9 and C-11 and peroxide at C-15. The peroxide is reduced by the POX site of COXs or any other cellular peroxidase leading to a formation of PGH₂. Molecules of COX require interaction with hydrogen peroxide to maintain activity and undergo a suicide inactivation. They also have allosteric regulation by fatty acids including common fatty acids that are not used as substrate for COXs. COX-1 and COX-2 gene expression is regulated in different ways. COX-1 is expressed constitutively by most cell types to maintain regular cell processes and for immediate responses to circulating hormones. In contrast, COX-2 is absent in the cell and appears only in response to cytokines, tumor promoters or growth factors. Formation of biologically active prostanoids from PGH₂ is a cell specific process and is determined and performed by appropriate enzymes: prostaglandin synthases and thromboxane A synthase on the cytosolic surface of the endoplasmic reticulum (ER). Formation of most of prostanoids is performed by isomerisation of PGH₂ without changes in oxidation state. The only exception is the formation of PGF_{2α}, where aldoketoreductase 1B1 with HADPH induce reduction of two electrons of PGH₂.^{15,16}

Prostaglandin D₂ (PGD₂) is synthesized from PGH₂ by two distinct PGD synthases (PGDS) that catalyze isomerization of 9,11-edoperoxide group of PGH₂ to 9-hydroxy and 11-keto group. Hematopoietic PGDS (H-PGDS) is localized in mast cells, T helper 2 (Th2) cells and microglia. Lipocaline-type PGDS (L-PGDS) is localized in the brain (leptomeninges, choroid plexus, and oligodendrocytes), male genital organs and cardiovascular tissues. The main difference between them is the requirement of glutathione: H-PGDS uses it for catalysis while L-PGDS does not use it. PGD₂ binds to two known receptors: Gs-coupled DP receptor (DP1) and Gi-coupled DP receptor (DP2 or CRTH2).¹⁵ Interaction of PGD₂ with DP1 increases the level of cAMP in cells via activation of adenylate cyclase. DP1 receptor is produced by vascular and bronchial smooth muscle cells that mediates vasodilation and bronchodilation, also it was found on platelets and participates in inhibition of platelets aggregation. Thereby PGD₂ plays an important role in allergic inflammation promoted by mast cells. However, the interaction of PGD₂ with DP1 can cause anti-inflammatory effects. On the surface of airway dendritic cells (DCs) and Langerhans cells (LCs) this interaction inhibits their migration thereby limiting T-cell activation. Also, this interaction on DCs inhibits their maturation. Thus, interaction PGD₂ with DP1 on DCs is an important way for T-cell regulation and airway inflammation control. In the brain, PGD₂ via interaction with DP1

regulates sleep, temperature and nociception. In sleep regulation, PGD₂ acts on DP1 on leptomeningeal cells of the basal forebrain that releases adenosine acting on the sleep center in the preoptic area. Also, it was shown involvement of DP1 on microglia and reactive astrocytes in neuroinflammation in Alzheimer's disease (AD) and on the other hand, its involvement in neuroprotection by rescue of neurons in paradigm of glutamate toxicity. Interaction of PGD₂ with DP2 inhibits cAMP generation and increases Ca²⁺ level in cells. DP2 is expressed in eosinophils, basophils and Th2 cells and its interaction with PGD₂ mediates chemotaxis of these cells in allergic inflammation sites, so a PGD₂-DP2 interaction shows a proinflammatory effect.¹⁷ PGD₂ can be metabolized by 11-keto PGD₂ reductase to 9 α ,11 β PGF2 α .¹⁵ Also, because of an instability in aqueous solutions, PGD₂ can be non-enzymatically dehydrated to PGs of J series: PGJ₂, Δ 12-PGJ₂, 15-deoxy- Δ 12,14-PGJ₂.¹⁷ For PGJs it was shown an ability to interact with the nuclear receptor Peroxisome Proliferator-Activated Receptor Gamma (PPAR γ) that promotes adipocyte and macrophage differentiation.¹⁵ Finally, it was shown that PGJs have neurotoxic effects and lead to chronic neuroinflammation and neurodegeneration.¹⁸

Prostaglandin E₂ (PGE₂) is the most abundant COX-derived AA metabolite.¹⁷ Three different proteins were found that show the ability to transform PGH₂ to PGE₂ in vitro: cytosolic PGE synthase (cPGES), microsomal PGE synthase-1 (mPGES-1) and microsomal PGE synthase-2 (mPGES-2). However, to date, for only for mPGES-1, it was proved to have an involvement to *in vivo* PGE synthesis. mPGES-1 is a member of membrane-associated proteins involved in eicosanoid and glutathione metabolism superfamily and requires glutathione as a cofactor. It functionally coupled with COX-2 more preferably than with COX-1 and as COX-2 induced by cytokines and growth factors and downregulated by anti-inflammatory glucocorticoids. However, constitutive formation of mPGES-1 in particular tissues and cells was reported. cPGES is constitutively produced in cytosol of different cells and tissues and requires glutathione as cofactor as well. It shows to be coupling with COX-1 preferably and seems to be able to convert only COX-1 derived PGH₂. mPGES-2 constitutively expressed in different tissues and cells as well, coupled with COX-1 and COX-2 nonselectively and requires reducing agents but not only glutathione can be used.¹⁹ PGE₂ is acting through four different receptors: EP1, EP2, EP3, EP4, which are encoded by distinct genes. EP3 and EP4 are most widely distributed and can be found in almost all tissues and have the highest affinity to PGE₂. EP1 can be found only in the lungs, stomach and kidneys and EP2 is the least abundant, and both show a much lower affinity to PGE₂. PGE₂ interacting with

different EP receptors can regulate the function of different cells such as macrophages, dendritic cells (DC), and T and B lymphocytes causing pro- and anti-inflammatory effects. EP1 acts through mobilization of intracellular Ca^{2+} concentration. It induces edema and hyperalgesia during the inflammation process. Also, through PGE_2 -EP1, the interaction sodium excretory mechanism can be regulated that can affect on cardiovascular homeostasis. It was shown that EP1 receptor on native T cells by inducing Th1 differentiation modulates the immune response. An important role of EP1 may be found in the Central nervous system (CNS) where its interaction with PGE_2 can regulate stress responses. EP2 and EP4 receptors act via an increase of cAMP levels as well as using β -arresting-mediated signaling. These receptors being on different immune cells such DC or T cells regulate their activity by inhibition or promotion. Also, showed involvement of EP2 in neuroprotection, neuroinflammation, and mediating pain perception. Together with EP1, EP2 mediates wakefulness-augmenting effects around the third ventricle. EP4 acts as a vasodilator, maintaining intestinal homeostasis, in the CNS in the way that EP2 performs neuroprotection, modulates cerebral flow dynamics, participates in sleep together with the DP1 receptor of PGD_2 . The EP3 receptor acts via a decrease in cAMP levels in the cell. It mediates fever generation in response to pyrogens, and together with EP1, regulates water and salt transport along the nephron.¹⁷ PGE_2 inactivation starts from its oxidation by 15-hydroxyprostaglandin dehydrogenases to a 15-keto compound. After that, reduction of the double bond between C-13 and C-14 and ω -oxidation follow.²⁰ Also dehydration of PGE_2 leads to prostaglandin A_2 that undergoes two steps of isomerisation and via prostaglandin C_2 , it transforms into prostaglandin B_2 .⁸

Prostaglandin $\text{F}_{2\alpha}$ ($\text{PGF}_{2\alpha}$) can be produced in different tissues but the exact mechanism of synthesis is not clearly understood. There are three known pathways of biosynthesis of PGFs that are performed by reductases involving NADH or NADPH to the reaction. PGH_2 9-,11-endoperoxide reductase produces $\text{PGF}_{2\alpha}$ reducing two electrons of the 9,11-endoperoxide group of PGH_2 . PGE_2 9-ketoreductase produces $\text{PGF}_{2\alpha}$ from PGE_2 and PGD_2 11-keto reductase produces $9\alpha, 11\beta$ - $\text{PGF}_{2\alpha}$ – stereoisomer of $\text{PGF}_{2\alpha}$ from PGD_2 .¹⁵ $\text{PGF}_{2\alpha}$ acts via the FP receptor that is coupled to G_q and increases the level of cytosolic Ca^{2+} in the cell.¹⁷ It is the least selective of the prostanoid receptors and can bind other PGs.¹⁹ $\text{PGF}_{2\alpha}$ is actively produced in female the reproductive system and plays an important role in luteolysis, ovulation, initiation of parturition and contraction of smooth muscles of uterine.¹⁵ It was shown that $\text{PGF}_{2\alpha}$ plays a significant role in renal function, contraction of arterial smooth muscles, stimulation of hair growth, pain, brain injury, myocardial

dysfunction, and regulation of ocular pressure (FP agonist is used in the treatment of glaucoma).^{15,19} PGF_{2α} is metabolized in 15-Keto-dihydro-PGF_{2α} that can be found in peripheral plasma and urine.¹⁹

Prostaglandin I₂ (PGI₂), also known as Prostacyclin, unlike other PGs, has ether linkage between C-9 and C-5. It is produced by Prostacyclin synthase (PGIS) – a member of cytochrome P450 monooxygenase superfamily. PGIS colocalizes with COX in the endoplasmic reticulum, plasma membrane and nuclear membrane and constitutively expressed in endothelial cells.¹⁹ Heme-iron of PGIS interacts with C-11 of PGH₂ causing hemolytic cleavage of the C-11 – C-9 endoperoxide bond and produces an ether bond between C-9 and C-5. This bond is very unstable that leads to its hydrolysis and formation of inactive product 6-keto PGF_{1α} that is usually used for monitoring PGI₂ formation.⁸ PGI₂ has one IP receptor that binds with G_s and acts via an increased level of cAMP in cells. This receptor is produced in the kidneys, liver, lungs, platelets, heart, and aorta.¹⁹ PGI₂-IP interaction plays an important role in vascular homeostasis causing vasodilatation and inhibiting aggregation of platelets.¹⁵ Together with the EP1 receptor, it induces pain and edema during the inflammation process.¹⁹ Also it was shown that PGI₂-IP interaction has a pro- or anti-inflammatory function in the immune system depending on the context.¹⁷ PGI₂ can act through Peroxisome Proliferator-Activated Receptor delta (PPARδ) and Peroxisome Proliferator-Activated Receptor beta (PPARβ) to modulate transcription in the uterus and lungs, respectively.¹⁵

Thromboxane A₂ (TxA₂) has unusual for prostanoids structure with 6-member oxane ring and its formation is performed by thromboxane A synthase (TXAS) that is similar to PGIS and is also a member of the cytochrome P450 superfamily. However, unlike in the PGIS reaction, here, heme iron interacts with C-9 endoperoxide oxygen of PGH₂, which allows for C-11 oxygen radical to interact with C-12 producing an oxirane ring of TxA₂. In parallel, in this reaction TXAS forms 12-hydroxyheptadecatrienoic acid and malondialdehyde.¹⁵ Because TxA₂ has labile ether linkage, it is rapidly hydrolyzed forming inert ThromboxaneB₂ (TxB₂).⁸ TxA₂ is predominantly produced in platelets via COX-1. TxA₂ interacts with the TP receptor that increases the level of Ca²⁺ in cells. Together with PGI₂, TxA₂ is the major prostanoids of the cardiovascular system but it acts in the opposite way: it causes vasoconstriction and platelets aggregation. TxA₂, like PGI₂, has a pro- or anti-inflammatory function in the immune system depending on the context.^{17,19}

1.1.3 Lipoxygenase pathway (LOX)

In LOX pathway central role play enzymes called lipoxygenases (LOX). There are 6 known lipoxygenases today: 5-LOX, 12-(S)-LOX, 12(R)-LOX, 15-LOX-1, 15-LOX-2 and eLOX-3. They all have nonheme iron – an essential component of catalytic activity. During a reaction, they introduce molecular oxygen to polyunsaturated fatty acids (predominantly AA) with the formation of lipid hydroperoxides in the first step of the reaction. The number in their name shows the carbon position in AA that is oxygenated in the initial step (Figure 1.5).²¹

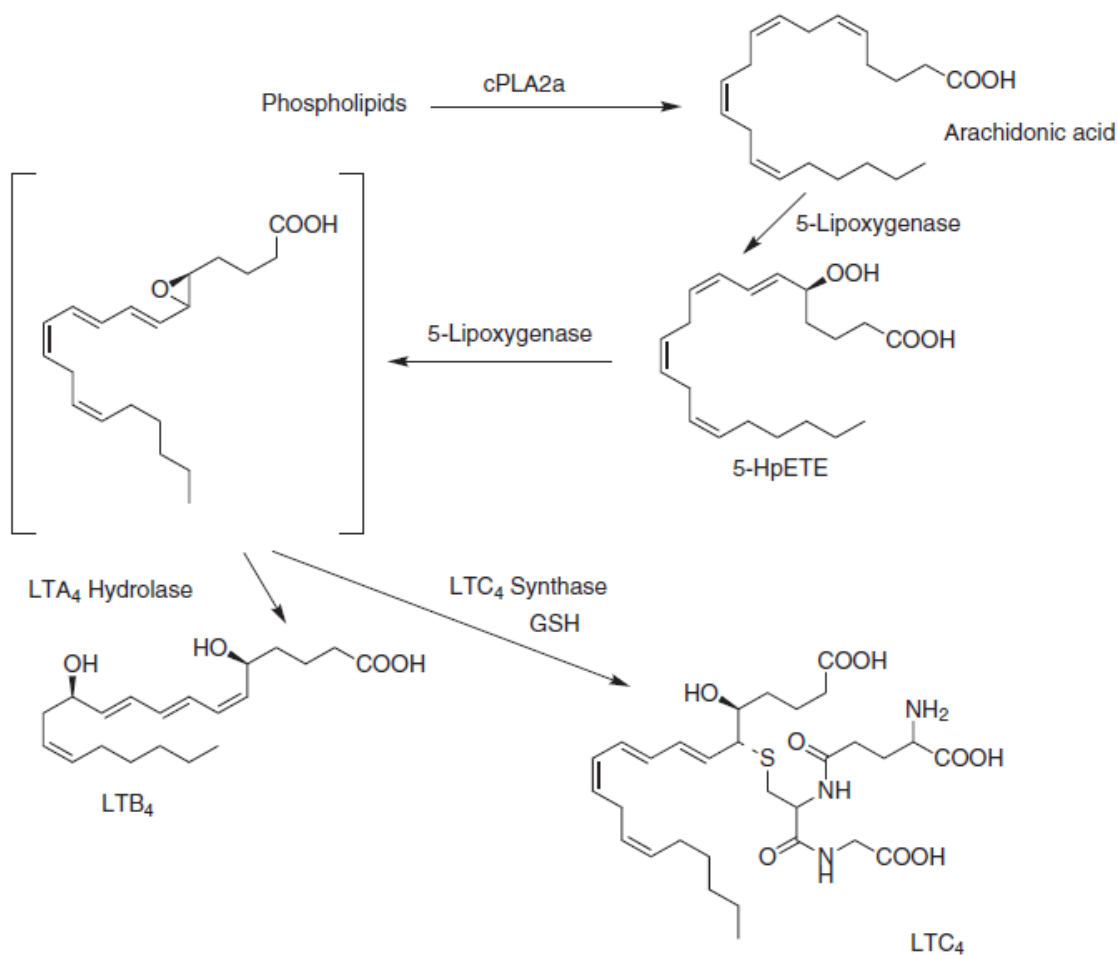


Figure 1.5 Biochemical pathway of the metabolism of arachidonic acid into the biologically active leukotrienes. Arachidonic acid released from phospholipids by cytosolic phospholipase A2 α is metabolised by 5-lipoxygenase to 5-hydroperoxyeicosatetraenoic acid (5 HpETE) and leukotriene A4 (LTA₄), which is then enzymatically converted into leukotriene B4 (LTB₄) or conjugated by glutathione to yield leukotriene C4 (LTC₄). Reprinted from reference 7, copyright 2016, with permission from Elsevier.

5-LOX performs the first two steps in leukotrienes biosynthesis.⁸ This enzyme is formed only in bone marrow derived cells such as mast cells, dendritic cells, macrophages, granulocytes, B-lymphocytes where its expression is regulated by different factors e.g. cytokines.²¹ 5-LOX activity is promoted by Ca^{2+} , cAMP, phosphorylation, also unlike other LOX, 5-LOX needs five lipoxygenase activation proteins (FLAP). 5-LOX activity is going in special nuclear envelope that is rich in phosphatidylcholine.⁷ At the first step, 5-LOX incorporates molecular oxygen to C-5 carbon of AA forming 5-hydroperoxy-eicosatetraenoic acid (5-HpETE) involving Fe^{3+} in the active center. At the second step, synthesized 5-HpETE is undergo by catalytic rearrangement by 5-LOX forming leukotriene A₄ (LTA₄). Also, depending on the conditions 5-HpETE can be secreted directly or reduced to a more stable 5-Hydroxyeicosatetraenoic acid (5-HETE) that can be further reduced by 5-hydroxyeicosatetraenoic acid dehydrogenase (5-HEDH) to 5-oxo-eicosatetraenoic acid (5-oxoETE). LTA₄ is a very labile molecule because of the epoxide group in its structure and can be hydrolyzed by LTA₄ hydrolase (LTAH) that relates to zinc metalloproteases family to leukotriene B₄ (LTB₄), or nonenzymatically forming stereoisomers of LTB₄: Δ 6-trans LTB₄, 12-epi LTB₄ and Δ 6-trans, 12-epi LTB₄. Also, LTA₄ can be conjugated with glutathione by LTC₄ synthase (LTCS) forming leukotriene C₄ (LTC₄). Glutathione of LTC₄ can be cleaved by endogenous peptidases e.g. γ -glutamyl transpeptidase that is located on the plasma membrane and removes glutamic acid forming leukotriene D₄ (LTD₄) from LTC₄. Dipeptidases, such as human membrane-bound dipeptidase-1, can hydrolyze the cysteinyl-glycine bond of LTD₄ forming leukotriene E₄ (LTE₄).⁸

LTB₄ has two specific receptors BLT1 and BLT2. BLT1 is mostly synthesized in polymorphonuclear leukocytes and in much lower amounts in macrophages, thymus and spleen. Unlike BLT1, BLT2 can be expressed in different tissues, most abundantly in the spleen, liver, ovaries and leukocytes. Transduction of signals initiated by these receptors depends on G-proteins coupled to a receptor and is different in different cells. LTB₄ plays an important role in the inflammatory process inducing migration and adherence of leukocytes and acts usually via the BLT1 receptor. On date LTB₄ is associated with several inflammatory events such as asthma, rheumatoid arthritis, psoriasis, atopic dermatitis, septic peritonitis.²² Inactivation of LTB₄ can be performed in two pathways: oxidative and reductive. Oxidation involves cytochrome P450s of the CYP4F family that converts LTB₄ to 20-hydroxy-LTB₄ (20-OH-LTB₄) that however has some biological activity. 20-OH-LTB₄ can be further metabolized to inactive 20-carboxy-LTB₄ (20-

COOH-LTB₄), 18-COOH-tetranor-LTB₄ and 16-COOH-tetranor-LTB₄. Reductive pathway starts from oxidation of LTB₄ by 12-Hydroxydehydrogenase/15-oxo-prostaglandin 13-reductase (13-PGR) forming inactive 12-oxo-LTB₄ and subsequent reductive products 12-oxo-10,11-dihydro-LTB₄, 10,11-dihydro-LTB₄ and 10-HOTrE.⁷

Cysteinyl leukotrienes LTC₄, LTD₄ and LTE₄ have two main receptors cysLT₁ and cysLT₂. Both receptors act via elevation of Ca²⁺ levels in cells. cysLT₁ can be synthesized in different cells, usually in cells that synthesized cysteinyl LTs. It has the following affinity to LTs: LTD>LTC>>LTE. cysLT₂ is more specified and can be found in the heart, brain, vasculature and has similar with cysLT₁ affinity to LTs: LTD=LTC>>LTE.⁸ Also it was found that LTE₄ has its own specific receptor, GPR99.⁷ Cysteinyl leukotrienes together are called “slow reacting substance of anaphylaxis” and play important roles in the inflammation processes. Through cysLT receptors, they induce smooth muscle contraction (e.g. bronchial smooth muscle contraction in asthma) and increase vascular permeability leading to edema.⁸ Inactivation of LTs is performed by cytochrome 450 by ω and β oxidation resulting in a series of chain-shortened products (Figure 1.6).⁷

It is suggested that 5-HETE doesn't play any significant role, however its metabolite 5-oxoETE is an important component of particular inflammation processes. 5-oxoETE is formed from 5-HETE via oxidation by 5-HEDH. 5-HEDH is an enzyme that requires NADP⁺ for enzymatic activity and level of NADP⁺ in cell regulate activity of 5-HEDH. This enzyme is usually formed in various inflammatory and structural cells such as epithelial and endothelial cells, airway smooth muscle cells, platelets, DC and monocytes. 5-oxoETE acts via specific receptors called OXE that increase the intracellular level of Ca²⁺ and inhibit the formation of cAMP. It was shown that 5-HETE and 5-HpETE also can interact with OXE receptors, however they have much lower affinity to it. This receptor is highly expressed in macrophages, neutrophils and eosinophils inducing their chemotaxis, calcium mobilization, actin polymerization, CD11b expression and L-selectin shedding. 5-oxoETE-OXE interaction plays an important role in the bronchial asthma process enhancing the influx of eosinophils and neutrophils, which increases the proliferation of prostate cancer cells and via affects on neutrophils it could be involved in cardiovascular disease. 5-oxoETE can be further metabolized via oxidation to different inactive metabolites, conjugated with glutathione (GSH) by LTCS or converted back to 5-HETE by 5-HEDH, however, here the oxidation reaction is dominant.²²

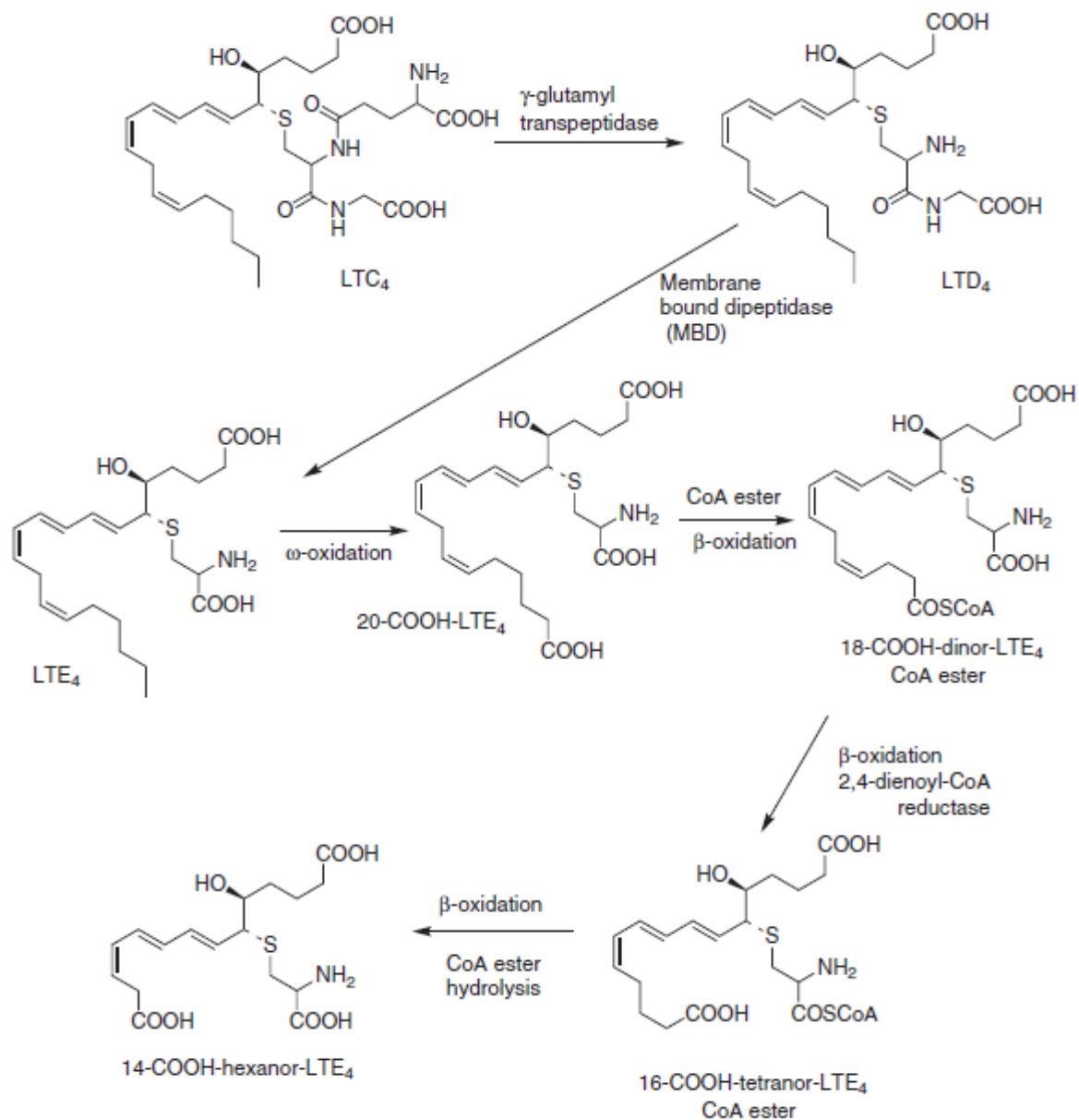


Figure 1.6 Common metabolic transformations of leukotriene C₄ (LTC₄) to the biologically active sulfidopeptide leukotrienes, LTD₄ and LTE₄. Subsequent ω -oxidation of LTE₄ by cytochrome P450 leads to the formation of 20-carboxy-LTE₄ that can undergo β -oxidation, after formation of the CoA ester, into a series of chain-shortened cysteinyl leukotriene metabolites. Reprinted from reference 7, copyright 2016, with permission from Elsevier.

Biological activities of other LOXs products are not clear and the significance of 12- and 15-LOX is not fully defined.⁷ 12(S)-LOX that localizes at platelets together with 15-LOX-1 and 2 can convert AA to either 12-HpETE and 15-HpETE that can further be metabolized to 12S-HETE-12-oxoETE and 15-HETE-15-oxoETE respectively, while 12(R)-LOX that localizes in skin can convert AA only to 12-HpETE and 12(R)-HETE with R-stereoconfiguration. Also, murine homolog of 15-LOX-2 produces 8-HpETE that converts to 8-HETE.²¹ Despite that mechanism of action of HETEs remains unclear it was shown that HETE demonstrates its participation in some biological activities including regulation of PPAR α and PPAR γ , expression of monocyte chemoattractant protein-1, angiogenesis, cancer growth and metastasis. Both 12-LOXs can produce Hepoxilins A₃ (HXA₃) and B₃ (HXB₃) from 12-HpETE incorporating epoxide across C-11 and C-12 and additional hydroxyl at C-8 for HXA₃ and C-10 for HXB₃. Because of instability of epoxide they can be further hydrolyzed to trioxilin A₃ and B₃ (TrXA₃ and TrXB₃). Some biological activities were shown by HXA₃ including Ca²⁺ release, neutrophil migration, insulin secretion, ichthyosis, and modulation of neuronal signaling. 12- and 15-LOXs participate in Lipoxins A₄ (LXA₄) and B₄ (LXB₄) formation that can be performed in three ways: neutrophil produces LTA₄ that then is taken up by platelets where it is converted to LXs by 12- or 15-LOXs; 15HpETE or 5-HETE are generated in platelets by 15-LOX and then are taken up by neutrophil where they are converted to LXs by 5-LOX; aspirin acetylated COX2 acts like 15-LOX producing LXs. LXs contain conjugated tetraene and hydroxyl at C-6 in LXA₄ and C-14 in LXB₄. LXs act via the ALX receptor, as well as via interaction with cysLT₁ and aryl hydrocarbon receptors and nuclear transcription factor. They demonstrate anti-inflammatory activity. 12- and 15-LOXs can form 14,15-LTA₄ incorporation epoxide across C-14 and C-15 of AA. 14,15-LTA₄ then can be conjugated with glutathione at C-14 forming analogues of LTs called eoxins (EXC₄, EXD₄, EXE₄), they demonstrate weak contractile activity.⁸

1.1.4 Cytochrome P450 pathway (CYP)

Cytochrome P450 (CYP) is a diverse superfamily of enzymes present in different cells and tissues. In eicosanoids biosynthesis they perform introduction of single oxygen atom to AA and in this term their activity similar to LOXs. However, unlike LOXs, CYPs contain heme-iron in active sites and NADPH as a cofactor. Depending on the oxidation mechanism, CYP products are divided into 3 classes: Hydroxyeicosatetraenoic acids (HETEs) formed by allylic oxidation, products of

oxidation of terminal alkyl chain region of AA (also HETEs) and cis-epoxyeicosatrienoic acids (EETs) formed by insertion of oxygen into the carbon-carbon bond of AA (Figure 1.7).⁸

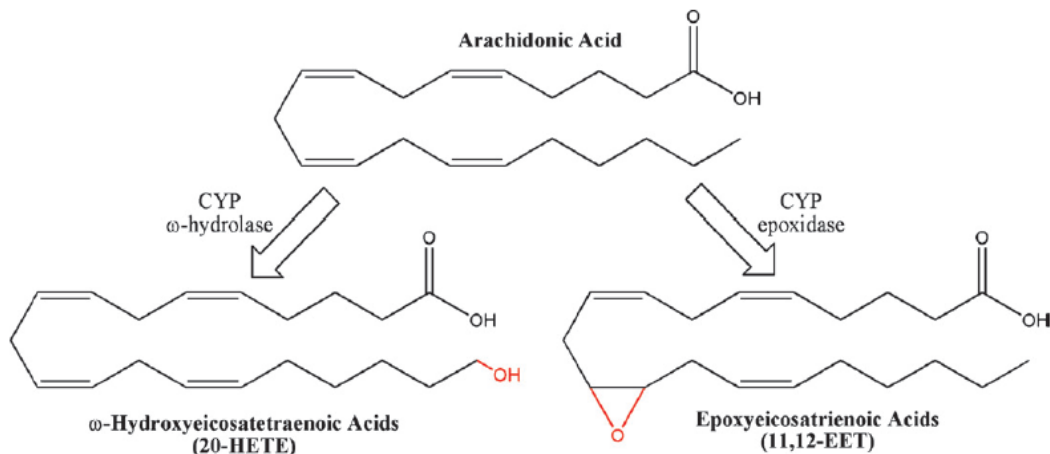


Figure 1.7 Structures of cytochrome P450 metabolites. Cytochrome P450 enzymes can catalyze ω -oxidation (example: 20-HETE) and epoxidation (11,12-EET) reactions. Reprinted from reference 8.

In process of HETEs formation, CYP reduces catalytic iron and oxygen forming reactive oxo-iron species that perform abstraction of sp^3 hybridized hydrogen of AA and the transfer of oxygen to this site to stabilize the AA molecule. If that occurs between C-5 and C-15 of AA, a molecule class similar to LOX products is formed. It contains 5-, 8-, 12-, 15-HETE that have the same structure as LOX products (some of them are epimeric). If CYP introduces hydroxyl to the sp^3 -hybridized ω -carbons of the AA unique class of HETEs is formed that contains 16-, 17-, 18-, 19-, 20-HETE. 20-HETE is most characterized of that HETEs and shows several important activities: it plays an important role in hypertension, inhibits K_{Ca} channels activity by that promoting systemic vasoconstriction, inhibits Na^+K^+ -ATPase activity in the kidneys by blocking sodium resorption. Other ω -HETEs show opposite to 20-HETE activities promoting vasodilatation and sodium reuptake in the kidneys. Also, it was shown that 16-HETE can inhibit neutrophil adhesion. Despite several activities were demonstrated for HETEs neither receptor nor second messenger were found for them, so their mechanism of action is still unclear.⁸

In process of EETs, formation reactive oxo-iron species formed by CYP, remove a single electron from sp^2 -hybridized carbon of AA and transfer oxygen there forming epoxy group. There are four known EET: 5,6-EET, 8,9-EET, 11,12-EET, 14,15-EET that can exist either as an R,S or the S,R enantiomer. EETs demonstrate their role in several processes such as angiogenesis, renal

function, vascular tone, leukocyte adhesion, and neuronal signaling. EETs have been identified as active ligands for cation channels and PPARs. However, the effect of specific EET isomers as well as mechanism of their action still unclear. EETs are metabolized by epoxide hydrolase (sEH) to dihydroxy-eicosatrienoic acids (DHETs) that were expected to be inactivated metabolites of EETs, however they show ability to activate BK_{Ca} channels as well as PPAR α and PPAR γ .⁸

1.1.5 Nonenzymatic pathway

Oxidative stress generates free radicals that can participate in the metabolism of AA (and other polyunsaturated fatty acids (PUFA)) in cells. PG-like compounds, called isoprostanes (IsoPs), can be formed by free radical catalyzed peroxidation of AA (Figure 1.8). Nonenzymatically derived analogs of PGF_{2 α} , PGD₂, PGE₂, PGJ₂, PGA₂ and Thromboxane exist. There are two main differences between IsoPs and COX derived PGs: IsoPs have side chains cis-oriented to the prostane ring and COX-PGs have trans-oriented side chains; IsoPs are formed *in situ* esterified to phospholipids and then released by phospholipase whereas COX-PGs are formed from released free AA. The formation of these abnormal phospholipids can affect fluidity and integrity of membranes during oxidative stress. Also, it is known that IsoPGs can interact with FP and TP receptors causing the same effects as COX-PGs.²³ Also, free radicals can metabolize AA in a LOX-like way, and as a result all LOX and CYP derived HETEs can be formed. Additionally, 9-HETE can be formed that doesn't have any biological activity and can't be formed by any enzymatic way. All these nonenzymatically derived eicosanoids can be used as biomarkers of oxidative stress.⁸

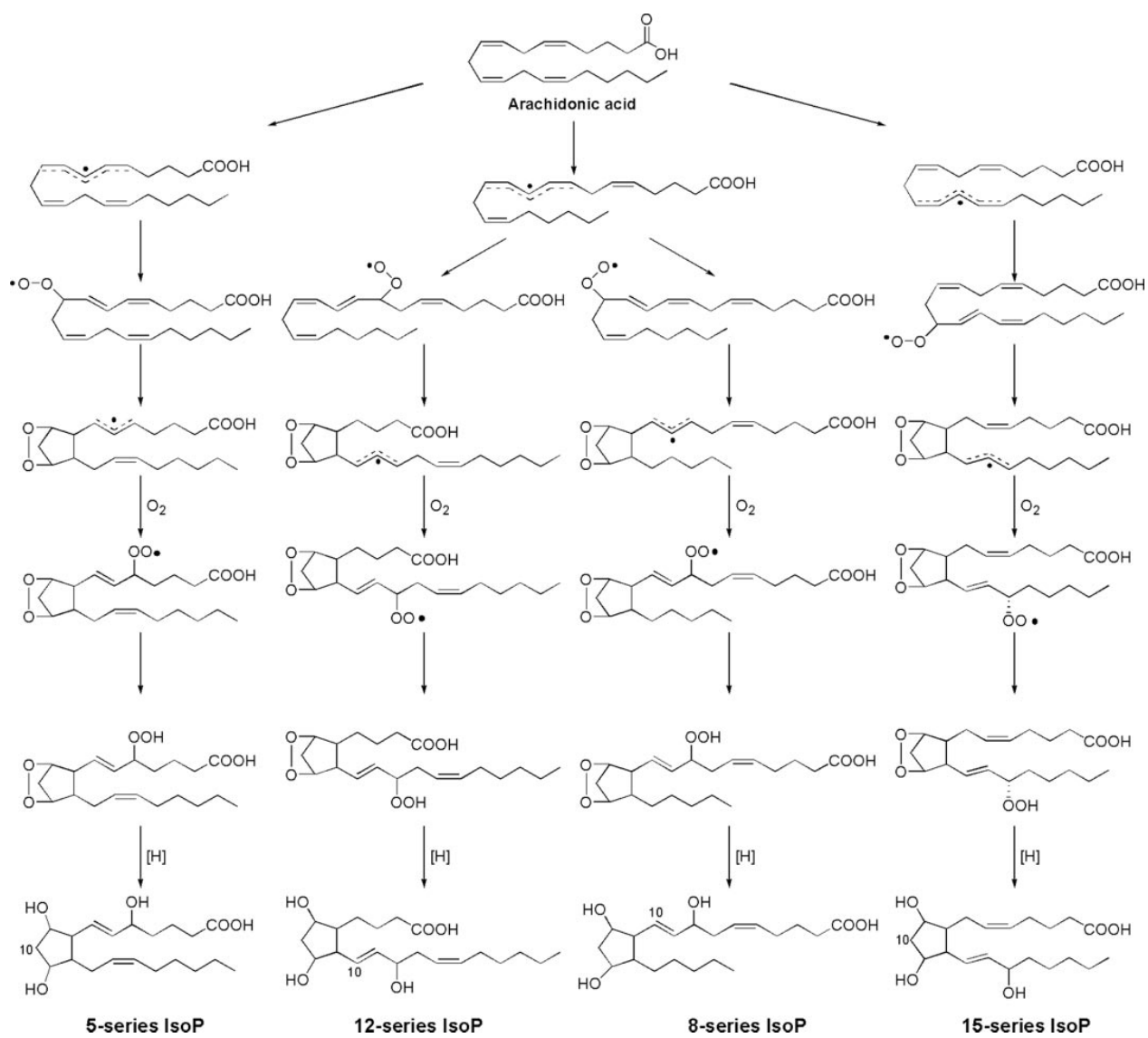


Figure 1.8 Mechanism of formation of the F2-IsoPs from the free radical-catalyzed peroxidation of arachidonate. Four regioisomers are generated, each consisting of 8 racemic diastereomers. For simplicity, stereochemistry is not indicated. Reprinted from reference 23.

1.2 Analysis of eicosanoids in brain tissue

Eicosanoids play an important role in brain processes such as temperature and sleep regulation, neuroinflammation, neuroprotection, brain maturation, regulation of synaptic activity and plasticity, cerebral blood flow regulation etc. (Table 1.1).²⁴ However, the function and mechanism of action of many eicosanoids in brain tissue is still unclear. Studying eicosanoids in the brain is not a trivial task due to several analytical challenges: extremely low concentrations of eicosanoids in brain tissue (1-50 pg/mg of protein, see Table 1.1), high chemical noise caused by the complexity and heterogeneity of the brain matrix, which decreases selectivity and sensitivity,

existence of many eicosanoid isomers, and the possible formation of eicosanoids during animal sacrifice in *in vitro* methods of analysis that therefore does not reflect real *in vivo* eicosanoid brain composition.

Table 1.1 Concentrations and functions of some eicosanoids in the brain

Eicosanoid	Detected concentrations pmol/g wet tissue	Functions
PGD ₂	27±5 (normal brain) ²⁵ 5.01±1.65 (post-injury) ²⁶ 2.91±0.06 (ischemic) ²⁷ 937 ± 305 (asphyxial cardiac arrest) ²⁸	Sleep regulation, ²⁴ synaptic plasticity (memory and learning), ²⁴ neuroinflammation, ²⁴ vasorelaxation ²⁹
PGE ₂	42.73±7 (normal brain) ³⁰ 11.311±2.62 (post-injury) ²⁶ 14.44±0.94 (ischemic) ²⁷ 35.5 ± 12.3 (asphyxial cardiac arrest) ²⁸	Sleep regulation, ²⁴ synaptic plasticity (memory and learning), ²⁴ neuroinflammation, ²⁴ vasorelaxation and vasoconstriction, ²⁹ nociceptive transmission, ²⁹ regulation of membrane excitability, ²⁹ apoptosis ²⁹
PGF _{2α}	14.4 ± 7 (asphyxial cardiac arrest) ²⁸	vasoconstriction ²⁹ , inflammation ¹⁹

Today several analytical methodologies are used for eicosanoid analysis including immunoassays,³¹ gas chromatography - (tandem) mass spectrometry (GC-MS or GC-MS/MS),^{32,33} liquid chromatography – (tandem) mass spectrometry (LC-MS³⁴ or LC-MS/MS³⁵). Enzyme-linked and radio-labeled immunoassays, despite their sensitivity, have poor reproducibility and specificity. HPLC with UV or fluorescent detection cannot be used due to lack of good chromophores or fluorescing systems in the eicosanoid structures, unless derivatization is used. However, derivatization makes the analytical process more complicated, and incomplete derivatization and side reactions may occur. GC-MS and GC-MS/MS can be used for analysis of most primary eicosanoids, however it is not suitable for labile compound like EETs (derivatization as well can help here). The most popular method in eicosanoid analysis is LC-MS or LC-MS/MS due to its sensitivity, resolution and high throughput. This helps to solve problems with low

abundance and separate many of the eicosanoid isomers of interest.³⁶ Due to these advantages, a LC-MS/MS method was used in this research and will be discussed in more detail below.

Sample preparation and extraction procedures that reduce matrix complexity and provide good recovery and/or enrichment of eicosanoids of interest are key steps in eicosanoid analysis.³⁷ *In vitro* sample preparation starts with a homogenization step with subsequent extraction of eicosanoids by liquid-liquid extraction (LLE) or solid phase extraction (SPE). The selected extraction method should be reproducible, fast, and cost effective. Matrix effects should be controlled and minimized as much as possible because a complex matrix can suppress signals from the analyte by decreasing ionization efficiency.³⁸ Also, new eicosanoids can be generated in the matrix from their precursors during the extraction process, therefore it is important to use inhibitors like indomethacin, ethylenediaminetetra-acetic acid (EDTA), diethylenetriaminepenta-acetic acid (DTPA) and butylated hydroxyl toluene (BHT) to prevent this.³⁶ Indomethacin is a known COX inhibitor, so its use prevents synthesis of PGs from AA in biological matrices where COX may be active.¹⁵ EDTA and DTPA are chelating agents and have the ability to sequester metal ions, therefore inhibiting activity of metal dependant enzymes (*e.g.* LOX). BHT is an antioxidant that scavenges a free radical species, therefore preventing non-enzymatic eicosanoid formation.³⁹ In brain samples, BHT is most widely used. Usually 0.1 mM of BHT is added to the homogenization solvent.^{28,40-42} Golovko *et al.* evaluated how BHT can prevent oxidation of PGs. They analyzed identical brain samples with 0, 0.1%, 0.005% (weight/volume) added to extraction solvents. They found that using 0.1% BHT can cause clogging of the LC system due to the of formation of precipitate, however 0.005% BHT does not form a precipitate but, it helps to decrease variability of analysis of PGs and prevents 2.8-fold reduction in an amount of 6-oxo-PGF_{1 α} .⁴³ In addition to the extraction procedure, sampling and tissue harvesting are critical steps. It was shown that during decapitation and sampling of the brain post-mortem, synthesis of eicosanoids can take place that influence the measured eicosanoid concentrations. Golovko and Murphy suggested to use microwave irradiation at 70-80⁰C in order to denature enzymes and prevent post-mortem formation of eicosanoids.⁴³ However, this method showed its efficiency mainly for PGs.

1.2.1 Brain tissue homogenization

Homogenization of brain tissue in eicosanoid analysis is usually performed by different types of homogenizers as well as via sonication. Masoodi *et al.* analyzed PGs³⁵ and HETEs⁴⁴ by homogenizing brain tissue in water using a Dounce glass mini homogenizer kept on ice during the process. This was followed by making an adjustment to 15% methanol, internal standard (IS) spiking and removal of any precipitated proteins, adjustment of supernatant to pH 3 and finally SPE. Yue *et al.*²⁶ homogenized cortex brain tissue in methanol with formic acid using micro ultrasonic cell disruptor, followed by centrifugation and dilution of the supernatant before loading on SPE. Miller *et al.*⁴⁰ and Liu *et al.*⁴¹ used the same sample preparation method for HETEs and PGs, where they homogenized brain tissue in 0.12 M potassium phosphate buffer containing 5 mM magnesium chloride and 0.113 mM BHT, centrifuged the homogenate, spiked the supernatant with IS, and performed SPE. Strauss *et al.*⁴⁵ homogenized brain tissue with high power sonication in a methanol extraction buffer containing 0.1% formic acid, 0.01% BHT and mix of IS, followed by centrifugation and dilution of supernatant before loading on SPE, for the successful measurement of HETEs and EETs. Furman *et al.*⁴² used a tip sonicator for a 60 second homogenization step in an autosampler vial containing Bligh-Dyer extraction monophasic solvent with subsequent addition of dichloromethane with water and sonication. Jouvène *et al.*⁴⁶ homogenized brain tissue in liquid nitrogen using mortar and pestle. The resulting powder was resuspended in Tyrode-HEPES buffer (pH 7.4), extracted with chloroform/ethanol (2:1 volume/volume (v/v)), followed by acidification to pH 3 and SPE. In summary, different approaches to date have been used for brain tissue homogenization, however in the experiments that were mentioned above, recovery evaluation was focused on the SPE step, so it is difficult to make a conclusion what approach in brain homogenization is most efficient in the eicosanoid analysis.

1.2.2 Liquid-liquid extraction (LLE)

Folch⁴⁷ and Bligh and Dyer⁴⁸ extraction protocols that are commonly used for lipid extraction can be utilized for the extraction of eicosanoids from brain tissue. In these protocols biphasic mixtures of methanol/chloroform/water are used for extraction.^{30,42,49} An important step in LLE of eicosanoids is the acidification of the lower layer to obtain eicosanoids in non-ionized form that allows to be extracted into the organic phase. However, excess acidification could cause alterations of eicosanoids.³⁶ More specific LLE methods for eicosanoid extraction that have higher efficiency were developed. Saunders *et al.*⁵⁰ used hexane/2-propanol extraction and observed a 12-

37% increase in recovery of PGs versus the Folch method. Golovko *et al.*⁴³ compared hexane/2-propanol extraction followed by acetone extraction against acetone extraction followed by hexane/chloroform extraction methods. Both methods showed comparable LOD and masses of extracted PGs from brain tissue, however acetone extraction followed by hexane/chloroform extraction produced much lower chemical background noise. Brose *et al.*²⁷ compared acetone extraction followed by hexane/chloroform extraction, Bligh and Dyer extraction and one-step methanol extraction of PGs from brain tissue. Methanol extraction showed a 20% higher recovery of IS (97%) than acetone extraction (77%). Bligh and Dyer extraction showed only 10% recovery in this experiment. The efficiency of methanol extraction might be the result of an elimination of losses during multiple-step extraction protocols. Also, one-step methanol extraction showed a 1.45x higher signal to noise ratios than acetone extraction. Even though some LLE protocols show high recovery of eicosanoids they all have several disadvantages: large solvent volume consumption and possible problems with separation of layers (e.g. emulsification).³⁶ SPE helps to address some of these problems, therefore it is the most popular *in vitro* extraction method for eicosanoids in brain tissue.

1.2.3 Solid-phase extraction (SPE)

Solid-phase extraction allows concentration of analytes along with removing some impurities from the sample, thus improving detection limits of analytical methods. For eicosanoid extraction, due to their lipophilic nature, reversed-phase SPE is usually used.³⁷ However, for the extraction of more hydrophilic eicosanoids, such as PGs, anion exchange can be used due to its ability to interact with the carboxyl groups of these eicosanoids.³⁷ Figure 1.9 shows the main steps of a typical SPE procedure. During reversed-phase SPE, the hydrophobic aliphatic moieties of the eicosanoids interact with the non-polar stationary phase allowing them to be retained while other polar and mid-polar compounds from the sample can be washed away by a polar wash solvent. Eicosanoids are then removed from the cartridge by an appropriate elution solvent such as methanol.³⁷

There are two widely used reversed phase SPE sorbents for eicosanoids: C-18 and Hydrophilic-Lipophilic Balanced sorbent (HLB). C-18 SPE stationary phase contains silica particles with bonded octadecyl alkyl chains (18 carbons hence C-18) that provide strong hydrophobic interactions with lipophilic compounds. HLB contains a resin made from a co-

polymer of divinylbenzene that provides hydrophobic interactions and vinyl pyrrolidinone that provides hydrophilic interactions.

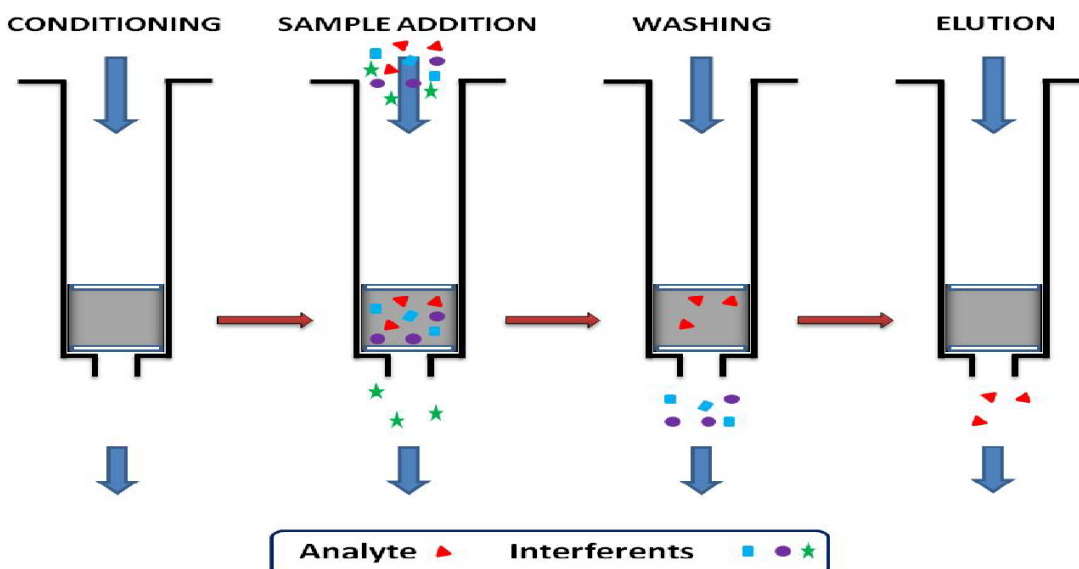


Figure 1.9 General SPE workflow. Reprinted from reference 51.⁵¹

Masoodi and Nicolaou³⁵ extracted 27 prostanoids from brain tissue using (Phenomenex) C-18 SPE. Sample pH was adjusted to 3 with 0.1 M hydrochloric acid and prostanoids were eluted with methyl formate. The recovery of analytes was 84-100%. The method was later expanded⁴⁴ to cover an additional 20 eicosanoids (mostly HETEs, hydroxyeicosapentaenoic acids (HEPEs) and Resolvins (Rvs)) from brain tissue with recovery between 76-115%. Farias *et al.*⁵² used (Strata) C-18 SPE cartridges for extraction of eicosanoids from rat brain, elution was with methanol. Yue *et al.*²⁶ extracted PGs, HETEs, EETs, DiHETrEs and AA from a rat brain using (Oasis) HLB SPE and eluted the analytes with acetonitrile and ethyl acetate with a final recovery between 72-99%. Miller *et al.*⁴⁰ also used HLB SPE for the extraction of the same groups of eicosanoids from brain cortical tissue. However, elution was with methanol, resulting in the final recovery of analytes ranging from 73-94%. HLB in combination with methanol elution was also used by Shaik *et al.*,²⁸ to extract PGs from rat brain. Ostermann *et al.*⁵³ compared extraction recovery of all classes of eicosanoids from plasma on different SPE cartridges: Oasis HLB, Strata-X, SepPak-C-18, BondElut strong and weak anion exchange. The comparison was performed in a plasma matrix. It was concluded that C-18 is the optimal cartridge for oxylipin analysis in plasma (Figure 1.10).

Since no single method covers all eicosanoids of interest, it was decided to develop new extraction method.

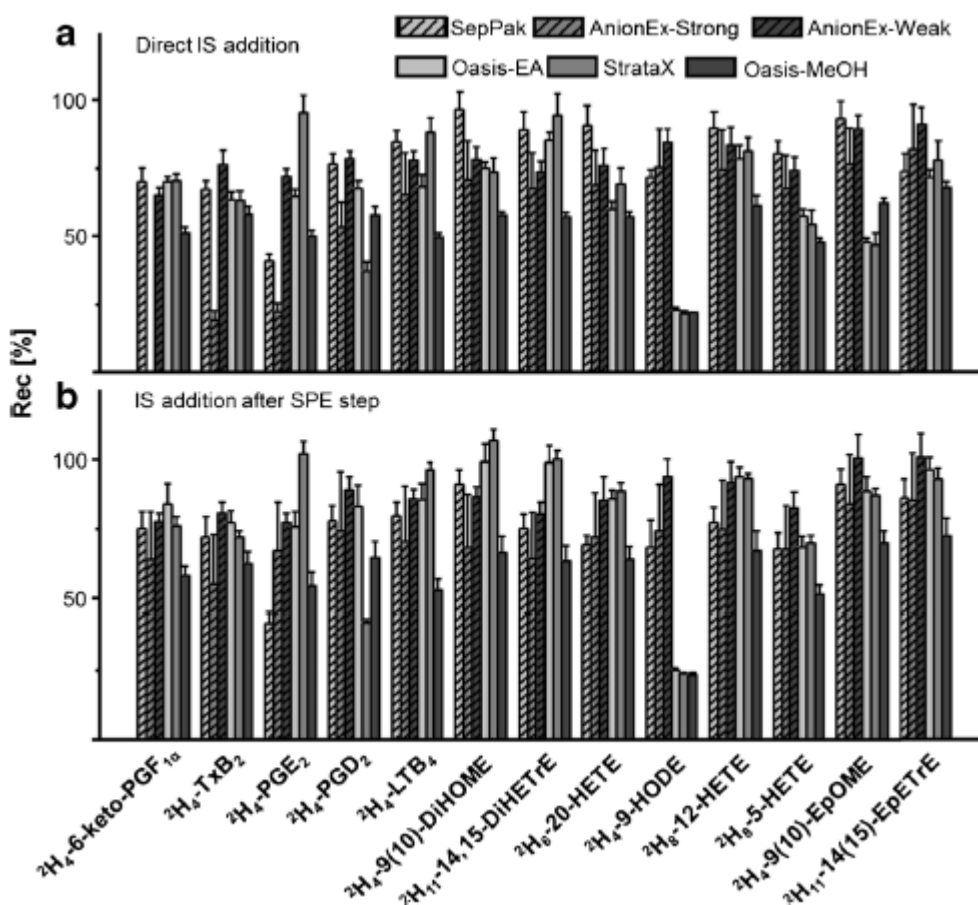


Figure 1.10 Recoveries of internal standards (IS) for the tested SPE protocols. IS was added to the samples either at the beginning of the analysis (panel A) or after the SPE step (panel B). Shown is the mean recovery rate \pm SD ($n=5$). Reprinted by permission from Springer Nature: from reference 53, copyright 2014.

Another important step in the sample preparation process using SPE is the evaporation of solvent after elution and reconstitution of the sample in injection solvent. Here, three main approaches were found: evaporation under a stream of nitrogen,²⁸ argon²⁶ or in a vacuum centrifuge⁵³. To minimize adsorptive losses of oxylipins, it was recommended to add 6 μL of 30% glycerol in methanol to the tubes where evaporation will be performed.⁵³ This prevents the interaction of eicosanoids with the walls of the tube after evaporation of the solvent, because glycerol is not volatile and after evaporation 1.8 μL of glycerol remains on the bottom of the tube forming “safety trap” for eicosanoids.⁵³

The above strategies for measuring the eicosanoids all aim to maximize recovery and ultimately accuracy but, they do not deal with the issue of ante-mortem/post-mortem changes in eicosanoids. Instead of focusing on solving the problems of post-mortem measurement perhaps it would be better to measure the correct levels of eicosanoids in living tissues. One technique that could potentially measure eicosanoids in particular brain regions, and at particular times, is *in vivo* solid-phase microextraction (SPME).

1.2.4 *In vivo* solid-phase microextraction (SPME)

Solid-phase microextraction (SPME) is a non-exhaustive extraction technique that combines sampling, analyte isolation and enrichment into one step. Using SPME, only a small portion of the analyte is extracted causing minimal perturbation to the living system, which allows this technique to be used for *in vivo* analysis. To use SPME for *in vivo* analysis, the device coating must be made with biocompatible materials such as polydimethylsiloxane (PDMS), polypyrrole (PPY) or polyethylene glycol (PEG). Biocompatibility is important even if exposure to fiber is not long because it prevents fouling of the fiber with large biomolecules such proteins. The sorbent of interest (e.g. C-18, HLB etc.) that is used in SPME coating needs to be covered by the biocompatible polymer but also allow analyte diffusion through it. This minimizes adverse reactions to the living system and prevents the adhesion of the macromolecules to the surface of the SPME devices. Different designs of SPME devices exist but fiber SPME is most widely used for direct *in vivo* sampling. Fiber SPME consists of a thin metal fiber core partially coated with sorbent and assembled within a hypodermic needle that covers and protects the fiber before and after extraction (Figure 1.11).⁵⁴

Typical fiber SPME workflow consists of several steps. After a preconditioning step, where the SPME fiber is immersed into organic solvent to condition the sorbent, the fiber is introduced into the biological matrix and analytes begin to diffuse between the matrix and the sorbent until the system reaches equilibrium. However, often in *in vivo* SPME shorter sampling times, without waiting for equilibrium, are used. At the next step, the fiber is removed from the biological matrix, quickly rinsed, in water, and immersed into a small amount of organic solvent (enough to fully immerse the coated part of the fiber, usually ~100 μ L for commercial 15 mm-long coatings) to desorb the analytes. This desorption solvent, containing the analytes, is analyzed or an evaporation/reconstitution step may be added to further improve limits of detection (Figure 1.12).⁵⁴

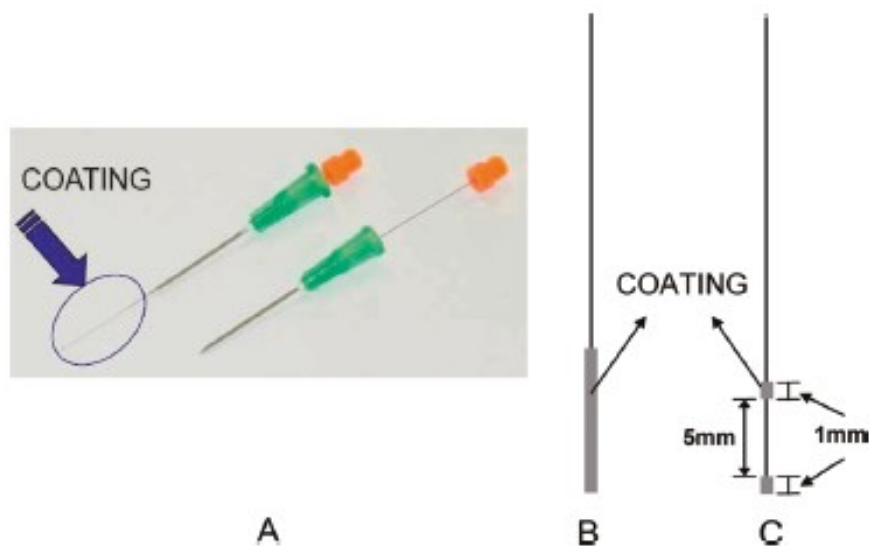


Figure 1.11 Commercial prototype SPME fiber assembly based on a hypodermic needle for *in vivo* applications (A) and schematic of conventional SPME fiber with typical coating length of 10–15 mm (B) and high-spatial-resolution fiber with discontinuous coating (C). Reprinted with permission from reference 54, Copyright 2011, American Chemical Society.

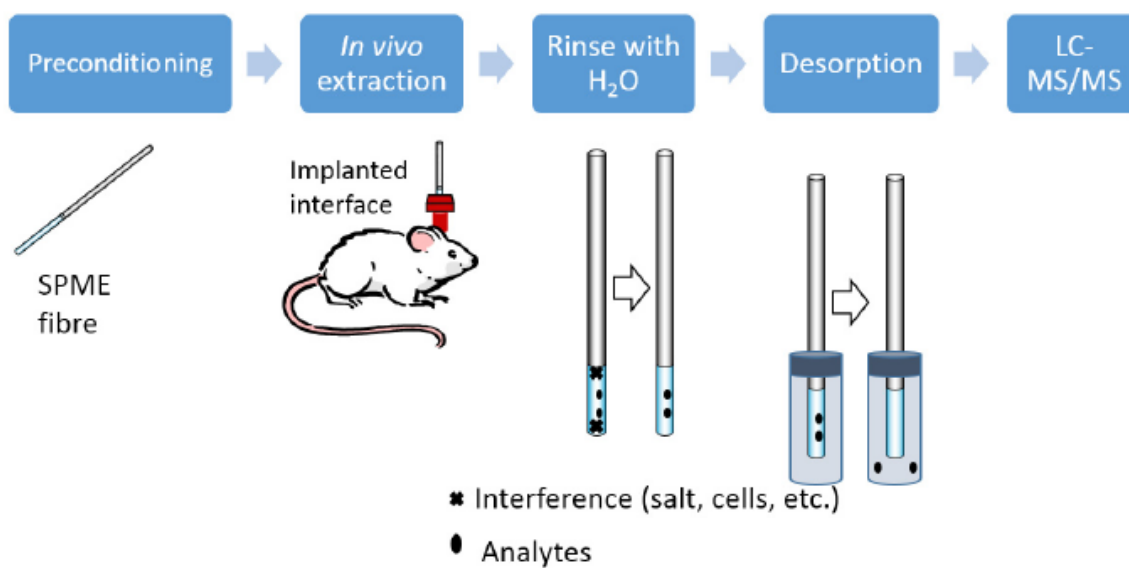


Figure 1.12 Workflow of *in vivo* extraction of analyte from brain tissue using SPME fibers. Reprinted from reference 58 with permission from John Wiley and Sons.

The extraction of the analyte by SPME is nonexhaustive and can be described by Equation 1.1.⁵⁴

Equation 1.1 Amount of analyte extracted by SPME⁵⁴

$$n_e = \frac{K_{fs} V_s V_f}{K_{fs} V_f + V_s} C_0$$

where n_e – concentration of analyte extracted at equilibrium, K_{fs} – distribution coefficient of the analyte between sorbent and sample matrix, V_s and V_f – volumes of sample and sorbent respectively, C_0 – initial concentration of analyte in the sample.

The distribution coefficient K_{fs} can be described by Equation 1.2.⁵⁴

Equation 1.2 Distribution coefficient⁵⁴

$$K_{fs} = C_f \div C_s$$

where C_f and C_s are the concentrations of the analyte in the sorbent and in the sample at equilibrium.

The distribution coefficient depends on different conditions including temperature, pressure and matrix composition.

In cases when the sample volume is much larger than $K_{fs} V_f$, Equation 1.1 can be simplified to Equation 1.3.⁵⁴

Equation 1.3 Amount of analyte extracted by SPME when sample volume is large⁵⁴

$$n = K_{fs} V_f C_0$$

Equation 1.3 allows calculation of the concentration of the analyte without defining the volume of the sample and can be used for *in vivo* extraction when the sample volume is unknown provided it is much larger than the volume of the sorbent.

Equations 1.1 and 1.3 are relevant only in situations when sampling time is long enough to reach equilibrium. In case of pre-equilibrium extraction Equation 1.4 must be used. In this thesis pre-equilibrium SPME were performed and time-averaged concentrations were measured.

Equation 1.4 Amount of analyte extracted by SPME at pre-equilibrium conditions⁵⁴

$$n = [1 - \exp^{-at}] n_e$$

where n is amount of extracted analyte at time t , n_e is amount of analyte extracted at equilibrium and a is a rate constant that is dependent on the volumes of the extraction phase and sample, the mass transfer coefficients, the distribution coefficients, and the surface area of the extraction phase.

In vivo SPME was applied to different living systems including microorganisms,⁵⁵ plants,⁵⁶ insects⁵⁷ and animals⁵⁸. Brain *in vivo* sampling was performed in several experiments. *In vivo* SPME sampling of rat brain tissue is performed via guide cannulae surgically implanted into the cranium, similar to what is used for microdialysis (MD) sampling.⁵⁹ Win-Shwe *et al.*⁶⁰ used fiber SPME to measure the pharmacokinetics of intraperitoneally injected toluene in mouse brain (hippocampus region). This experiment showed that the level of toluene in the hippocampus rapidly increased in the first 30 minutes after injection and returned to the basal level after 2 hours. Cudjoe *et al.*⁵⁹ measured levels of serotonin and dopamine in rat brain before and after administration of fluoxetine using *in vivo* SPME and MD. Fluoxetine is an anti-depressant drug that affects the serotonin levels without changing dopamine levels in the brain. Both methods demonstrated the same trends where the level of serotonin increased after drug administration and the level of dopamine was not changed. However, SPME showed better precision than MD potentially because matrix effects are higher for MD.

To date *in vivo* SPME of eicosanoids was performed only once by Bessonneau *et al.*⁶¹ in circulating rat blood. The goal of the experiment was to monitor rapid changes in blood concentrations of eight eicosanoids (TXB₂, PGD₂, PGE₂, LTB₄, 15-HETE, 12-HETE, DHA and AA) after lipopolysaccharide (LPS)-induced inflammation. Extraction was performed using a biocompatible C-18 SPME fiber via catheters implanted into carotid artery and diffusion-based calibration was used for quantitative analysis. 15-HETE, PGE₂ and PGD₂ could not be measured *in vivo* because their concentrations in blood were lower than the lower limit of quantitation (LLOQ) for the method, however, they were detected. TXB₂ and LTB₄ did not show significant changes upon LPS treatment, while the levels of AA, docosahexaenoic acid (DHA) and 12-HETE were increased. Additionally, validation experiments were performed where the concentrations obtained via SPME and the precipitation method were compared. The concentrations that were measured using SPME were slightly higher, which was explained by the higher stability of eicosanoids on SPME fibers. Despite its small sample size of only 2 rats, this experiment showed that fiber SPME can be used for sampling of eicosanoids *in vivo*. However, the inability to detect

three of eight selected eicosanoids in this experiment also demonstrates some of the key difficulties with this analysis. Eicosanoids are effectively protein-bound (99%) in blood and *in vivo* SPME can extract only a small fraction of the free concentration of a given eicosanoid. This thesis will expand on this preliminary work in order to use fiber SPME for the measurement of eicosanoids in rat brain *in vivo* and it will be the first experiment of this kind. However, to be able to measure such low levels of eicosanoids method limits of detection must be further improved.

1.2.5 Liquid chromatography (LC)

Many oxylipin species have the same molecular formula, the same mass and thus cannot be resolved by even high-resolution mass spectrometry. This makes liquid chromatography an essential part of any analysis since chromatographically it is possible to separate many eicosanoid isomers prior to MS detection.

It is known that smaller particle size decreases the height equivalent of a theoretical plate (HETP) and thus improves the efficiency of the separation.⁶² Thus, the popularity of ultra-high performance liquid chromatography (UHPLC) columns containing 1.7-1.8 μm fully porous particles or 1.7-2.6 μm particles containing solid core has grown over the last decade.⁶³⁻⁶⁶ Solid core particles improve peak shape and resolution because mobile phase containing analytes cannot penetrate into particle pore thus decreasing axial diffusion.^{36,67} Unfortunately, smaller particles in UHPLC columns increase the backpressure up to 1000 bar, compared with 400 bar for traditional HPLC. Solid-core particles can give resolution similar to UHPLC but with traditional HPLC backpressure. Ecker showed that with both UHPLC and solid-core HPLC excellent separation and peak shapes can be obtained, however for higher volumes of complex matrices UHPLC are preferable.⁶⁷ Kortz *et al.*⁶⁸ showed improvement of resolution between PGD_2 and PGE_2 using a Kinetex core-shell column rather than traditional fully porous C-18 HPLC. Brose *et al.*²⁷ using UHPLC obtained five times narrower chromatographic peaks for PGE, PGD and isoprostanes from mouse brain as compared to the peaks obtained using traditional HPLC. In summary, the use of UHPLC or solid-core particles, such as Kinetex core-shell from Phenomenex, can improve sensitivity and separation of oxylipins and will be examined in this thesis.

Different LC modes can be used for separation of arachidonic acid metabolites including reversed-phase (RP-HPLC), normal-phase (NP-HPLC), chiral HPLC, and nanoLC that will be discussed below. RP-HPLC with C-18 columns is the most widely used method of separation in

eicosanoid analysis and is based on hydrophobic interactions between the stationary phase and eicosanoids.^{63–66} However, sometimes NP-HPLC can help in separation of particular eicosanoids. For example, Qu *et al.*⁶⁹ separated 19-HETE and 20-HETE using NP-HPLC where it was not possible to with RP-HPLC. Chiral HPLC is useful for separation of prostaglandin/isoprostane stereoisomers⁷⁰, R- and S-enantiomers of HETEs and HpETEs^{71,72} and enantiomers of EETs⁷³. Brose *et al.*⁷⁰ separated PGE₂ and its enantiomer (entPGE₂) from brain tissue using a Lux Amylose2 column. Neilson *et al.*⁷¹ separated R- and S-enantiomers of 5-, 12- and 15-HETE in mouse colonic mucosa using a Chiral-Pak AD-RH column. Mesaros *et al.*⁷³ analyzed enantiomers of 8,9-EET, 11,12-EET, 14,15-EET using NP-chiral-LC-MS employing a Chiralpak AD-H column. Jouvène *et al.*⁴⁶ used a Chiralcel OD-H column to resolve R- and S-enantiomers of HETEs and hydroxydocosahexaenoic acids (HDoHE) – oxidation products of docosahexaenoic acid (DHA) in rat brain tissue. They used ratio between R- and S-enantiomers of these eicosanoids to determine their origin because enzymatic oxidation of PUFA produces mainly S-enantiomers meanwhile nonenzymatic oxidation produces racemic mixtures. The drawback of chiral chromatography is the limited availability of UHPLC columns. UHPLC chiral columns were developed recently, however, and there are no reports about analysis of eicosanoids on this type of column.

Recently, Kumari *et al.*⁷⁴ also applied supercritical fluid chromatography (SFC) for separation of eicosanoids. SFC utilizes supercritical carbon dioxide (CO₂) as the mobile phase. Its high diffusivity, and low viscosity, allow higher flow rates on UHPLC columns in order to decrease analysis time. The addition of modifiers (2-40% v/v of e.g. methanol) can improve the elution strength and solvating power of CO₂. Kumari *et al.* assessed seven SFC columns to choose one that gives the best separation of eicosanoid standards, mobile phase was modified with methanol (MeOH) and 10 mM ammonium acetate (AmAc) at a flow rate of 1.5 mL/min. A 2-picolylamine (2-PIC) column was chosen as the best, and after optimization of the method, allowed separation of five eicosanoids within 3 minutes. Despite the efficient and fast separation only five hydrophilic eicosanoids were analyzed in this experiment and it is not clear how other classes of eicosanoids would be separated by this method.

The main difference between nanoLC and HPLC/UHPLC is the much lower flow rate in nanoLC (nL/min). Nanoflow provides improved sensitivity because less solvent is going to the mass spectrometer electrospray ionization (ESI) source where ionization of analytes occurs. which

can decrease the matrix effect and increase ionization efficiency. NanoLC is mainly used in proteomics, however Ando *et al.*⁷⁵ suggested using nanoLC for the analysis of eicosanoids in brain tissue. They hypothesized that the sensitivity of nanoLC-MS/MS could help to detect low concentrations of eicosanoids. In this approach, brain tissue was homogenized with methanol and formic acid, transferred to a Captiva ND lipids 96-well plate to remove ion-suppressing phospholipids and proteins then centrifuged for 2 min and injected onto a nanoLC-MS/MS system using an 50 μm i.d. column, and flow rate of 200 nL/min with water/acetonitrile/isopropanol:acetone (95:5:5) mobile phases, containing 0.1% acetic acid. They analyzed seven eicosanoids and achieved LOQs of 0.05 ng/ml for most of them. However, nanoLC usually requires long separation times and this analysis took 85 min. Also, it is not as robust as HPLC/UHPLC methods and retention times are less reproducible.

1.2.6 Mass spectrometry (MS)

Due to their low concentrations, analysis of eicosanoids in brain tissue requires highly sensitive MS instruments. Also, its coupling with UHPLC requires fast data acquisition capability because of high flow rate. Electrospray ionization (ESI) in negative mode is used in the majority published LC-MS methods because eicosanoids readily ionize to form $[\text{M}-\text{H}]^-$ ions. For eicosanoid analysis in negative ESI two main additives are used: acetic acid^{63-65,76} and formic acid^{45,49,77} in different (low) concentrations ranging from 0.005 to 0.1% (v/v). However, positive ESI is sometimes used for ionization of leukotrienes and eoxins.⁷⁸ Different MS instruments are used in eicosanoid analysis including triple quadrupole (QQQ), Quadrupole-Time-of-Flight (QTOF) and hybrid quadrupole-linear ion trap (QqLIT) mass analyzers. Selected reaction monitoring (SRM) or multiple reaction monitoring (MRM) on QQQ is the most popular method for targeted eicosanoid analysis.^{28,35,40,75} In this analysis, a selected precursor ion is filtered in the first quadrupole then it is fragmented via collision induced dissociation (CID) in the second quadrupole using low collision energy (usually between -15 and -35 eV), after that specific product ions are filtered in the third quadrupole and go to the detector. Masoodi and Nicolaou³⁵ performed an analysis of 27 prostanoids from brain tissue using HPLC-QQQ and MRM mode, the LLOQ for the prostanoids was 2-100 pg on-column. Shaik *et al.*²⁸ analyzed 11 prostanoids in rat brain tissue using UHPLC-QQQ and SRM mode, the LLOQ for the majority of prostanoids was 6.25 pg on column (0.104 ng/ml). Miller *et al.*⁴⁰ performed an analysis of HETEs, EETs, and DiHETrEs from brain tissue using UPLC-QQQ and SRM mode and obtained LLOQ 0.208 ng/ml in solvent for the analyzed compounds. Using

linear ion trap (LIT) instead the third quadrupole can help to increase sensitivity and popularity of QqLIT in targeted eicosanoid analysis is growing.^{25,42,46,63} Similar to quadrupole, LIT uses electrical fields to manipulate ions, however using additional endcap electrodes LIT can not only pass ions like a quadrupole but also trap and accumulate these ions according to their masses with their subsequent ejection to the detector. For the analysis of 43 brain oxylipins Wong *et al.*²⁵ used QqLIT and MRM mode to reach LLOQ of 0.01 nmol/g tissue. Jouvène *et al.*⁴⁶ analyzed 16 eicosanoids from rat brain tissue using QqLIT. Thakare *et al.*⁶³ analyzed 34 eicosanoids in different biological matrices (including plasma, bronchoalveolar lavage fluid (BALF) and sputum) with LLOQ of 0.2-3 ng/ml.

In a QTOF mass spectrometer the third quadrupole is replaced by a time-of-flight mass analyzer to increase resolution compared to QQQ. In TOF, product ions (if fragmentation took place in the quadrupole) or only parent ions (without fragmentation) travel through the drift tube to the detector and separate according to their mass-to-charge ratios. Lighter ions move faster than heavier ones (for the same charge). QTOF is used much less than QQQ in eicosanoid analysis. It belongs to high resolution MS and has higher resolving power and mass accuracy which is important in complex biological matrixes where it is possible to have interferences with the same nominal mass as the analyte(s). Also, QTOF is useful because it can collect full product ion spectra rapidly in order to confirm the identification of isomers that cannot be resolved chromatographically. Brose *et al.*²⁷ analyzed nine PG and Isoprostanes from mouse brain using UHPLC-QTOF without fragmentation and observed LLOQ of 1±0.5 pg on column. Tajima *et al.*⁴⁹ performed an analysis of 31 eicosanoids of different classes on UHPLC-QTOF with fragmentation, however LLOQs were not reported. In this thesis targeted analysis and untargeted profiling of oxylipins will be performed on QTOF MS.

1.2.7 Summary of the LC-MS methods for oxylipin measurement in brain

Existing analytical methods to measure brain eicosanoids are summarized in Table 1.2. Generally, these methods focus on specific classes of eicosanoids and only three of them cover all main classes of eicosanoids derived from AA (Wong²⁵, Petta⁷⁶, Furman⁴²). However even these methods do not cover all eicosanoids of interest. For example, Wong's method²⁵ does not include measurement of PGF_{2α} isomers, LTD₄, LXA₄, 5-oxoETE; Petta's method⁷⁶ does not include measurement of PGF_{2α} isomers, 8-HETE, 11-HETE, 16-HETE, (±)14(15)-EET, (±)11(12)-EET; Furman's method⁴² does not include measurement of LTD₄, LTE₄ and oxoETEs. Moreover,

Wong²⁵ and Furman⁴² used LLE for extraction of eicosanoids from brain tissue and LLE has several drawbacks such as large solvent consumption and possible problems with separation of layers. Also, in descriptions of these methods recovery of analytes was not shown so it is difficult to evaluate the efficiency of these methods. Thus, it was decided to use SPE for the extraction of oxylipins from brain tissue and, because no existing method covers all analytes of interest, we decided to develop and optimize our own SPME method and evaluate its recovery.

As it was mentioned in Section 1.2.4 for *in vivo* SPME, maximum sensitivity is required because we expect very low levels of eicosanoids in these extracts. Among these three methods with maximum coverage of oxylipins the LLOQ were shown only for Wong's method,²⁵ however LLOQ of 3 ng/g tissue is not acceptable for our analysis because we expect levels lower than this of 3 ng/g. Among other existing methods (see Table 1.2) the lowest LLOQ were reached by Ando⁷⁵ and Shaik²⁸ of 0.05 and 0.1 ng/ml respectively. However, these LLOQs were shown only for PGs and only in solvent. Also, Ando *et al.* used nanoLC and it takes 85 minutes for separation of more hydrophilic PGs and TxS. For the separation of all eicosanoids of interest including more hydrophobic compounds it possibly will take much longer, drastically reducing sample throughput. Another drawback of these two methods is that they use QQQ MS which means that they can analyze only known eicosanoids that are resolved chromatographically or have different fragmentation patterns. However, *in vivo* SPME may possibly extract some oxylipins that are not in the list of targets and that may not have been described before. Thus, it is important to use full scan mode and resolve the analytes chromatographically as much as possible as some isomeric eicosanoids of interest will have the same fragmentation patterns. Among existing methods (see Table 1.2) only two used full scan mode Tajima *et al.*⁴⁹ and Brose *et al.*²⁷, however they do not cover all eicosanoids of interest and they do not report, or report very high, LLOQ (10 ng/ml) respectively. Thus, for analysis of the SPME extracts we had to develop a novel, sensitive, LC-MS method that can resolve chromatographically all eicosanoids of interest, or when that it is impossible, resolve them using MS/MS and perform it in full scan mode to be able to find other eicosanoids that are not in our list of targets.

Table 1.2 Summary of the LC-MS methods for oxylipin measurement in brain

Reference	Target analyte classes / number of analytes covered	Extraction method	LC-MS method/scan mode	LLOQ	Analysis time (min)
Masoodi <i>et al.</i> ³⁵	PGs, TxS / 27	SPE (C-18)	HPLC-QQQ MS/ MRM	in solvent 1-20 ng/ml	30
Yue <i>et al.</i> ²⁶	PGs, DiHETrEs, HETEs, EETs/19	SPE (HLB)	HPLC-Q MS/ SRM	in solvent 0.2-2 ng/ml	45
Golovko <i>et al.</i> ⁴³	PGs, TxS / 5	LLE	HPLC-QQQ MS/ MRM	n.r.	50
Farias <i>et al.</i> ⁵²	PGs, LTs, HETEs/13	SPE (C-18/HLB)	HPLC-QQQ or QTRAP MS/ MRM	in solvent 1.76-10.51 ng/ml	45
Masoodi <i>et al.</i> ⁴⁴	HODEs, HEPEs, HETEs, LTB ₄ , Rvs, PDs, 17S-HDHA/19	SPE (C-18)	HPLC-QQQ MS/ MRM	in solvent 4-10 ng/ml	35
Miller <i>et al.</i> ⁴⁰	HETEs, EETs, DiHETrEs/10	SPE (HLB)	UPLC-QQQ MS/ SRM	in solvent 0.208 ng/ml	4.8
Brose <i>et al.</i> ⁷⁰	PGs, isoPGs/5	LLE	HPLC and Chiral HPLC-QQQ MS/ MRM	n.r.	80
Strauss <i>et al.</i> ⁴⁵	HETEs, EETs/20	SPE (HLB)	HPLC-QQQ MS/ MRM	n.r.	8
Tajima <i>et al.</i> ⁴⁹	PGs, HETEs, HEPEs, HDoHEs, DiHETEs/62	LLE	UPLC-TOF MS/ Full Scan	n.r.	67
Liu <i>et al.</i> ⁴¹	PGs/4	SPE (HLB)	UPLC-QQQ MS/ SRM	n.r.	n.r.
Brose <i>et al.</i> ²⁷	PGs/9	MeOH extraction	UPLC-QTOF/ Full Scan	in solvent 10±5 ng/ml	16.5
Shaik <i>et al.</i> ²⁸	PGs/11	SPE (HLB)	UPLC-QQQ MS/ SRM	in solvent 0.1- 0.2ng/ml	12

Wong <i>et al.</i> ²⁵	PGs, LTs, DiHETs, HETEs, EETs/49	LLE	HPLC-QTRAP MS MRM	in matrix 3ng/g tissue	n.r.
Petta <i>et al.</i> ⁷⁶	PGs, LTs, DiHETs, HETEs, EETs/23	SPE (C-18)	HPLC(fused core)- QQQ MS/ MRM	n.r.	30
Ando <i>et al.</i> ⁷⁵	PGs, TxS, LTB ₄	MeOH extraction	nanoLC-QQQ MS/ SRM	in solvent 0.05 ng/ml	85
Furman <i>et al.</i> ⁴²	PGs, LTs, HETEs, EETs/55	LLE	HPLC-QTRAPMS/ MRM	n.r.	35
Jouvene <i>et al.</i> ⁴⁶	HETEs, HDoHES, LTB ₄ , RvD ₁ , PDs/16	SPE (MAX)	UPLC and Chiral HPLC-QTRAPMS/ MRM	n.r.	40/27

*n.r-not reported

1.3 Research objectives

The existing methods for the analysis of eicosanoids in brain tissue require sacrifice of the animal followed by tissue homogenization and subsequent extraction of eicosanoids using LLE or SPE. However, post-mortem synthesis can change eicosanoid levels, so that the existing *in vitro* methods may not reflect *ante mortem* levels of eicosanoids in living/functioning brains. For this reason, it is important to develop an *in vivo* method that can measure accurately levels of eicosanoids in living brain with good spatial and temporal resolution. The single existing *in vivo* method for brain analysis is MD but it has limitations for lipid analysis because they can interact with the MD device tubing causing analyte losses. *In vivo* MD was used for extraction of oxylipins from brain, however, representatives of only one class of more hydrophilic oxylipins (PGs) were detected. SPME can solve this problem of losses during sampling and become the first *in vivo* method for the analysis of oxylipins in brain tissue that covers all main classes. Thus, the main objective of this thesis was to demonstrate this capability of SPME for the first time. However, because of the low abundance of eicosanoids and because SPME is a non-exhaustive method that can extract only a small portion of the analyte, very sensitive LC-MS was required. Thus, the first step of this work focused on the development of the LC-MS method that was capable of detecting and quantifying all oxylipins of interest. According to the literature review, RP C-18 was selected for the separation method and columns packed with both fully porous and core-shell particles will be compared. After that, SPME fibers were used for *in vivo* sampling from the rat brain and the resulting samples were analyzed using the developed LC-MS method. Authentic standards were used to confirm the identification of as many oxylipins as possible that were extracted by *in vivo* SPME. The second objective of this thesis was to develop a reliable SPE method capable of extracting all oxylipins of interest from brain tissue and plasma *in vitro*. This optimized method was then be applied to brain tissue samples and human plasma samples. Oxylipins were detected and quantified in these samples. Coverages of *in vivo* and *in vitro* methods for the brain tissue were compared.

2 Ultra-high performance liquid chromatography – high resolution mass spectrometry method for detection and quantitation of oxylipins in plasma.

Alexander Napylov, Dajana Vuckovic

Department of Chemistry and Biochemistry, Concordia University, Montreal, Quebec, Canada

2.1 Abstract

Oxylipins are bioactive oxygenated products of long chain (18-22) polyunsaturated fatty acids (PUFA). They play important roles in different physiological processes acting as local hormones, so they may be used as biomarkers of these processes. In addition, the pathways and exact biological functions of many members of this family are not clear and need further investigation. To enable such investigations, it is important to have a reliable and accurate analytical method for oxylipin measurements. The objective of this work was to develop a multi-class oxylipin analytical method to detect and quantitate oxylipins in plasma samples. High-resolution scan mode is used for further identification and annotation of unknown oxylipins. A sensitive liquid chromatography-mass spectrometry method was developed for 65 oxylipins and 7 internal standards that was used to detect 38 oxylipins in human plasma and accurately quantitate 25 of them. The method relied on Strata C-18 SPE followed by two LC-MS analyses on an Agilent QTOF 6550 iFunnel, one of 2.5x pre-concentrated and one of 40x diluted samples. Chromatographic separation of oxylipins, including their isomers, was achieved with a C-18 UHPLC column using water/acetonitrile:isopropanol mobile phases, containing 0.02% acetic acid in 40 min. Three pairs of standards required MS/MS for positive identification/quantitation. The average recovery was 70-97 % and the matrix effect was 27-105%. The chromatographic selectivity of the method was further investigated using shallower gradient and different chromatographic columns to ensure selectivity of the identifications. The results showed that shorter methods could suffer from oxylipin misidentifications even when authentic standards and very narrow accurate retention time matching was used due to the existence of very large numbers of oxylipin isomers.

2.2 Introduction

Oxylipins are bioactive oxygenated products of long chain (18-22) PUFA.⁷ The main precursors of oxylipins are AA, DHA, EPA, Linoleic acid (LA), Alpha-linolenic acid (ALA), Dihomo-gamma-linolenic acid (DGLA) and 11,14-eicosadienoic acid. Membrane phospholipids are the main source of PUFA that are released from cell membranes by PLA₂ enzyme.¹¹ After mobilization, PUFA can be oxidized by COX, LOX and CYP enzymes as well as nonenzymatically.⁸ Oxygenated PUFA act through specific G-protein-coupled receptors close to the place of their synthesis.^{7,8} In living systems, eicosanoids, and other oxylipins, play important roles in various physiological processes such as inflammation,¹⁹ sleep and memory,²⁴ cerebrovascular function⁷⁹ and others^{29,80}. Depending on their roles, oxylipins may be used as therapeutic targets or biomarkers of different disorders. To investigate these and other biological roles of oxylipins, reliable quantitative analytical methods for various biological tissues and fluids are needed.

Different analytical methodologies can be used for the analysis of oxylipins in biological matrices including immunoassays³¹, GC-MS or GC-MS/MS^{32,33} and LC-MS or LC-MS/MS^{34,35}. Radio-labeled and enzyme-linked immunoassays were historically popular for oxylipin analysis. However, their key disadvantages include cross-reactivity and they cannot be used for simultaneous measurement of multiple oxylipin analytes of interest. GC-MS and GC-MS/MS can be used for the analysis of most primary oxylipins (*e.g.* PGs) but are not suitable for labile oxylipins (*e.g.* EETs). In addition, GC-based methods require derivatization which makes the analytical process more complicated because of factors such as incomplete derivatization and side reactions. To date, LC-MS/MS is the most popular methodology for oxylipin analysis due to its sensitivity, resolution and high throughput.³⁶ Reversed-phase liquid chromatography on C-18 is commonly used for the effective separation of isomeric compounds, followed by MS analysis of oxylipins in negative ESI, mostly on QQQ or QqLIT mass analyzers in SRM or MRM modes.^{53,65,81-83} For example, Zhang *et al.*⁸¹ successfully quantified 15 oxylipins in human plasma with LOQs of 20-33 pg/ml. Miller *et al.*⁸² quantified 10 oxylipins in human plasma and achieved 0.416 ng/ml LOQ for all analytes. These targeted methods generally provide high sensitivity and good limits of detection, but they only allow quantification of the oxylipins that were included in the target list before analysis. However, many unknown oxylipins and oxylipins are still being annotated⁸⁴ and typical target lists usually do not even contain all the known oxylipins that could be possibly detected.

Thus, using high-resolution mass spectrometry for oxylipin profiling is of significant interest in order to expand the range of oxylipin species that can be monitored.⁸⁵ Only a few methods to date have examined QTOF performance for oxylipin profiling,^{27,49,86,87} and among these only Berkecz *et al.*⁸⁶ used MS1 scan mode for analysis. The identification of known oxylipins with authentic standards was performed based on retention time and accurate mass while unknown oxylipins were further characterized using data-dependent acquisition (DDA) mode to obtain fragment ions. As a result, 31 oxylipins from the target list were identified in plasma and an additional 20 potential oxylipins that were not on the target list were identified due to using the scan mode and DDA in the 20 min analysis time. One potential issue with the use of such short chromatographic times is possible co-elution of isomeric oxylipins, and this requires further investigation.

Sample preparation and extraction procedures are also critical steps in oxylipin analysis. For the extraction of oxylipins from plasma, LLE,⁸¹ protein precipitation^{83,88,89} and SPE^{65,82,86,90} are frequently used. Among these, SPE is the most popular due to its robustness, reproducibility and high recoveries.⁵³ There are many existing SPE methods for oxylipin extraction from plasma showing different oxylipin coverage, recoveries of standards and reproducibility. However, most often they are optimized for a particular class of oxylipins with similar properties. For methods covering a wide range of oxylipins the reported validation does not usually reflect real recovery or the matrix effect of each oxylipin but, rather for a small group of internal standards to avoid problems with endogenous levels of oxylipins. For example, the methods developed by Strassburg *et al.*³ and Wang *et al.*⁹¹, that used SPE for extraction of more than 100 oxylipins used 11 and 26 internal standards respectively for method validation, evaluation of recovery and matrix effect. With so few validation species, the results cannot really reflect recovery and matrix effect for every analyte. For that reason, it was decided to develop and optimize a SPE method for extraction of oxylipins from plasma with evaluation of recovery and matrix effect for every oxylipin analyte.

The aim of this study was to develop a sensitive analytical method for quantitative analysis and profiling of eicosanoids and other oxylipins in plasma and to investigate, in detail, the possible interferences of isomeric species for the analysis of 65 oxylipins. The optimized method includes solid phase extraction optimized for plasma and LC-HRMS in scanning mode for broad oxylipin profiling and is suitable for detection of 38 oxylipins, among which 25 oxylipins could be accurately quantified.

2.3 Materials and methods

2.3.1 Chemicals

LC-MS grade water, methanol, acetonitrile, isopropanol and HPLC grade ethyl acetate were purchased from Fisher Scientific (Ottawa, Ontario, Canada). Acetic acid (HAc, ACS grade, 99.7%) and formic acid (FA, for mass spectrometry, 98%), trichloroacetic acid solution (TCA, 6.1 N), ammonium acetate (AmAc, for mass spectrometry), ammonium hydroxide solution (NH₄OH, ≥25% in H₂O, eluent additive for LC-MS) were purchased from Sigma-Aldrich (Oakville, Ontario, Canada). Ethanol (EtOH, ACS grade) was purchased from MP Biomedicals, LLC. Pooled human plasma and individual human plasma with sodium citrate as anticoagulant was purchased from Bioreclamation Inc. (Baltimore, MD, USA).

2.3.2 Oxylipin standards

In total, 76 oxylipin standards including 8 deuterated standards (Supplementary Tables S1 and S2) were purchased from Cayman Chemicals (Ann Arbor, MI, USA). During the initial method development four of them (Table S1) were excluded from further analysis: LTC₄ was not detectable in negative mode, TXB₂ showed a very broad peak with unacceptable tailing, whereas 5(6)-EET and 5(6)-EET-d₁₁ gave very low signal relative to other EETs making them undetectable in low concentrations. 12-oxoETE, 5-HpETE and 15-HpETE did not pass an autosampler 24-hour stability test (Supplementary Figure S14) and were excluded from all quantitative analyses, however they were used in Mix 65 and Mix 72 to preserve the possibility for their detection in samples. All standard solutions were prepared in MeOH and stored at -80°C, unless otherwise noted. Individual standard stock solutions were prepared at 10 µg/ml. Three 100 ng/ml working solutions were prepared: one of all non-labelled oxylipins and internal standards (Mix72), second of all non-labelled oxylipins (Mix 65), and third of deuterated internal standards (Mix 7d).

2.3.3 Optimized C-18 SPE procedure for standards in solvent

C-18 (Strata Phenomenex 200 mg) SPE was performed as follows: (i) conditioning with 1 ml of MeOH and 1 ml of 20% MeOH, (ii) loading 100-1000 µl of sample, percentage of organic solvent in sample should be ≤20% (iii) washing with 1 ml of 20% MeOH, (iv) elution with 1 ml of 99% MeOH with 1% HAc into a 5 ml culture glass tube. After elution, all eluent was transferred to a 1 ml amber glass round-bottom tube contained 20 µl of 30% glycerol in MeOH and evaporated in a speedvac to dryness (6 µl of glycerol remaining at the bottom of the tube). The evaporation required different times depending on the matrix (~2 hours for standard solutions). After

evaporation, the samples were reconstituted with 40 μ l of MeOH with vortex mixing. Samples were then transferred to 250 μ l glass inserts placed in 1.5 ml Eppendorf tubes for centrifugation at 15 000 x g for 10 minutes at 4°C. Finally, 20 μ l of supernatant was transferred to a new HPLC glass insert for LC-MS analysis.

2.3.4 C-18 SPE with TCA precipitation

Pooled plasma (100 μ l) was added to a 1.5 ml polypropylene Eppendorf tube and spiked at final concentration of 5 ng/ml ISTDs mix and then placed in the freezer at -80°C for 1 hour. Samples were thawed and mixed with 100 μ l of 10% (v/v) TCA, vortexed and then centrifuged at 15000 x g for 15 min at 4°C. 150 μ l of supernatant was transferred to a clean 1.5 ml polypropylene Eppendorf tube and pH was adjusted to 3 using NH₄OH and pH paper. The samples (approximately 150 μ l, taking into account a few drops of NH₄OH that were added for pH adjustment) were then extracted by SPE followed by evaporation/reconstitution as described in Section 2.3.3.

2.3.5 C-18 SPE without prior protein precipitation step

Plasma (100 μ l) was added to a 1.5 ml polypropylene Eppendorf tube and spiked to a final concentration of 0.5 ng/ml ISTDs mix and placed in the freezer at -80°C for 1 hour. Samples were thawed and loaded on SPE and evaporation/reconstitution as described in Section 2.3.3. After reconstitution, samples were transferred from the glass inserts and placed into 1.5 ml Eppendorf tubes for centrifugation. Centrifugation was performed at 15 000 x g for 10 minutes. 20 μ l of final supernatant were transferred to the HPLC glass inserts for LC-MS analysis of low abundance oxylipins. 10 μ l of supernatant was diluted 100X with 100% MeOH, 20 μ l of diluted sample was transferred to an HPLC glass insert for LC-MS analysis of high abundance analytes. Samples were injected in 100% MeOH as no impact on accuracy or peak shape was observed during development experiments (Supplementary Figure S7).

2.3.6 IPA protein precipitation

Pooled plasma (100 μ l) was added to a 1.5 ml polypropylene Eppendorf tube and spiked to a final concentration of 0.5 ng/ml ISTDs mix then placed in the freezer at -80°C for 1 hour. Samples were then mixed with 300 μ l of IPA, vortexed and then centrifuged at 15000 x g for 15 minutes at 4°C. Finally, 350 μ l of supernatant was transferred to a new 1.5 ml Eppendorf tube. In HPLC glass inserts, 10 μ l of supernatant was diluted with 27.5 μ l of water before LC-MS injection.

2.3.7 Final LC-MS method

The chromatographic separation was performed on an Agilent 1290 Infinity II UHPLC system with a ZORBAX Eclipse plus C-18, 1.8 μm (2.1 mm x 100 mm) Rapid Resolution High Definition (RRHD) column (Agilent Technologies, Santa Clara, CA, US) protected by a guard column (2.1 mm x 5 mm; Agilent) made of the same packing material. The temperature of the column was held at 50°C with a mobile phase flow rate of 0.4 ml/min. Mobile phase (A) consisted of 0.02% acetic acid in LC-MS grade water and (B) 0.02% acetic acid, 10% isopropanol and 90% acetonitrile. The MP started at 95% A : 5% B for 1 min, then the % B was increased to 20% over 0.1 min, followed by a linear gradient from 20% to 80% B over 29.9 min. Then, %B was increased to 95% over 0.1 min where it remained for 3.9 min followed by column re-equilibration to initial conditions for 5 min. Total run time per sample was 40 min. Injection volume was 10 μl .

Mass spectrometric analysis was performed on an Agilent Q-TOF 6550 iFunnel equipped with Dual AJS ESI operated in negative mode. The following MS parameters were used: capillary voltage 3500 V, nozzle voltage 500V, drying gas temperature 250°C, drying gas flow 15 l/min, sheath gas temperature 275°C, sheath gas flow 12 l/min, mass range 100-1000 m/z. The LC-MS method was divided into 3 time segments: first (0-22.08 min.) and third (22.48-40 min) segments MS mode, acquisition rate 2 spectra/second; second segment (22.08-22.48 min), acquisition rate for MS - 2 spectra/second plus MS/MS mode for detection of 8-HETE (parent ion 319.22787/fragment ion 155.07) and 12-HETE (parent ion 319.22787/fragment ion 179.1). For MS/MS - 3 spectra/second, collision energy 16, iso. width – narrow (~1.3 m/z), delta retention time 0.2 min. To individually quantitate 10,17-DiHDHA+MaR1 and 11-HEDE+15-HEDE, two additional time segments were used 15.53-16.13 min with CID 15 for 10,17-DiHDHA (parent ion 359.22280/fragment ion 153.09) and MaR-1 (parent ion 359.22280/fragment ion 250.12) and 23.99-24.59 with CID 20 for 11-HEDE (parent ion 323.259173/fragment ion 199.13) and 15-HEDE (parent ion 323.259173/fragment ion 223.17), all other MS/MS settings are the same as the MS/MS segment in the basic method. Internal calibration was performed using Dual AJS system and an isocratic pump with a flowrate of 0.1 ml/min. Calibrant masses 119.03632 (purine), 980.01638 (HP-0921 acetate adduct) from Agilent mass reference solution were used. Data acquisition was controlled using MassHunter software version B.07.00 (Agilent).

2.3.8 Data analysis

Data analysis was performed using Agilent Masshunter software (TOF Qualitative Analysis B.07.00 and QTOF Quantitative Analysis B.07.00). Extraction window of $[M-H]^-$ was 10-30 ppm depending on the compound. All calibration curves were built using $1/x$ weighted linear regression.

2.3.9 Calibration curves

For the quantitation of oxylipins in plasma samples four types of calibration curves were used. (i) Solvent calibration curve. A mixture of 72 standards and ISTDs at 100 ng/ml in methanol was serially diluted with methanol to obtain the following standards: 100, 50, 25, 12.5, 6.25, 3.12, 1.56, 0.781, 0.391, 0.195, 0.098 ng/ml. 10 μ l of each sample were injected. (ii) SPE calibration curve. A mixture of 65 standards at 16, 8, 4, 2, 1, 0.5, 0.25, 0.125, 0.063, 0.031 ng/ml concentration were prepared in 20% methanol by serial dilution. Prior to SPE, each sample was spiked at 0.4 ng/ml with ISTDs. Volume of the standard loaded was 125 μ l (100 μ l 20% MeOH + 20 μ l of 65 analytes + 5 μ l ISTDs mix). Samples were subjected to SPE as described in Section 2.3.3 with 10 μ l of reconstituted sample injected. The peak area ratio, between analyte and selected ISTD, was used to build the calibration curve (iii) SPE standard addition curve for the measurement of low abundance oxylipins in plasma with 2.5x enrichment was prepared by performing SPE on three 100 μ l pooled plasma replicates spiked at 40 ng/ml of 15-HETE-d8 and 0.4 ng/ml concentration of the other six ISTDs and a series of 100 μ l plasma samples spiked with Mix 65 standards at increasing concentration from 0.031 to 16 ng/ml and with Mix of seven ISTDs at 0.4 ng/ml concentration. Final volume of the sample at loading was 125 μ l (100 μ l of pooled plasma + 20 μ l spike with Mix 65 + 5 μ l spike with ISTDs mix). All steps were the same as for SPE calibration curve. The endogenous levels of oxylipins, in the pooled plasma, were calculated using three blank pooled plasma samples and were subtracted from each calibration point. (iv) SPE standard addition calibration curve in plasma with 40x dilution for the measurement of high-abundance oxylipins. All steps were the same as for the curve described in (iii), but samples were spiked with Mix 18 standards that contains the 18 most abundant oxylipins in plasma (Supplementary Table S1) at 800, 400, 200, 100, 50, 25, 12.5 ng/ml concentration prepared in 20% methanol and with 15-HETE-d8 at 40 ng/ml concentration. Final volume at the loading step was 125 μ l (100 μ l of pooled plasma + 20 μ l spike with Mix 18 + 5 μ l spike with 15-HETE-d8). Samples were loaded on SPE as described in Section 2.3.3. After reconstitution and centrifugation 10 μ l of supernatant was diluted 100x with 100% MeOH and 10 μ l of diluted sample was injected. 15-HETE-d8 was used as internal standard

for building all calibration curves for high abundance oxylipins. The endogenous levels of oxylipins in pooled plasma were determined using three pooled plasma samples spiked with ISTD only and were subtracted from each calibration point. These samples were described in (iii) and were diluted 100x after reconstitution and prior to LC-MS analysis.

2.3.10 Method evaluation – recovery and matrix effects

For the fully optimized method, the recovery and matrix effect were assessed. To measure the recovery in solvent, 100 µl of 4 ng/ml Mix 72 standard (containing all analytes and internal standards) in 20% MeOH were loaded on SPE as described in Section 2.3.3 (n=3). The obtained peak areas from these pre-extraction spiked samples were measured against the peak areas obtained for post-extraction spiked samples. These were prepared by subjecting 20% methanol to SPE as described in Section 2.3.3 and reconstituting the samples after evaporation using 40 µl of 10 ng/ml Mix 72 standard in MeOH (n=3). This corresponds to the final expected oxylipin concentration in SPE samples at the time of injection. To measure the oxylipin recovery in plasma for low abundance oxylipins, the procedure was the same as for solvent recovery but Mix of 72 standards was spiked in pooled plasma at 4 ng/ml concentration, analysis was performed for 6 pre- and 6 post-spiked samples. To measure the recovery in plasma for high abundance oxylipins, the pooled plasma samples were spiked with Mix 25 that contains 18 most abundant oxylipins and 7 ISTDs at 40 ng/ml concentration and loaded on SPE as described in Section 2.3.3 (n=6). After reconstitution, 10 µl of each sample were diluted 100X with MeOH and 10 µl of diluted sample were injected. The obtained peak areas were measured against the peak areas in post-extraction spiked plasma, so final equation is $\text{Recovery} = (\text{Area in pre-extraction spiked} / \text{Area in post-extraction spiked}) * 100$. In all cases, the absolute matrix effect was assessed by measuring the peak areas in post-spiked samples, at an expected concentration of 10 ng/ml, against the peak areas of 10 ng/ml oxylipin standards in methanol as per the commonly employed Matuszewski *et al.*⁹² procedure.

2.4 Results and discussion

2.4.1 SPE method development

Sample preparation is a critical step in oxylipin analytical methods. Many oxylipins exist in very low concentrations (*e.g.* 0.1 ng/ml) in biological matrices. Thus, sample preparation should provide enrichment and decrease matrix complexity. Today C-18, or polymeric, reversed-phase

materials (e.g. HLB) SPE, are the most commonly used methods for sample preparation in oxylipin analysis.^{53,67,93,94} Both of these approaches show high recovery for particular groups of oxylipins, however these methods were rarely applied to all of the diverse classes and do not cover all oxylipins of interest. In the first step of method development in this work, a detailed comparison of HLB and C-18 SPE was performed. Supplementary Figure S1 shows the method efficiency results for oxylipin standard solutions. For most oxylipins, the method efficiency was higher than 60% ranging from 62 to 102 for C-18 SPE and 60 to 100 for HLB SPE and comparable for both SPE. Only RvD1, LXA₄, LTE₄ and LTD₄ showed low recoveries between 10-57% (Supplementary Figure S1). The eluents, after loading and washing steps, were analyzed and contained no detectable concentrations of oxylipins. This means that a possible source of loss in recovery was incomplete elution from the SPE cartridge. Next, the composition and volume of the elution solvent were optimized to maximize recovery (Supplementary Figures. S2-S3). Methanol was selected as elution solvent due to better elution of HETEs, LTEs, EETs and PUFA precursors. Elution with 1 ml of 99% MeOH + 1% HAc was determined as optimal for the standards of interest. Acidification of the elution solvent was required for leukotrienes, but if this subclass is not of interest elution with methanol provides quantitative recoveries for all other subclasses (78-130%). Despite comparable recovery, C-18 was chosen for further development because C-18 can decrease the complexity of the matrix by not retaining polar compounds, similar to the results obtained by Ostermann *et al.*⁵³ who investigated optimal sample preparation method for analysis of oxylipins in plasma and found that C-18 SPE outperforms other sample preparation methods.

Enrichment of the sample is an important component of the sample preparation procedure in oxylipin analysis. By comparing method recovery, with and without the inclusion of evaporation/reconstitution step, it was determined that the evaporation/reconstitution step is a critical step in contributing to oxylipin losses (up to 80%) during sample preparation. In the literature, evaporation of the SPE eluent is commonly performed in speedvac, or under a stream of nitrogen, or argon,⁹³ but the recovery losses of oxylipins during evaporation/reconstitution step were not reported. In order to further evaluate the extent of losses during this critical step, a comparison of speedvac versus nitrogen evaporation was performed. The results for this comparison showed 15-30% higher recovery by Speedvac evaporation in comparison with nitrogen evaporation and much better precision (Supplementary Figure S4). However, too few replicates were used in this experiment and additional experiment with at least 30 replicates is needed to

make final decision what evaporation is better. But at that time speedvac evaporation was chosen for the final sample preparation method, and then further optimized to decrease losses during this important step. For that, the optimal vessel for evaporation, the composition and volume of reconstitution solvent were determined. In addition, other ways to decrease the adsorptive losses such as the addition of glycerol in the evaporation tube, preliminary rinsing of evaporation tube with acid and the evaporation to 2 μ l, rather than to dryness were assessed. The results of these experiments are shown in Supplementary Figures S5-S7. As a result, the final optimized evaporation/reconstitution method includes using 1 ml glass tubes with the addition of 20 μ l of 30% glycerol in MeOH, evaporation in speedvac, and subsequent reconstitution in 40 μ l MeOH. The use of glycerol to minimize non-specific adsorption of oxylipins during evaporation/reconstitution step has also been successfully employed in other studies.^{53,95-97}

The final optimized method is summarized in Figure 2.1. The recovery and precision of the final method were evaluated for standard solutions as shown in Figure 2.2. The oxylipins were sorted according to their elution order on C-18 and in most cases this corresponds to ascending LogP values (Supplementary Table S3). As shown in Figure 2.2, more hydrophilic oxylipins (e.g. PGs) have a higher recovery than more hydrophobic (e.g. EETs) oxylipins. In general, the recovery of standard solutions was >50%: PGs (88-109%), DiHETEs (59-78%), HEPEs (72-90%), HETEs (74-93%), HDoHEs (63-81%) and EETs (57-64%). The most hydrophobic compounds: DHA and AA-d8 had recoveries around 40% and AA was not detected at this low concentration (0.4 ng/cartridge) but can be quantitatively recovered at higher concentrations (e.g. Supplementary Figure S1). Lower recoveries for the more hydrophobic oxylipins shown in Figure 2.2 are likely due to increased non-specific adsorptive losses at very low oxylipin concentrations. This is supported by Supplementary Figure S1 where all oxylipins, at higher concentrations of 3.125 ng/ml, could be recovered with acceptable performance (except leukotrienes) and with recovery data obtained in plasma (Figure 2.3)

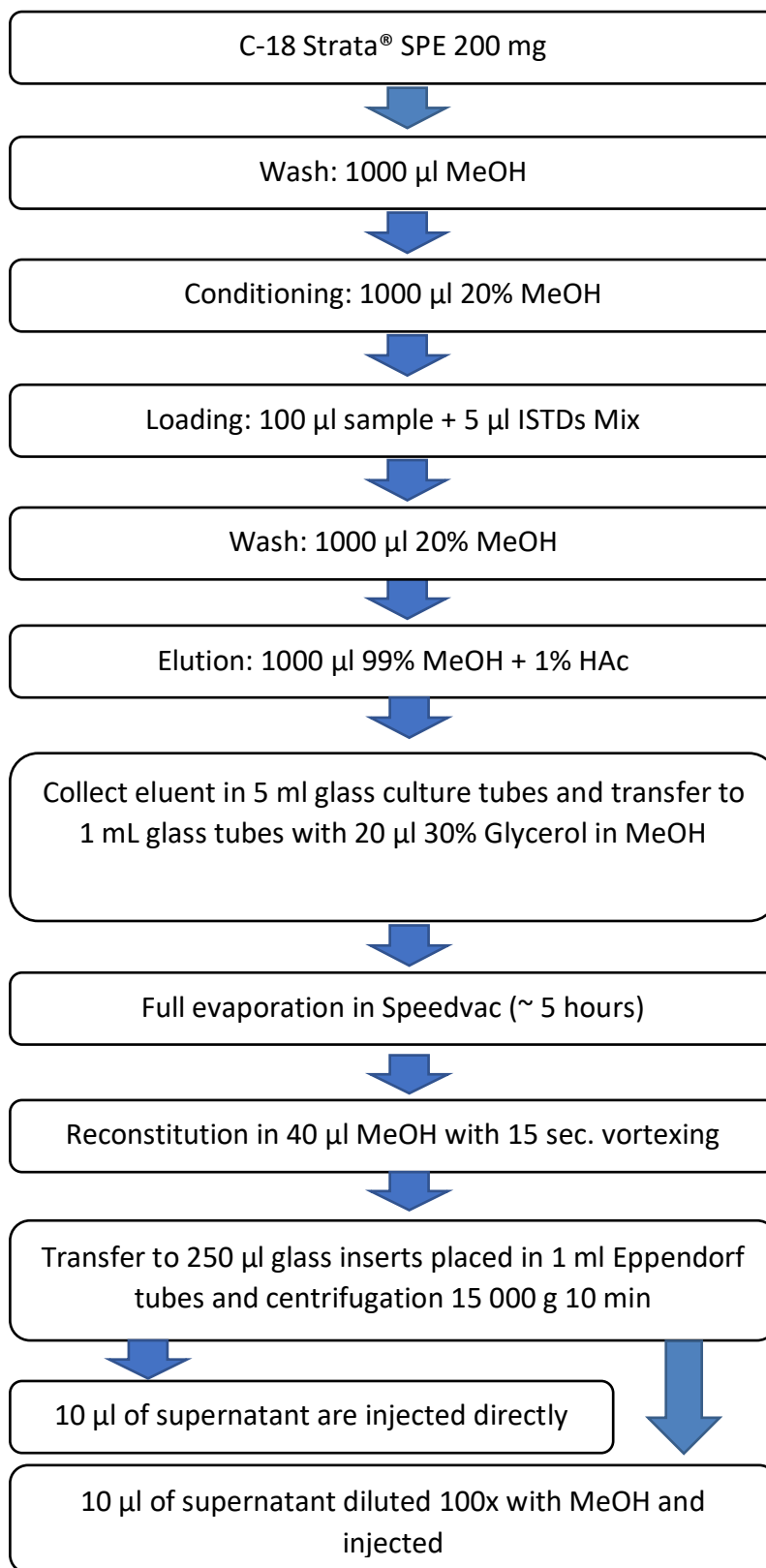


Figure 2.1 Final optimized SPE method workflow. For plasma samples ISTD mix contains six ISTDs at 10 ng/ml and 1000 ng/mL 15-HETE-d8 in MeOH

At a spiking mass of 0.4 ng/cartridge in simple solvent which is at the low/high end of the expected masses, the recoveries of LTE4, LTE4-d5, LTD4 were 0. Experiments with higher loading masses (concentrations) in solvent (Supplementary Figures S1-S3) as well as spiking plasma with 0.4 ng of these oxylipins (Figure 2.3 and 2.5a) showed higher recovery, ranging from 2 to 24% in solvent and 40-55% in plasma. These losses are attributed to non-specific adsorption throughout the procedure, and poor long-term stability of leukotrienes under acidic conditions at elevated temperatures such as those during speedvac evaporation. To reduce non-specific adsorption, “active sites” throughout the procedure can be first be filled with blocking molecules that decrease losses of targeted oxylipins (sequential loading). For instance, when LTE4-d4 was first loaded on a SPE cartridge to block such sites, the recovery of LTE4 increased to 70% even at the 0.4 ng loaded level. This strategy can be used for matrices where problems with oxylipin recovery, due to excessive non-specific adsorption, are observed. Similar challenges in the extraction of leukotrienes were reported by Astarita *et al.*⁹⁴ and the majority of papers that describe oxylipin methods do not report the recovery of LTE4 and LTD4. In terms of method precision, the average RSD in this experiment (n=3) was 7% confirming that the developed method has acceptable precision for the oxylipin extraction.

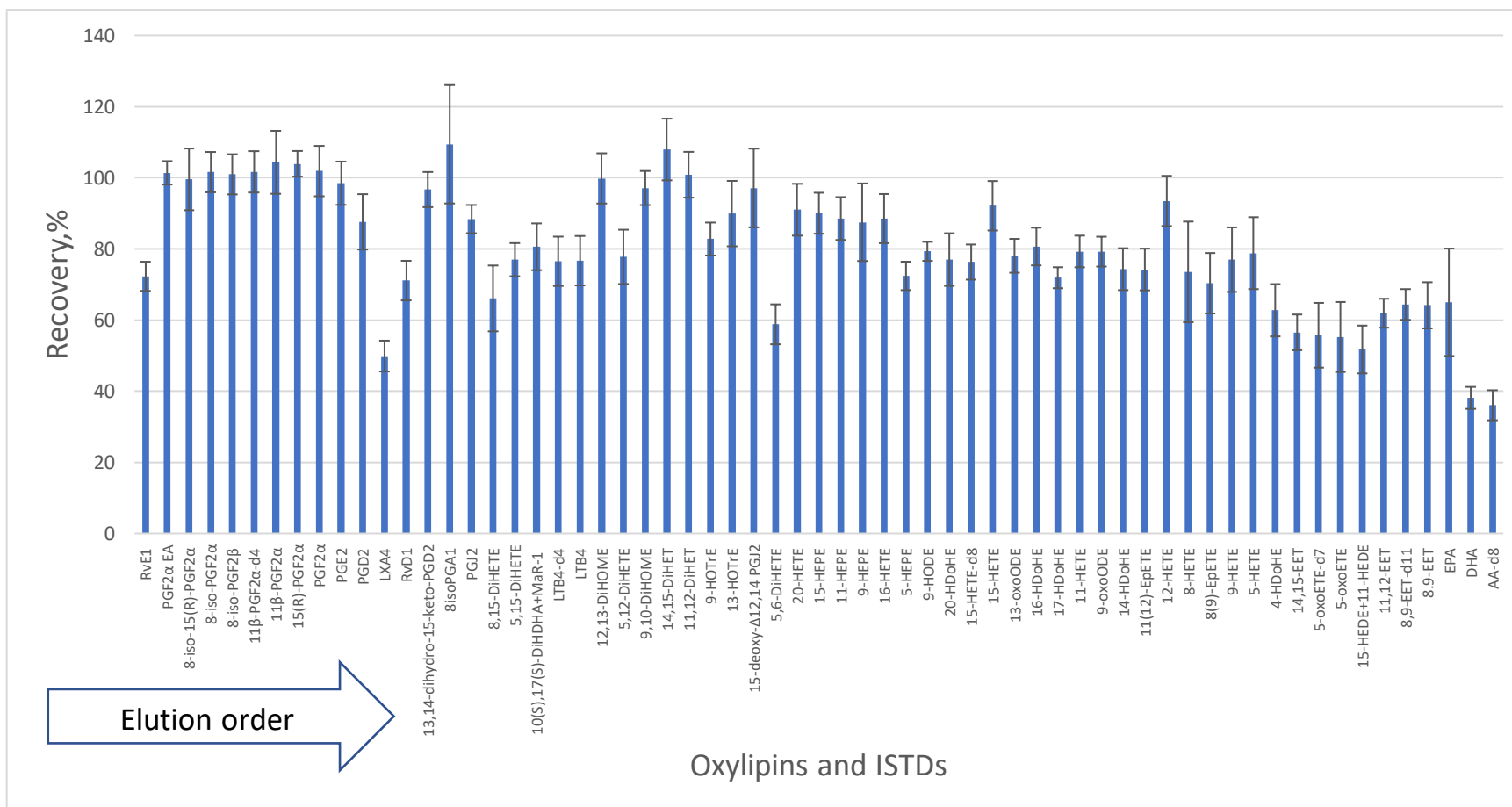


Figure 2.2 Extraction recovery of oxylipin standards using the optimized SPE method. Recovery % = $\frac{A_{pre}}{A_{post}} \times 100\%$, pre- and post-extraction spikes were performed at 4 ng/ml mix. The results show mean recovery (n=3), error bars show mean values (n=3) of SD for each oxylipin. This figure shows 65 oxylipins (including two unresolved pairs: 10(S),17(S)-DiHDHA+MaR1 and 11-HEDE + 15-HEDE) out of 72 that were used in this experiment, 7 oxylipins were excluded: LTE4, LTE4-d4, LTD4, AA were not detectable as discussed in Section 2.4.1; 12-oxoETE, 5-HpETE and 15-HpETE were excluded due to their instability as discussed in Section 2.4.4

2.4.2 Protein precipitation of plasma samples before SPE

The optimized SPE method was next applied for the analysis of oxylipins in pooled human plasma. Protein precipitation with TCA prior to SPE was initially selected instead of precipitation with MeOH or ACN.^{90,95,98} The use of an organic solvent for precipitation requires subsequent dilution of the sample after precipitation to decrease high organic solvent level to 20% to enable sample loading on SPE without losses of oxylipins. The use of TCA can avoid such step while providing efficient protein removal from plasma. A TCA to plasma ratio of 1:1 was used^{99,100} followed by pH adjustment to 3 with NH₄OH prior to SPE loading. When 100 µl pooled plasma samples were spiked to 5 ng/ml ISTDs (Table 2.1) before precipitation, several endogenous oxylipins were detected, however none of the ISTDs were detectable indicating possible losses during the precipitation step. In follow-up experiments, the concentration of spiked ISTDs was 5, 10 and 20 ng/ml. In the 20 ng/ml samples, no ISTDs, except for the most hydrophilic 11βPGF2α-d4 were detected (recovery of 15%, data not shown). These experiments showed that severe losses of oxylipins occur during the precipitation step. To further confirm this finding, the extraction was repeated without preliminary precipitation by loading spiked pooled plasma samples directly on equilibrated SPE cartridges as reported in other studies^{65,101}. In this experiment, the detected concentrations of oxylipins were much higher than in the preliminary experiment with TCA precipitation. The concentration range of detected oxylipins was very wide from 0.26 to 821 ng/ml (Table 2.1). The direct loading of plasma for SPE was then further compared to IPA protein precipitation of plasma and showed comparable oxylipin levels. Altogether, these results show that tremendous losses of oxylipins were specific to TCA precipitation and that organic solvent precipitation, or direct loading, for SPE are preferred for oxylipin analysis.

The direct loading of plasma samples on the SPE cartridge (without preliminary protein precipitation) caused the appearance of precipitate after the reconstitution of evaporated sample. For that reason, an additional centrifugation step was added after reconstitution. This centrifugation step should be performed in a 250 µl glass insert placed in 1.5 mL Eppendorf tube at 15 000 x g for 10 min. It is necessary to use a glass insert, instead of an Eppendorf tube, because plastic tubes can cause losses of oxylipins (Supplementary Figure S5).

Table 2.1 Comparison of TCA protein precipitation versus direct loading on oxylipin recovery in human plasma. The results show the mean in ng/ml \pm SD (n=3). The HMDB column shows the range of oxylipin concentrations, in ng/ml, reported in the Human Metabolome Data Base (HMDB)¹⁰² (accessed November 2018). ND-compound was not detected. NR-concentrations were not reported. For both TCA protein precipitation and direct loading of plasma for SPE a solvent calibration curve was used for quantitation.

Oxylipin	TCA protein precipitation followed by SPE (ng/mL)	Direct loading of plasma on SPE (ng/mL)	HMDB [104]
8-iso-15(R)-PGF2 α	0.06 \pm 0.006	0.26 \pm 0.01	NR
15-HETE	0.6 \pm 0.2	376 \pm 34	0.26-358
9-HETE	0.64 \pm 0.29	408 \pm 35	0.05 \pm 0.55
5-HETE	0.76 \pm 0.46	681 \pm 54	0.29-1123
14,15-EET	ND	2.71 \pm 0.14	0.04-0.56
5-oxoETE	ND	24 \pm 2	0.04-0.05
EPA	1.41 \pm 0.88	248 \pm 27	0.12-635250
DHA	0.95 \pm 0.89	821 \pm 111	1.1-160965

The observed dynamic range of oxylipins in plasma is very high, roughly 3 orders of magnitude, as shown in Table 2.1, and the very high concentrations of some oxylipins in plasma caused detector saturation. To address this issue, it was necessary to use two injections of the reconstituted and centrifuged plasma. The first injection is a direct injection of the reconstituted sample, corresponding to 2.5x pre-concentration from the initial plasma and is used to detect and quantitate the low abundance oxylipins. For the second injection, the reconstituted sample is diluted 100x with MeOH, i.e. 40x dilution compared to the initial plasma and is used to quantitate the more abundant oxylipins. However, even with this dilution arachidonic acid is still too concentrated for accurate quantitation. The use of two injections with different dilution/enrichment factors also allows the method to provide accurate results for oxylipins whose concentrations can vary widely across individuals (Table 2.2), so the appropriate low or high abundance calibration curve can be used, as needed, for quantitation of each analyte in each individual.

2.4.3 Evaluation of recovery and matrix effect of the developed SPE method in plasma

The developed method was evaluated for matrix effect and recovery in human plasma as described in Section 2.3.10 The assessment was performed only for oxylipins from Table 2.3 that can be measured accurately, and all internal standards. The recoveries of oxylipins in plasma were higher than in solvent with an average of 83% (range from 70 to 97%), Figure 2.3. The higher

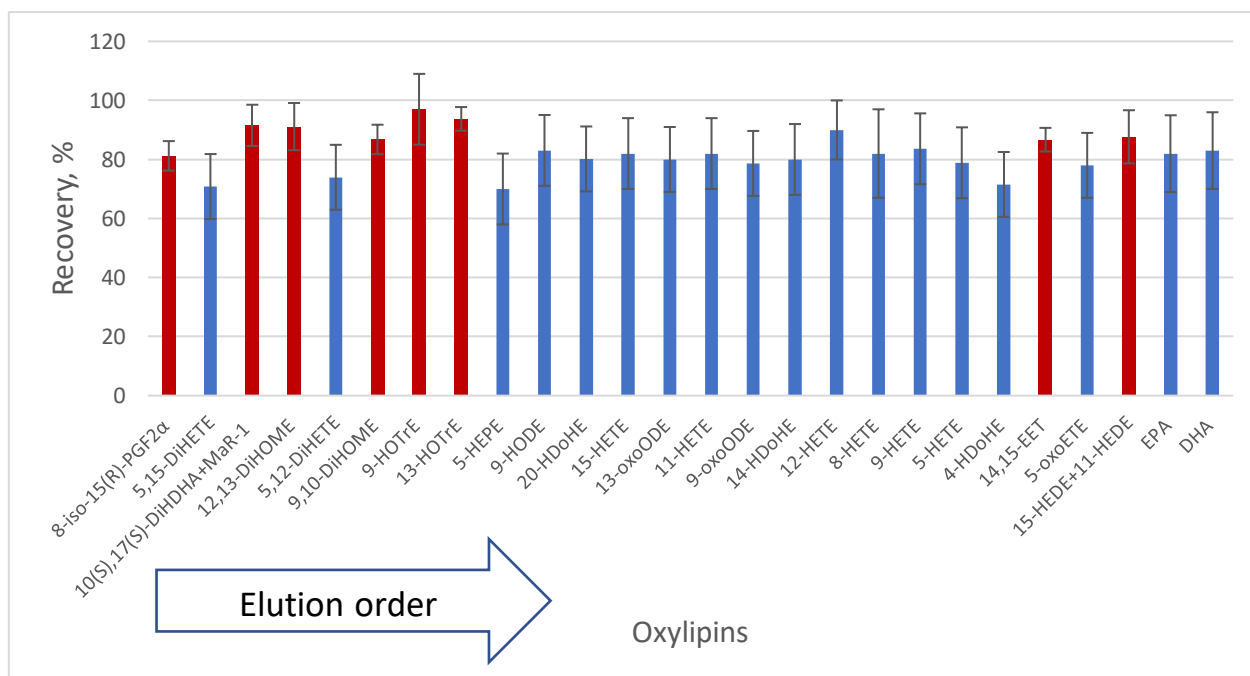
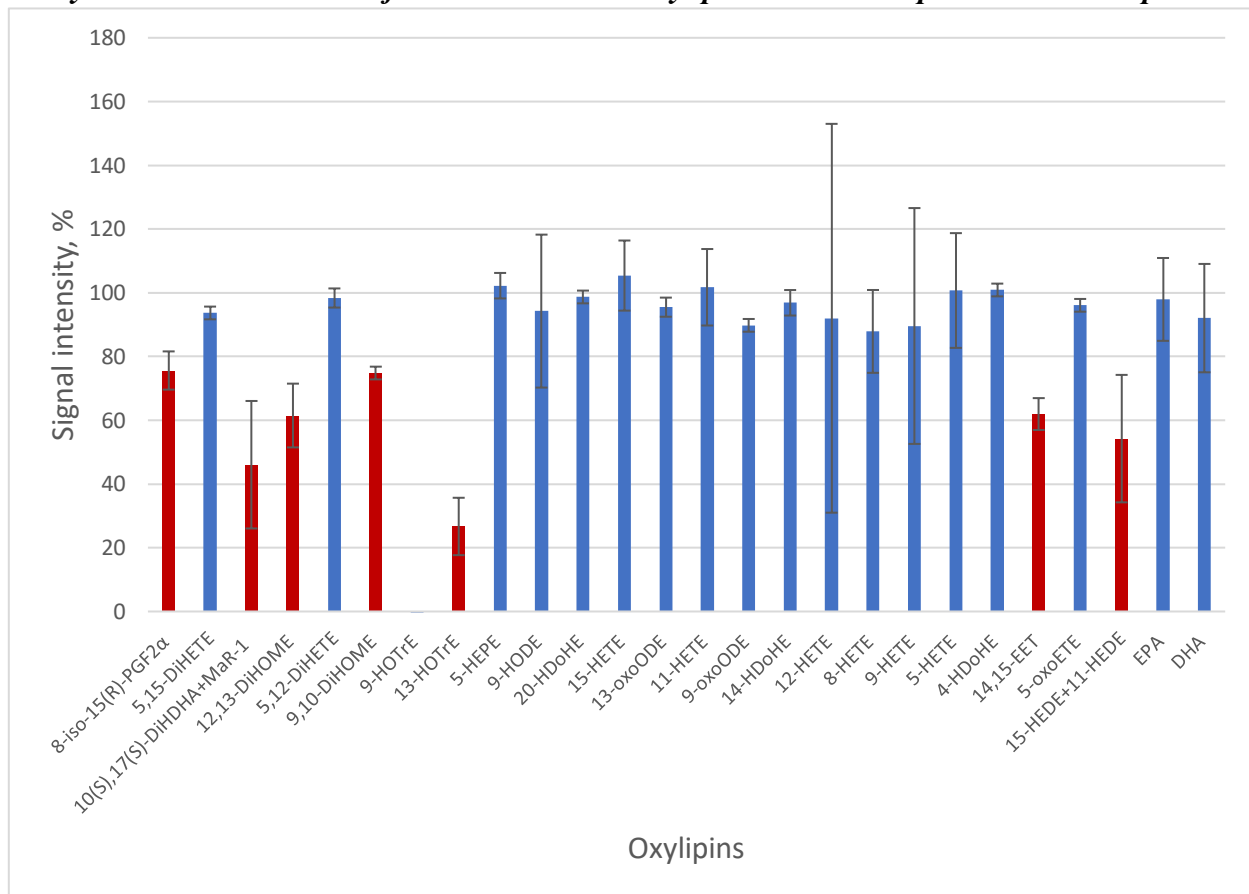


Figure 2.3 Evaluation of extraction recovery of oxylipins from human plasma. $Recovery\% = A_{pre}/A_{post} * 100\%$, where red colour is used for less abundant oxylipins, there pre- and post-extraction spikes were performed at 4 ng/ml mix of standards accounting for 2.5x enrichment. For more abundant oxylipins (highlighted in blue) pre- and post-extraction spikes were performed at 40 ng/ml mix of 18 most abundant standards and ISTDs accounting for 40x dilution. The results show mean values ($n=6$), error bars show mean values of SD for each standard.

recovery, from a complicated biological sample such as plasma, compared to the very simple standard solutions can be explained by the fact that, in addition to the analytes, there are also many hydrophobic compounds in plasma that can interact with the high activity binding sites of the cartridge that would otherwise irreversibly bind oxylipins leading to their loss. The recovery of internal standards showed the same trend (range: 36-88%) and among them LTE4-d5 showed: 0% in solvent at 0.4 ng/ml, 36% in plasma at 0.4 ng/ml and 55% at 4 ng/ml (Figure 2.5a). The recovery evaluation was performed using 6 replicates, RSD for all standards was $\leq \pm 15\%$ showing excellent method precision. In the majority of recent studies only method efficiency for SPE that incorporates both recovery and matrix effect was reported and ranged from 15 to 95% (approximately, because only bar graphs reflecting recoveries were demonstrated) for 22 oxylipins in plasma,²⁷ from 6.7% to 73.4% for 17 oxylipin ISTDs⁹⁰ and from 54.3 to 112.7% for 26 oxylipin ISTDs⁹¹. These values can be compared with the method efficiency of our method calculated using ISTDs (Supplementary Figure S15) that ranged from 42 to 76%. Recoveries of our method, Figure 2.3 and Figure 2.5a are comparable to those calculated by Rago *et al.*⁹⁵ and Strassburg *et al.*³. Rago *et al.* showed recoveries

for 18 oxylipins ranging from 55.6 to 97.4%. Strassburg *et al.* showed recoveries for 11 oxylipin ISTDs ranging from 45 to 84%. Both methods used HLB SPE for extraction which is expected to affect the recovery.

Figure 2.4 Comparison of matrix effect in plasma. Signal intensity $\% = A_{post}/A_{solvent} * 100\%$. Analytes in red colour are for less abundant oxylipins where the post-extraction spike was



performed at 10 ng/ml mix of standards and measured against 10ng/ml mix of standards in solvent. For the more abundant oxylipins (in blue) the post-extraction spike was performed at 10 ng/ml mix of the 18 most abundant standards and ISTDs accounting for 40x dilution standards and measured against 10 ng/ml mix of standards in solvent. The results show mean values (n=6), error bars show mean values of SD for each standard.

Matrix effect was not observed for oxylipins in the 40x diluted plasma samples because this dilution decreases the amount of competing compounds sufficiently to minimize it (Figure 2.4). For the less abundant oxylipins that were measured in 2.5x pre-concentrated samples, absolute matrix effect was more noticeable and generally decreased the signal intensity by 2x. The most severe matrix effect was observed for 9- and 13-HOTrEs, that eluted close to each other, and suffered complete suppression or signal intensity drops to 27%. A possible reason for this severe

suppression is the co-elution of an interference with m/z 277.145 and showed 1×10^7 signal intensity. For the internal standards, in diluted samples, the matrix effect was not observed any of them. In the preconcentrated samples, the matrix effect was more noticeable and signal intensity was 60-80% depending on compound. According to the matrix effect results, at least 9-HOTrE has to be excluded from the quantitative analysis list due to such pronounced matrix effects. Adding labelled HOTrE as an internal standard would likely improve method performance for this/these compound(s). The LLOQ was 0.1 ng/ml for the majority of oxylipins tested in solvent and in plasma.

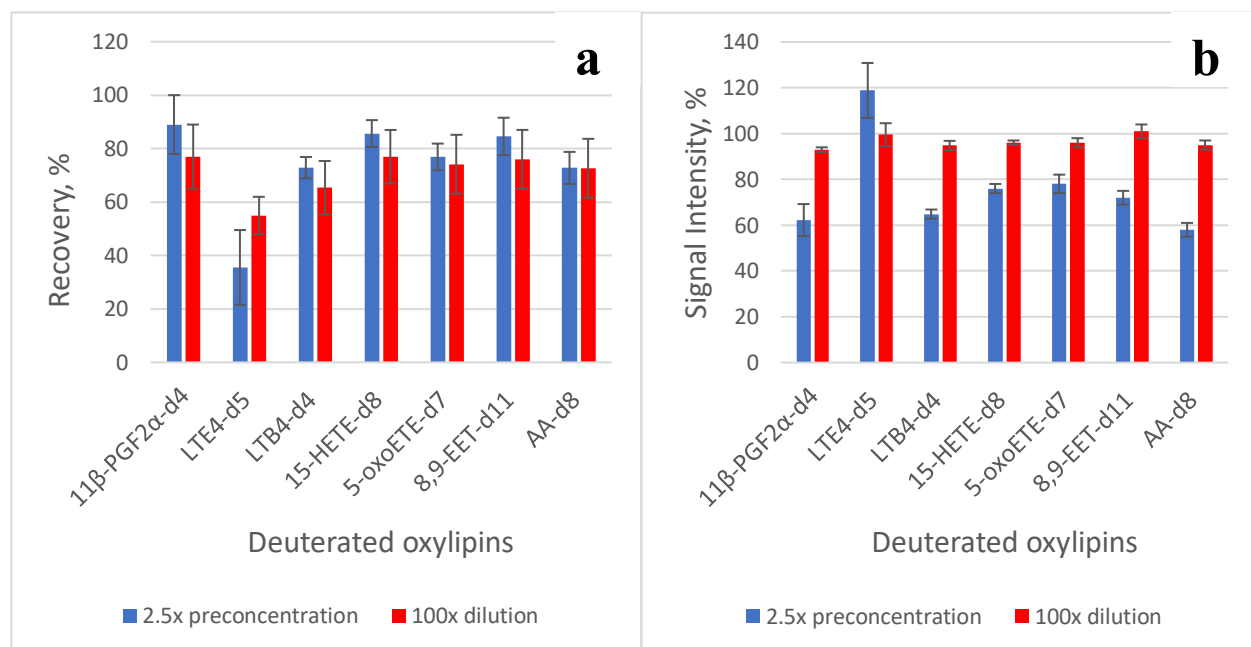


Figure 2.5 Comparison of (a) recovery and (b) matrix effect of deuterated oxylipins in plasma. (a) Recovery% = $A_{pre}/A_{post} \times 100\%$, where red colour is used for 2.5x enrichment, there pre- and post-extraction spikes were performed at 4 ng/ml mix of standards accounting for 2.5x enrichment. For 40x dilution (highlighted in blue) pre- and post-extraction spikes were performed at 40 ng/ml mix of 18 most abundant standards and ISTDs accounting for 40x dilution. (b) Signal intensity % = $A_{post}/A_{solvent} \times 100\%$, where red colour is used for 2.5x enrichment, there post-extraction spike was performed at 10 ng/ml mix of standards and measured against 10ng/ml mix of standards in solvent. For 40x dilution (highlighted in blue) post-extraction spike was performed at 10 ng/ml mix of 18 most abundant standards and ISTDs accounting for 40x dilution standards and measured against 10ng/ml mix of standards in solvent. The results show mean values ($n=6$), error bars show mean values of SD for each standard.

2.4.4 LC-MS method development

The effect of three mobile phase additives: HAc, FA and AmAc on ionization efficiency of oxylipins was evaluated (Supplementary Figures S11-S12).¹⁰³ Similar to what was observed for

other lipid classes in negative ESI, 0.02% HAc provided the maximum sensitivity, with an average improvement of 8x versus AmAc and minor improvement 1.25x versus FA. This agrees with the study by Berkecz *et al.*⁸⁶ who also evaluated mobile phase additives for oxylipin analysis and determined that 0.02% HAc was the optimal choice.

For oxylipin separations, reversed-phase C-18 chromatography is the most widely used. UHPLC C-18 columns, with sub-2 μm particles, are increasingly in popularity as they provide higher efficiency and better resolution.^{67,93,94} However, the smaller particle size requires higher operating pressure. Core-shell columns that provide comparable efficiency with fully porous UHPLC columns can also be used to enhance the separation without the need for dedicated UHPLC equipment.⁶⁷ During method development, four LC columns were evaluated: Zorbax Eclipse plus C-18, 1.8 μm (2.1 mm x 100 mm) RRHD UHPLC column; Kinetex core-shell C-18, 2.6 μm (2.1 mm x 50 mm) HPLC column; Cortex T3, 1.6 μm (2.1 mm x 100mm) UHPLC column and Kinetex Pentofluorophenyl (PFP) 2.6 μm (2.1mm x 50mm) HPLC column to determine the column that gives maximum chromatographic separation of oxylipins. The Zorbax C-18 was determined to provide the best separation for this application. Core-shell Kinetex C-18 showed comparable performance for many standards versus Zorbax C-18, but for critical pairs of isomeric oxylipins (e.g. 8isoPGF_{2 α} /8isoPGF_{2 β}) Zorbax C18 showed better separation than Kinetex due to narrower chromatographic peaks (Supplementary Figure S8). T3 columns are C-18 columns optimized for separation of polar compounds since they are compatible with 100% aqueous mobile phases. T3 columns were previously used for oxylipin analysis, however, for more hydrophilic PGs only.²⁷ The UHPLC Zorbax C18 and core-shell Cortex T3 columns showed comparable separation for the majority of standards. For more hydrophilic oxylipins, T3 showed better separation than the Zorbax column, possibly because of the smaller particle diameter of the T3 column giving narrower chromatographic peaks and optimization of T3 for more polar compounds. However, for more hydrophobic compounds T3 showed poorer separation and for some isomeric oxylipins (e.g. 11,12-EpETE and 8,9-EpETE) (Supplementary Figure S9). To the best of our knowledge PFP columns were not evaluated previously for oxylipin analysis. PFP columns have highly negatively charged fluorine atoms and much less hydrophobic interactions, so retention of hydrophobic oxylipins on these columns is not efficient that was showed by our experiment, when isomeric peaks eluted together with minimal separation (Supplementary Figure S10).

The LC gradient (2% per min, 20-80% organic) used in this work was optimized to obtain chromatographic separation of as many of the isomeric oxylipins listed in Supplementary Table 1 as possible using a 40-min analysis time. This method is longer than many contemporary LC-MS methods for oxylipins that have average analyses times of 25 min and focus on a wide range of oxylipins.⁸⁵ However, all these methods use a SRM mode for oxylipin quantification, so that chromatographic separation is deemed not important for oxylipins provided that they have different fragmentation patterns. However, considering the large number of oxylipin isomers with a given formula, it is likely that it may not be possible to select SRM transitions that have no overlap with other possible interferences, resulting in misidentification and inaccurate quantitation. In our case, where full-scan mode HRMS detection is used, it is important to resolve all isomeric compounds. Although our chromatographic method provides baseline resolution for the majority of standards of interest, 3 pairs of standards co-eluted and required MS/MS fragmentation for their individual quantification (see Section 2.3.7). Also, three pairs: 15-HEPE/11-HEPE, 16-HDoHE/17-HDoHE, 11,12-EpETE/8,9-EpETE elute with a separation of less than 0.2 mins and consequently they may not be resolved enough for individual quantitation but need to be reported together (Figure 2.6).

Figure 2.6 shows the comparison of chromatographic separation obtained for oxylipin standards in solvent versus pooled human plasma sample. It clearly shows that additional isomeric interferences are observed in the biological matrix which precludes correct quantification of some oxylipins in plasma due to partial co-elution of the analyte of interest and the isobaric interference. (Figure 2.6 m/z 353, 351, 313, 337). We further examined if changing the LC gradient could help to solve this problem. Shallower (1% and 0.5% per min) gradients were assessed, however they could not help to separate the analytes from the unknown interferences (data not shown). The use of these shallower gradients with Zorbax column as well as application of these gradients on Cortex T3 column (that has slightly different selectivity) allowed us to further evaluate the correctness of the identifications for oxylipins observed in human plasma samples tested in this work. As summarized in Supplementary Table S1, this approach showed several misidentifications which were discovered by the retention time of standard and unknown oxylipin no longer matching on the long chromatographic method e.g. PGE2 and PGD2. These standards were excluded from list of oxylipins that can be detected in plasma using current method. Table 2.3 lists 25 oxylipins that can be accurately quantified in human plasma without interferences and that were detected at

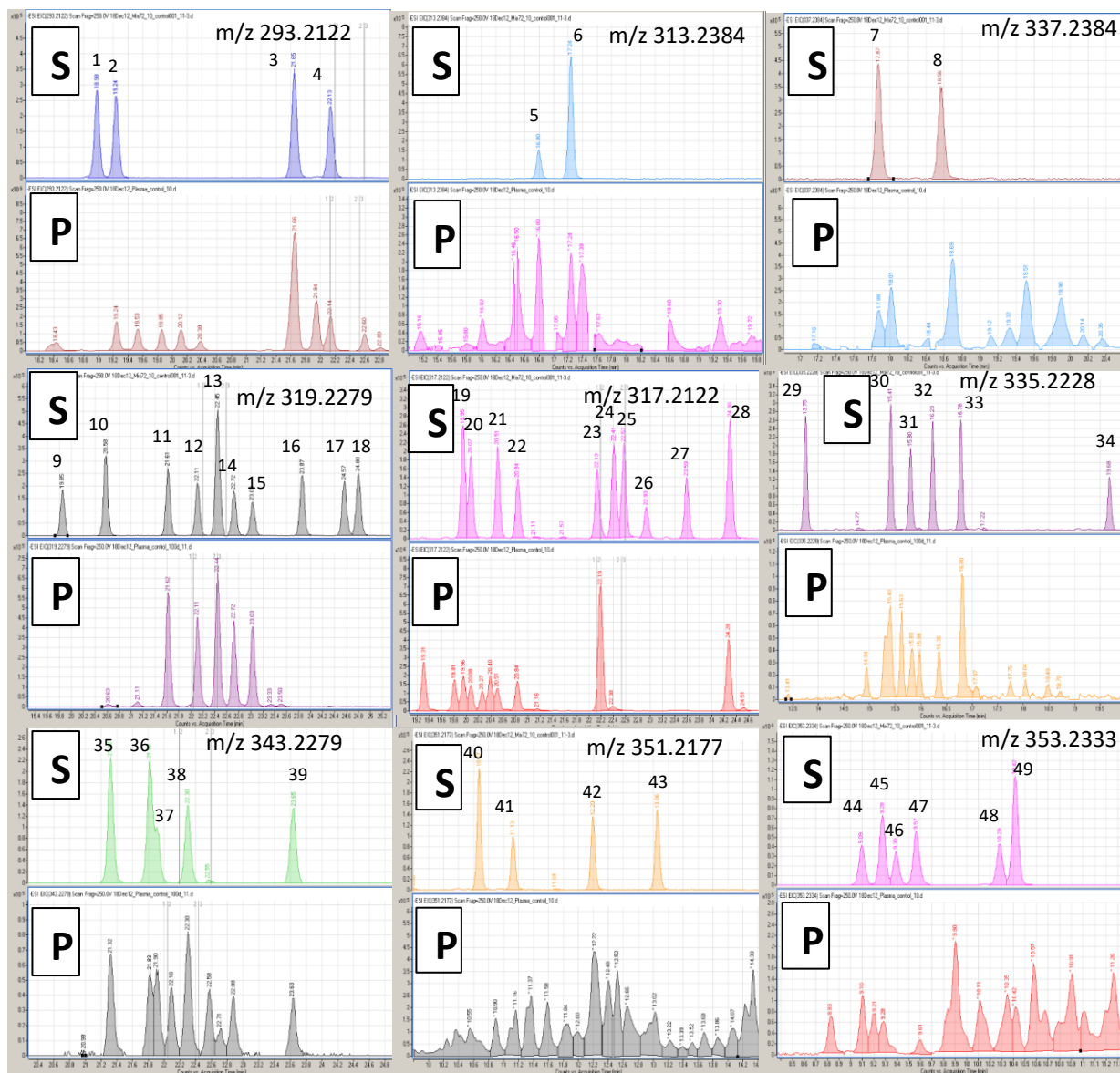


Figure 2.6 Chromatographic separation of oxylipin isomers. *S* – EIC of standards in solvent, *P* – EIC of endogenous oxylipins in human plasma. *m/z* window ± 10 ppm. 1)- 9-HOTrE, 2)- 13-HOTrE, 3)- 13-OxoODE, 4)- 9-OxoODE, 5)- 12,13-DiHOME, 6) 9,10-DiHOME, 7)- 14,15-DiHET, 8) 11,12-DiHET, 9)-20-HETE, 10)-16-HETE, 11)-15-HETE, 12)-11-HETE, 13)-12-HETE+8-HETE, 14)-9-HETE, 15)-5-HETE, 16)- 14,15-EET, 17)- 11,12-EET, 18)- 8,9-EET, 19)-15-HEPE, 20)-11-HEPE, 21)-9-HEPE, 22)-5-HEPE, 23)-15-HpETE, 24)-11,12-EpETE, 25)-8,9-EpETE, 26)-12-oxoETE, 27)-5-HpETE, 28)-5-oxoETE, 29)- 8-iso-PGA1, 30)-8,15-DiHETE, 31)-5,15-DiHETE, 32)-LTB4, 33)-5,12-DiHETE, 34)-5,6-DiHETE, 35)- 20-HDoHE, 36) 16-HDoHE, 37)-17-HDoHE, 38)-14-HDoHE, 39) 4-HDoHE, 40)-PGE2, 41)-PGD2, 42)-LXA4, 43)-13,14-dihydro-15-keto-PGD2, 44)-8-iso-15(R)-PGF2 α , 45)-8-iso-PGF2 α , 46)-8-iso-PGF2 β , 47)-11 β -PGF2 α , 48)-15(R)-PGF2 α , 49)-PGF2 α

endogenous levels in current study. Other group of 38 oxylipins that incorporates 25 oxylipins from Table 2.3 is oxylipins that were accurately detected using our method, and are highlighted in green

in Supplementary Table S1. Twenty-five of them were detected and quantitated and 13 of them were detected only and were not quantitated due to the reasons mentioned in Supplementary Table S1. The third small group of five oxylipins determined as ND-P in Supplementary Table S1 includes oxylipins that can be detected in plasma using our method if present above LOQ in a given plasma sample. In conclusion, based on these results we strongly recommend that existing oxylipin methods, especially very short methods, should be carefully evaluated for the possibility of interferences in biological matrices using orthogonal and/or very long chromatographic separations. As our results for PGE2 and PGD2 show the reliance on the match with the retention time of authentic standard is not sufficient, and this may be especially problematic for fast multi-class oxylipin separations. Isomeric and isobaric interferences still pose a significant issue in oxylipin analysis and may be an under-appreciated source of error.

Also, according to the stability experiments that were performed (Supplementary Figure S14) unstable 15-HpETE, 5-HpETE and 12-oxoETE were excluded from this list as well as AA that with even 40x dilution is in the high concentration in plasma.

2.4.5 Individual plasma samples: inter-individual variability and comparison to HMDB and other studies

As was seen in Table 2.2, the pooled plasma sample analyzed using direct loading of plasma on SPE showed unexpectedly high concentrations of several oxylipins, specifically 9-HETE, 5-oxoETE and 14,15-EET. The concentrations for these oxylipins were 5-740x higher than the highest concentrations of that analyte reported in HMDB database. The concentrations in Table 2.1 which represented preliminary development work were quantitated using the solvent calibration curve, so this may represent an important source of error in calculation of correct concentrations. To further investigate this and examine inter-individual variability of oxylipin concentrations, we next analyzed six individual plasma samples (three male and three female). The results showed noticeable variability of the levels of oxylipins between samples regardless gender, and much higher variability than method precision which was below 15% as indicated by replicate analyses of pooled sample (Table 2.2). For example, 5,15-DiHETE level ranged from 0.38-0.44 ng/ml in Samples 3 and 4 was to 156 ng/ml in sample 5, almost three orders of magnitude. Interestingly, the average of these six randomly selected individual samples, was close to the concentration of the pooled plasma obtained from 30 individuals not related to individual plasma samples. One trend that can be noted in Table 2.2 is that a high correlation between oxylipin samples is observed. If in

a sample high levels of one oxylipin were observed, high levels for all oxylipins were also observed.

Table 2.2 Individual variability of oxylipin concentrations in human plasma. For individual plasma samples F-Female, M-Male, (n=1), concentration in ng/ml, individual plasma samples were not diluted so some oxylipins showed saturated peaks-S. Results for pooled plasma (n=30) show mean concentrations (n=3) in ng/ml \pm SD. “-“– oxylipin was not used in experiment. For individual plasma samples solvent curves were used for quantitation, for pooled plasma sample SPE solvent curve was used for quantitation.

	Plasma-1 F	Plasma-2 M	Plasma-3 F	Plasma-4 M	Plasma-5 F	Plasma-6 M	Average of individual samples	Pooled plasma (n=30 individuals)	HMDB Concentration range ¹⁰²
8-iso-15(R)-PGF2 α	ND	0.34	ND	ND	0.31	0.12	0.16 \pm 0.16	0.26 \pm 0.01	-
5,15-DiHETE	1.02	95.6	0.38	0.44	156	41.3	49.1 \pm 64.4	48.6 \pm 5.98	0.02-0.18
10(S),17(S)-DiHDHA +MaR1	ND	100	ND	0.09	154	26.9	70.25 \pm 70	11.3 \pm 0.63	-
12,13-DiHOME	1.38	12.18	1.36	1.10	2.76	5.01	3.96 \pm 4.28	1.27 \pm 0.09	1.57-5.22
5,12-DiHETE	1.41	130	0.39	ND	184	87.3	80.57 \pm 80.34	84.8 \pm 9.23	-
9,10-DiHOME	0.92	7.50	1.28	0.67	2.12	3.13	2.6 \pm 2.56	0.48 \pm 0.03	9.34-19.03
13-HOTrE	0.42	11.8	0.22	0.13	30.9	16.2	9.94 \pm 12.35	7.61 \pm 0.31	0.15-0.56
5-HEPE	5.74	45.1	1.43	0.28	45.4	28.6	21.1 \pm 21.3	26.7 \pm 1.9	0.07-0.37
9-HODE	-	-	-	-	-	-	-	49.1 \pm 6.17	1.93-3.47
20-HDoHE	-	-	-	-	-	-	-	56.3 \pm 3.68	0.08
15-HETE	6.29	S	3.19	0.95	S	S	S	376 \pm 34	0.26-358
13-oxoODE	-	-	-	-	-	-	-	71.7 \pm 4.4	0.14-1.41
11-HETE	4.72	S	2.56	0.30	S	S	S	355 \pm 27.4	0.13-0.33
9-oxoODE	0.64	16.3	0.67	0.32	60.2	21.8	16.7 \pm 23.2	21 \pm 3.64	0.71-1.56
14-HDoHE	3.11	S	2.52	0.21	S	S	S	89.5 \pm 9.4	0.57
12-HETE	7.96	S	9.74	0.50	S	S	S	197 \pm 25.2	1.3-112
8-HETE	2.88	S	1.23	0.17	S	S	S	172 \pm 49	0.16-0.67
9-HETE	3.70	S	1.79	0.29	S	S	S	408 \pm 35	0.05-0.55
5-HETE	87.7	S	27.6	2.04	S	S	S	681 \pm 54	0.29-1123
4-HDoHE	-	-	-	-	-	-	-	57.8 \pm 2.29	0.45
14,15-EET	0.43	9.35	0.42	0.26	9.39	3.99	3.98 \pm 4.41	2.71 \pm 0.14	0.04-0.56
5-oxoETE	2.18	86.9	0.38	0.04	163	54.8	51.3 \pm 65.4	24 \pm 2	0.04-0.05
11-HEDE + 15-HEDE	0.33	103	0.19	0.07	85.7	89.5	46.5 \pm 51	14.05 \pm 0.85	-
EPA	S	S	136	130	S	S	S	248 \pm 27	0.12-635250
DHA	S	S	S	S	S	S	S	821 \pm 111	1.1-160965

Willenberg *et al.*⁸⁵ discussed oxylipin variability in their review article and suggested this may be caused by pharmacological and/or nutritional intervention, however the exact mechanism is not clear. Individual variability of oxylipin concentrations were previously reported by Yasumoto *et al.*⁹⁰, however the observed inter-individual variability was much lower than in our experiment. For example, reported 5-HETE concentrations ranged from 69-231 pg/ml while in our experiment it was from 2 ng/ml to saturation peak level which means that the concentration exceeded 400 ng/ml in some samples. The accurately calculated mean concentration of 5-HETE in pooled plasma was 681 ng/ml, which is significantly higher than the pg/ml level reported by Yasumoto *et al.* For 5-HETE, HMDB reports a wide range that is consistent with our results (0.29-1123 ng/mL). Analysis of recent publication showed that in all cases levels of oxylipins in human plasma taken from healthy persons without any preliminary treatment are in 0.1-10 ng/ml range.^{82,89,104} Even with direct loading of plasma on HLB SPE as was performed Gouveia-Figueira *et al.*⁶⁵ experiment, concentration range of oxylipins was 0.1-10 ng/ml. On the other hand, Galvao *et al.*⁹⁸ showed high concentrations for oxylipins such as 12-HETE and 5-HETE in 100-1000 ng/ml range consistent with our results. However these concentrations were obtained from patients receiving drug treatment, whereas for baseline cohort 0.1-10 ng/ml concentrations were observed.

Looking at the HMDB¹⁰² and oxylipins beyond 5-HETE, some oxylipin levels detected in our study correspond to the levels reported in the HMDB e.g. level of 15-HETE with high calculated concentration 376 ± 34 ng/ml corresponds to 0.26-358 ng/ml in (HMDB) (Table 2.2). However not all calculated concentrations correspond to the levels reported in the HMDB. For example, calculated concentration of 9-HETE was 408 ± 35 ng/ml and in HMDB level was 0.05-0.55 ng/ml only. Considering, that this high level for 9-HETE was not reported before, it is necessary to have additional evidence confirming 9-HETE identification and accurate measurement. Thus, an additional experiment was performed for all abundant oxylipins that were quantitated where the pooled plasma was spiked with high levels of particular standard. This standard addition experiment confirms that doubled peak area in comparison to initial peak area (Supplementary Figure S13) and accuracy of our initial quantitation. For additional evidence, these standard addition samples were also subjected to 1 and 0.5 % per min shallower gradient to provide additional chromatographic resolution in case of possible interference peaks. No interferences or differences in peak areas were detected in these experiments further confirming the accuracy of our measurement (data not shown).

Table 2.3 Oxylipins that can be detected and quantitated accurately in plasma.

Oxylipin	m/z	RT	Formula	Precursor
8-iso-15(R)-PGF2 α	353.2334	9.06	C ₂₀ H ₃₄ O ₅	AA
5,15-DiHETE	335.2228	15.72	C ₂₀ H ₃₂ O ₄	
5,12-DiHETE	335.2228	16.71	C ₂₀ H ₃₂ O ₄	
15-HETE	319.2279	21.58	C ₂₀ H ₃₂ O ₃	
11-HETE	319.2279	22.03	C ₂₀ H ₃₂ O ₃	
12-HETE	319.2279	22.41	C ₂₀ H ₃₂ O ₃	
8-HETE	319.2279	22.41	C ₂₀ H ₃₂ O ₃	
9-HETE	319.2279	22.68	C ₂₀ H ₃₂ O ₃	
5-HETE	319.2279	22.99	C ₂₀ H ₃₂ O ₃	
14,15-EET	319.2279	23.84	C ₂₀ H ₃₂ O ₃	
5-oxoETE	317.2122	24.27	C ₂₀ H ₃₀ O ₃	
10(S),17(S)- DiHDHA +MaR1	359.2228	15.93	C ₂₂ H ₃₂ O ₄	
20-HDoHE	343.2279	21.21	C ₂₂ H ₃₂ O ₃	
14-HDoHE	343.2279	22.21	C ₂₂ H ₃₂ O ₃	
4-HDoHE	343.2279	23.49	C ₂₂ H ₃₂ O ₃	
DHA	327.2330	29.01	C ₂₂ H ₃₂ O ₂	EPA
5-HEPE	317.2122	20.77	C ₂₀ H ₃₀ O ₃	
EPA	301.2173	27.26	C ₂₀ H ₃₀ O ₂	LA
12,13-DiHOME	313.2384	16.71	C ₁₈ H ₃₄ O ₄	
9,10-DiHOME	313.2384	17.16	C ₁₈ H ₃₄ O ₄	
9-HODE	295.2279	20.99	C ₁₈ H ₃₂ O ₃	
9-OxoODE	293.2122	22.04	C ₁₈ H ₃₀ O ₃	
13-oxoODE	293.2122	21.51	C ₁₈ H ₃₀ O ₃	
13-HOTrE	293.2122	19.15	C ₁₈ H ₃₀ O ₃	ALA
11-HEDE+15- HEDE	323.2592	24.39	C ₂₀ H ₃₆ O ₃	11,14-eicosadienoic acid

2.4.6 Calibration curves for plasma oxylipins

Oxylipins are present endogenously in plasma, and their concentrations can vary widely across different individuals. This poses a significant problem regarding how to best perform accurate quantitation of these species. Choosing the proper calibration curve for the calculation of oxylipins in plasma is important and not a trivial task. Three types of calibration curves were assessed: standard calibration curve in solvent, SPE standard calibration curve, which takes into account the extraction recovery and any matrix effects due to SPE procedure, and the calibration curve that was built in a pooled plasma matrix and subjected all sample preparation procedures including SPE (equivalent to standard addition curve). The standard addition plasma calibration curves were built at two levels of concentration: regular concentrations that allow to measure 0.04-20 ng/ml concentration range and high-concentration curve that allows to measure 15.6-1000 ng/ml

concentrations. The standard addition plasma calibration curves that underwent all sample preparation procedures allows to consider all losses that can occur during sample preparation as well to compensate for any matrix effect of the plasma. Although this is theoretically the best approach, pooled plasma contains endogenous levels of oxylipins that must be considered and subtraction of peak area of endogenous levels must be performed. However, if the oxylipin levels in a sample is lower than in the pooled sample used to prepare the calibration curve, this approach will fail to provide accurate quantitation for that oxylipin. Considering very high inter-individual variability of some oxylipins, the likelihood of this scenario is very high. One way to minimize this issue is to obtain and use pooled plasma with the lowest possible concentrations of oxylipins. Even using two calibration curves (low and high) does not completely solve this problem due to high variability of the levels of oxylipins in plasma. To further improve the performance of this calibration method, additional 7-10 calibration points are needed, but together with 18 existing points it will make this method too expensive and time consuming for routine implementation.

The slopes of three types of calibration curves were compared to evaluate the possibility of using other types of calibration curve instead of matrix-matched (Figure 2.7). The slope of SPE calibration curve of standards in solvent is closer to matrix-matched plasma calibration curves than the slope of standard calibration curve in solvent. Because of this, we suggest the use of standard SPE calibration curve for the final quantitation method. The availability of data from enriched and diluted injection allows to evaluate the extent of matrix effects, and together with internal standards, this can be used to determine the systematic bias inherent in this approach.

In literature, there is no consensus regarding the best calibration method to use for oxylipin analysis. Some authors used standard calibration curves built in solvent for quantitation of oxylipins in plasma.^{65,81,104} Hu *et al.*¹⁰⁵ used standard calibration curve after SPE to take into account losses during extraction, similar to our proposed approach. Miller *et al.*⁸² evaluated different matrices suggested human serum albumin is the best choice to build calibration curve because of low endogenous oxylipins level and better compatibility with human plasma. Mazaleuskaya *et al.*⁸⁹ built curve in charcoal-stripped fetal bovine serum (FBS), but charcoal stripping drastically changes the matrix composition. Galvao *et al.*⁹⁸ built calibration curve in plasma, however subtraction of endogenous level was not reported. Their approach also uses separate calibration curves for low and high abundance oxylipins that is similar to our suggestion.

Another possibility is to build calibration curves in plasma using labelled standards, but for panels with 50-70 oxylipins of interest this rapidly becomes extremely expensive and impractical.

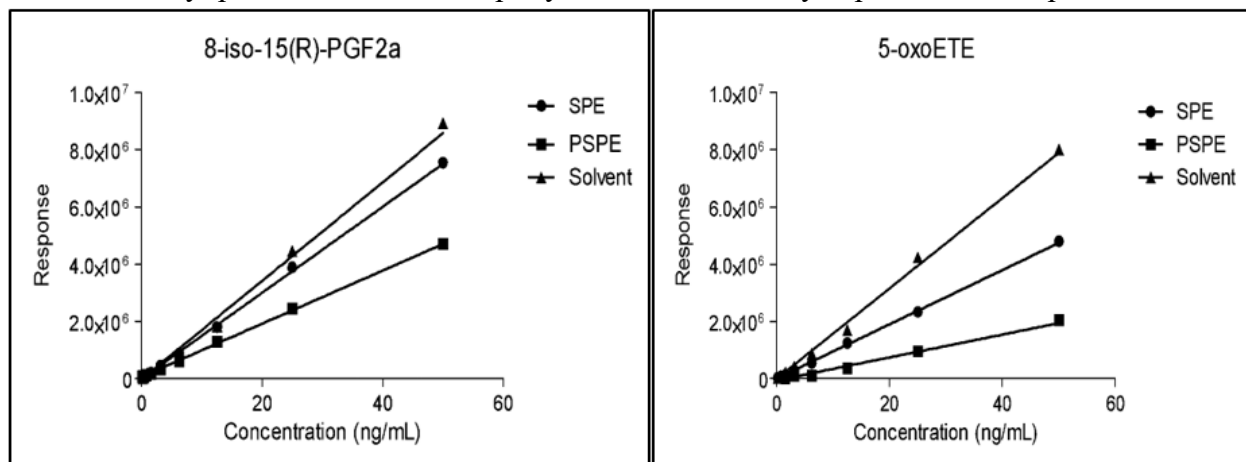


Figure 2.7 Comparison of calibration curves for (a) 8-iso-15(R)-PGF2a and (b) 5-oxoETE. SPE-curve prepared in solvent and passed SPE. PSPE-curve prepared in plasma covering range from 1-50 ng/mL and subjected to SPE. Solvent-curve in solvent. Response on y-axis means signal intensity obtained at particular level.

2.5 Conclusions

The goal of this study was to develop a sensitive and reliable LC-MS method for the detection and quantitation of oxylipins representing different classes in plasma samples. To reach maximum sensitivity, the sample preparation, chromatographic separation (stationary phase/column), mobile phase additive, and MS/MS fragmentation were optimized. The developed method was applied to the analysis of oxylipins in pooled and individual plasma samples and was able to detect 38 and accurately quantitate 25 out of 38 detected oxylipins. The results showed high inter-individual variability of many oxylipin concentrations, and it is the first time that such high concentrations were detected and confirmed for some of the oxylipins such as 9-HETE and 11-HETE. Also, one of the main findings was that checking peak purity in oxylipin analysis should be mandatory to prevent misidentifications.

3 *In vivo* solid-phase microextraction for sampling of oxylipins from the brain of awake, moving rats

Alexander Napylov¹, Nathaly Reyes Garces², German Gomez-Rios², Mariola Olkowicz², Sofia Lendor², Cian Monnin¹, Barbara Bojko², Clement Hamani³, Janusz Pawliszyn², Dajana Vuckovic¹

Affiliations:

¹Department of Chemistry and Biochemistry, Concordia University, Montreal, Canada

²Department of Chemistry, University of Waterloo, Waterloo, Canada

³Centre for Addiction and Mental Health, Toronto, Canada

Abstract

Oxylipins are key lipid mediators that play important roles in a brain including pain, sleep, oxidative stress and inflammation. For the first-time, an in-depth profile of up to 52 oxylipins can be obtained from the brains of awake moving animals using *in vivo* solid-phase microextraction (SPME) in combination with liquid chromatography – high resolution mass spectrometry. This new approach successfully eliminates changes in oxylipin concentrations routinely observed during the analysis of post-mortem samples, allows time-course monitoring of their concentrations with high spatial resolution in specific brain regions of interest and can be performed using the same experimental set-up as *in vivo* microdialysis (MD) thus providing a new and exciting tool in neuroscience and drug discovery.

3.1 Introduction

Eicosanoids are highly bioactive oxygenated products of long chain 20-carbon polyunsaturated fatty acids where AA plays a central role as a precursor. In addition to AA, other common precursors include ω 3 polyunsaturated fatty acids such as EPA and DHA.⁷ As these precursors have different number of carbon atoms, the term oxylipin is used to broadly define the family of oxygenated fatty acids derived from unsaturated fatty acids by pathways involving at least one step of dioxygen-dependent oxidation.⁴ Oxylipins can be derived from the appropriate polyunsaturated fatty acid precursor via oxidation by COX, LOX, CYP and via nonenzymatic oxidation.⁸ They generally act locally, close to the place of their synthesis through G-protein-coupled receptors.² In the brain, eicosanoids and other oxylipins play an important role in many physiological processes²⁹ such as neuroinflammation,¹⁹ cerebral blood flow regulation,⁷⁹

neuroprotection,¹⁰⁶ regulation of temperature¹⁰⁷ and sleep¹⁰⁸, maturation of brain¹⁰⁹ and pain¹¹⁰, thus making these pathways critical targets in drug discovery. They can also be used as possible biomarkers of pathological processes such as oxidative stress¹¹¹ and inflammation¹¹². For instance, AA-derived eicosanoids, such as prostaglandins can have both pro- and anti-inflammatory roles, but are generally involved in the onset of inflammation, whereas lipid mediator class switching and the release of EPA- and DHA-derived oxylipins occur during its resolution.¹¹³ Thus, simultaneous monitoring of multiple oxylipin classes is needed to further elucidate their biological roles and better understand these dynamic time-dependent processes *in vivo*.

Measuring oxylipins in brain tissue is extremely challenging due to their low abundance, the existence of numerous isobaric and isomeric species including stereoisomers with different biological activity, poor stability/short lifetime of some members of this family, and the inherent complexity, and heterogeneity of the brain matrix.^{36,94} Current methods for oxylipin measurement in the brain are mainly *in vitro* post-mortem methods that rely on tissue collection, homogenization and subsequent extraction using either LLE or SPE most commonly in combination with reversed-phase LC-MS analysis.³⁶ More rarely, gas chromatography – mass spectrometry and immunoassays may also be used. LLE methods include general lipid extraction methods such as Folch⁴⁷ and Bligh and Dyer⁴⁸, as well as hexane/2-propanol⁵⁰, ether and acetone/chloroform methods⁴³ for selected oxylipin classes. SPE methods predominantly utilize C-18 and Hydrophilic-Lipophilic Balanced (HLB) sorbents to achieve high oxylipin recovery.³⁶ Post-mortem oxylipin formation is one of the major sources of error in a traditional measurement of oxylipins in brain and is caused by phospholipase activation and the release of phospholipids and oxylipin precursors.^{43,114,115} For instance, Trepanier *et al.*¹¹⁴ showed CO₂ asphyxiation results in the tremendous release of lipid mediators, such as the 522x increase in prostaglandinE2 (PGE2) concentration. The magnitude of this post-mortem oxylipin release is much higher than the typical magnitude of the effect under study and also results in the increased variability of measured oxylipin concentrations, thus further preventing appropriate interpretation of oxylipin results. Head-focused microwave irradiation can address some of these limitations by minimizing post-mortem oxylipin release, but *in vivo* methods remain preferable in order to monitor oxylipin concentrations in individual animals over time.

Here, we introduce *in vivo* SPME sampling as a new method to accurately measure oxylipin profiles in the brains of living, awake rats. This new approach successfully eliminates post-mortem changes in oxylipin concentrations, allows time-course monitoring of their concentrations with high spatial resolution and can be performed using same experimental set-up as *in vivo* MD, which is considered the gold standard method in neuroscience. *In vivo* MD is poorly suitable for oxylipin measurements due to their hydrophobicity, which makes them poorly soluble in aqueous buffers used for MD and highly susceptible to non-specific adsorptive losses during sampling. Some adaptations to optimize MD recovery *in vitro* were evaluated¹¹⁶ but the only successful *in vivo* measurements focus on prostaglandins and prostanoids in human muscle^{117,118}, rat brain^{119–121} and human brain¹²². To the best of our knowledge, there is no data on *in vivo* concentrations of hydrophobic oxylipins from other classes.

3.2 Results and discussion

3.2.1 Oxylipin profiling using *in vivo* SPME

SPME is a non-exhaustive extraction technique that combines sampling, analyte isolation and (potentially) enrichment into one step.^{54,123} *In vivo* SPME was previously successfully employed to measure the circulating concentrations of three eicosanoids and two precursors in rat plasma in response to lipopolysaccharide-induced inflammation.⁶¹ However, the levels of other prostaglandins of interest remained below the limit of detection for the method. In brain, *in vivo* SPME was validated against *in vivo* MD for the measurement of neurotransmitters.⁵⁹ This comparison showed better method precision of *in vivo* SPME and similar capability of both techniques to accurately measure temporal changes in neurotransmitter concentrations in response to drug dosing. The objective of the current work was to introduce SPME technology to enable accurate oxylipin measurement of the large panel of oxylipins using *in vivo* SPME for the first time. *In vivo* SPME sampling from the brain was performed using SPME fibers covered with thin biocompatible coatings, which were introduced directly to the brain via microdialysis guide cannulae surgically implanted into the cranium. This new approach together with the extensive optimization of LC-MS method to achieve low limits of detection¹⁰³ allowed us to detect up to 20 oxylipins in SPME samples from the 54-oxylipin panel initially tested (Supplementary Table S4). Among these, 15 oxylipins could be accurately quantitated. The two precursors AA and DHA exceeded the highest level of calibration due to their high abundance but can be accurately measured in future by extending the calibration range for these analytes. 12-HETE and 8-HETE

can be accurately individually quantified in MS/MS dimension of our LC-MS method. However, signal intensity of the fragment ions in SPME samples was too low, so the sum of these two oxylipins is reported instead in the current study. 12-oxoETE was detected above LOQ in 18 out of 30 *in vivo* SPME samples, but its autosampler stability is poor as indicated by unacceptable precision of pooled quality control sample for this oxylipin in the current study and further confirmed during the stability investigation of standard solutions. Figure 3.1 summarizes the concentrations of 10 oxylipins which were measured above the LOQ in the majority of samples. 12,13-DiHOME and 9,10-DiHOME were detected above the LOD in 30 and 25 of *in vivo* SPME samples respectively, but their levels were below the LOQ in many of them, so these two oxylipins are not included in Figure 3.1

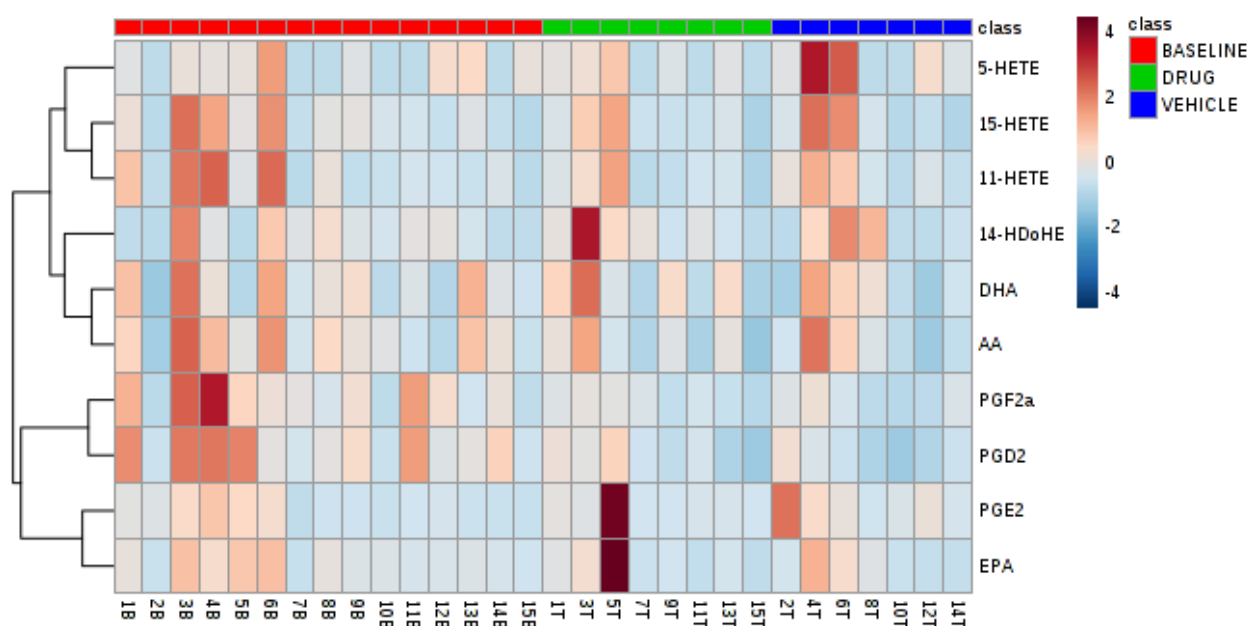


Figure 3.1 Hierarchical clustering by class (baseline, drug and vehicle) using Euclidian distance of the oxylipins measured by *in vivo* SPME in a minimum of 50% of all study samples above LOQ. Clustering was performed using concentrations (ng/mL) using Metaboanalyst 4.0^{124,125}

Figures 3.2 and 3.3 show example changes in the concentration of three representative oxylipins and one precursor: prostaglandin D2 (PGD2), PGE2, 14-hydroxy Docosahexaenoic Acid (14-HDoHE) and EPA. Comparing the drug-dosed cohort to vehicle-dosed cohort, as would be performed traditionally, showed no statistically significant differences between the cohort and vehicle group for any of the oxylipins accurately measured. These results are in agreement with other studies that have examined the effect of dosing fluoxetine on a murine brain in combination

with microwave irradiation to prevent post-mortem oxylipin formation and found no changes in oxylipins except for 20-HETE which was not detected in the current study.¹²⁶ Figures 3.1 and 3.3 also show inter-animal variability of oxylipin concentrations. The variability of these concentrations is very high depending on the oxylipin of interest (% RSD range from 23 to 171%). However, the individual results shown in Figure 3.1 and the percent difference plots of the individual animals shown in Figure 3.2 confirm that the observed variability is true inter-animal variability. Post-dose sampling of an animal with an elevated baseline concentration of a given oxylipin generally resulted in high concentrations of the same oxylipin. For example, comparing highly variable baseline data in Figure 3.3 and individual animal data in Figure 3.2 for PGD2, shows that the changes in PGD2 are consistent across animals (median decrease of 66 and 65% for vehicle and drug groups respectively). For all quantified oxylipins, median change across animals showed the decreases of 28% and 21% for vehicle and drug groups respectively, thus confirming that intra-animal variability is much lower than inter-animal variability. Finally, the hierarchical clustering and correlation analysis of quantified oxylipins show the expected trends whereby different subclasses cluster closely together as shown in Figure 3.5 (a). For example, all quantified HETEs cluster together, and all quantified prostaglandins cluster together. However, within the same class interesting trends showing low correlation between PGE2 and PGD2 are also observed in agreement with previous results observed for hippocampus region.¹²⁷

3.2.2 Comparison of *in vivo* SPME to post-mortem SPE extraction of pooled brain homogenate

Next, the *in vivo* SPME results were compared to the C18 SPE extraction of pooled rat brain homogenate. Using post-mortem SPE after CO₂ asphyxiation, 43 oxylipins were detected, and 41 of them were accurately quantitated (Supplementary Table S7). These SPE results show comparable or higher oxylipin coverage to other methods. Hennebelle *et al.*¹²⁷ detected 16-30 oxylipins in control rat brain depending on brain region and 34-53 in ischemic rat brain. Wong *et al.*²⁵ detected 7 oxylipins in different regions of normal rat brain. Yue *et al.*²⁶ detected 14 oxylipins in rat brain 72h post-injury. Shaik *et al.*²⁸ detected 11 oxylipins in rat brain cortex tissue samples collected 5 min after the resuscitation of animals subjected to 12 min asphyxial cardiac arrest. Figure 3.4 shows the distribution of all quantified identified oxylipins that were detected by both

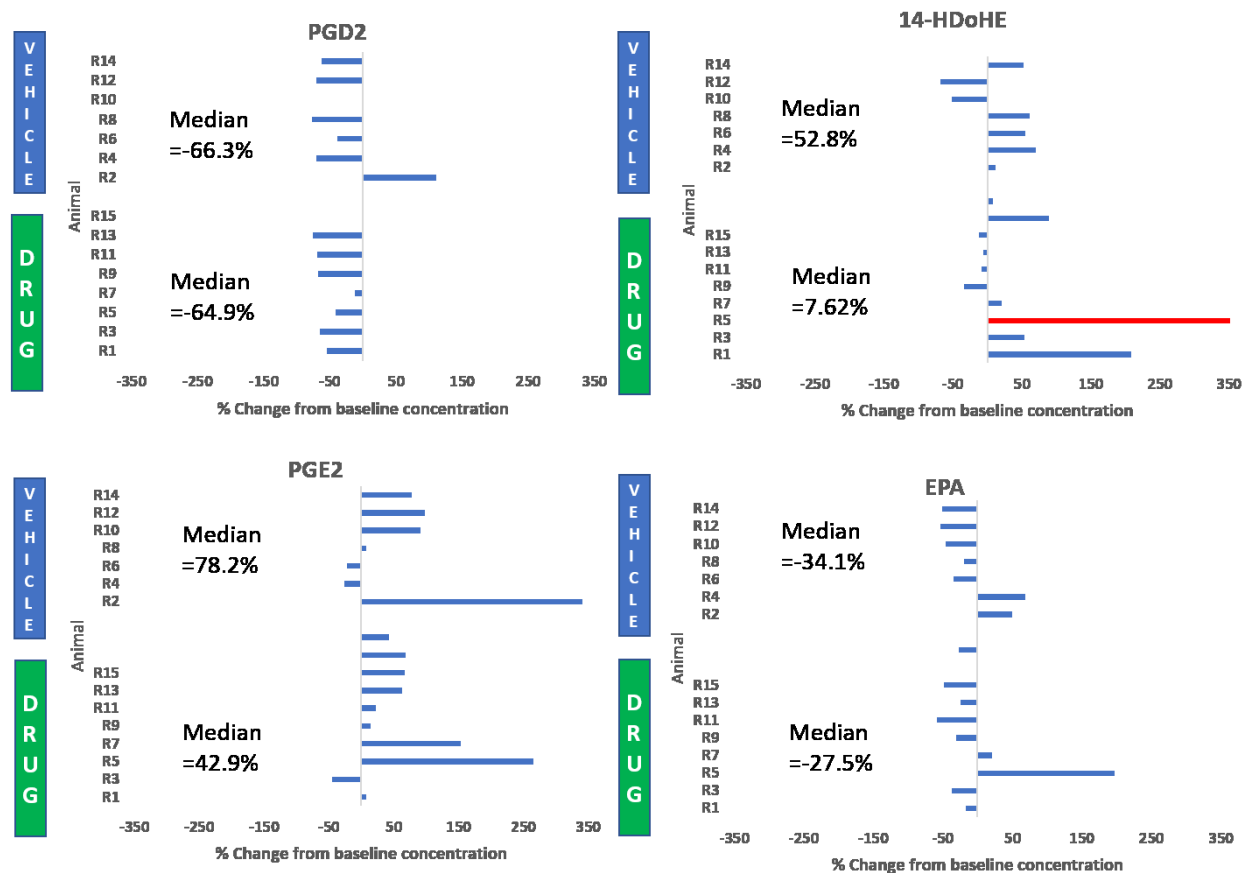


Figure 3.2 Relative change in the concentration of the selected oxylipins (PGD2, PGE2, 14-HDoHE and EPA) for each animal with respect to its baseline value when dosed either vehicle only (n=7) or fluoxetine+vehicle (n=8). Missing bar means that oxylipin was below LOD in one of the samples detected. One red bar shown for 14-HDoHE indicates that the observed change is off-scale (480%). Median % change for each group is also shown directly on the panels.

in vivo SPME and SPE methods, excluding the high-abundance precursors. The obtained distributions show significant differences, in particular much higher proportion HETEs was observed in SPE samples. HETEs and prostaglandins have been shown to be highly elevated during brain ischemia,^{114,127} and the observed difference in the distributions is consistent with post-mortem release of oxylipins. The correlation analysis of SPE versus SPME results shows the same trend, with the Pearson correlation coefficient of 0.12. When comparing SPE and SPME data, it is also important to note that 16-HETE and 20-HETE were not detected in any of *in vivo* SPME samples. 16-HETE was detected in post-mortem brain samples at comparable concentrations as 9- and 11-HETE (Supplementary Table S7), but in SPME only 9- and 11-HETE were detectable. 16-HETE is produced through CYP enzymatic pathway,⁸ indicating that its release may have occurred during anesthesia and/or asphyxiation and was not present *in vivo* at the same concentrations measured

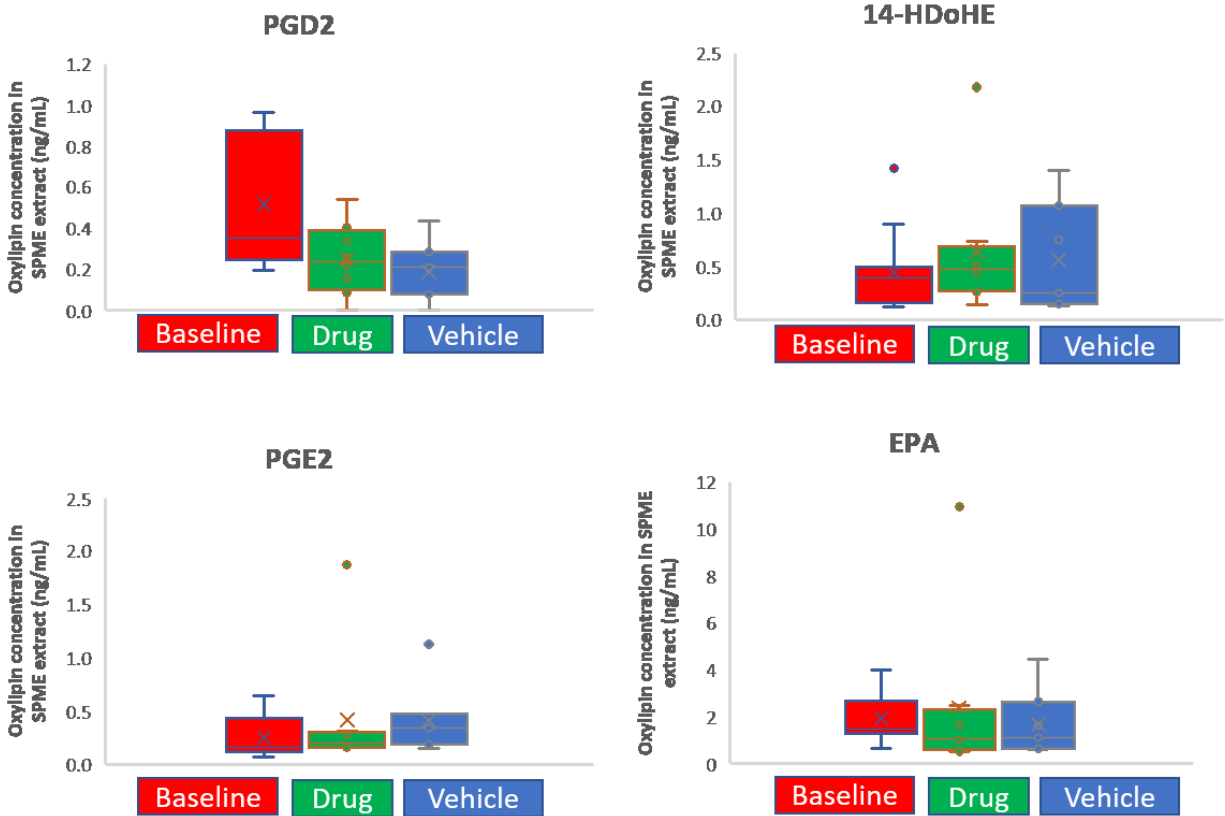


Figure 3.3 Inter-individual variability in the measured concentrations of the selected oxylipins (PGD2, PGE2, 14-HDoHE and EPA) shown by time point and dosing status: baseline ($t=0$, $n=15$), vehicle only ($n=7$) or fluoxetine+vehicle ($n=8$). Box shows Q1, median and Q3. The X shows mean of all the concentrations measured for that animal. Any missing values are not shown and not used in the calculation.

during the post-mortem tissue analysis. This is supported by the absence of 20-HETE, known marker of cerebral ischemia,¹²⁸ from *in vivo* SPME samples, but its presence in post-mortem SPE samples. In *in vivo* SPME samples, the most abundant quantified oxylipins after precursors were PGE2, PDE2, 14-HDoHE and 9-oxo-10,12-octadecadienoic acid (9-oxoODE). PGE and PDE2 are known to be highly abundant across many brain studies^{25–28,30,127}, but the *in vivo* results for 14-HDoHE and 9-oxoODE were surprising. 14-HDoHE can be synthesized enzymatically via the LOX pathway and through auto-oxidation of DHA. 9-oxoODE was previously detected in very high abundance in the cortex, and at lower abundance in the hippocampus, cerebellum and the brain stem showing important differences in its spatial distribution.¹²⁷ The same study did not report 14-HDoHE in any of the regions tested. However, in a comprehensive study of DHA-derived oxylipins, Derogis *et al.*¹²⁹ showed high levels of 4-, 11-, 14- and 20-HdoHE in brain homogenates, whereas Jouvène *et al.*⁴⁶ reported high-abundance of 4-, 14- and 17- HDoHE in whole brain

homogenate. Thus, at this time it is not yet clear whether 14-HDoHE high abundance is regiospecific to the hippocampus or represents more accurate capture of its true *in vivo* concentration.

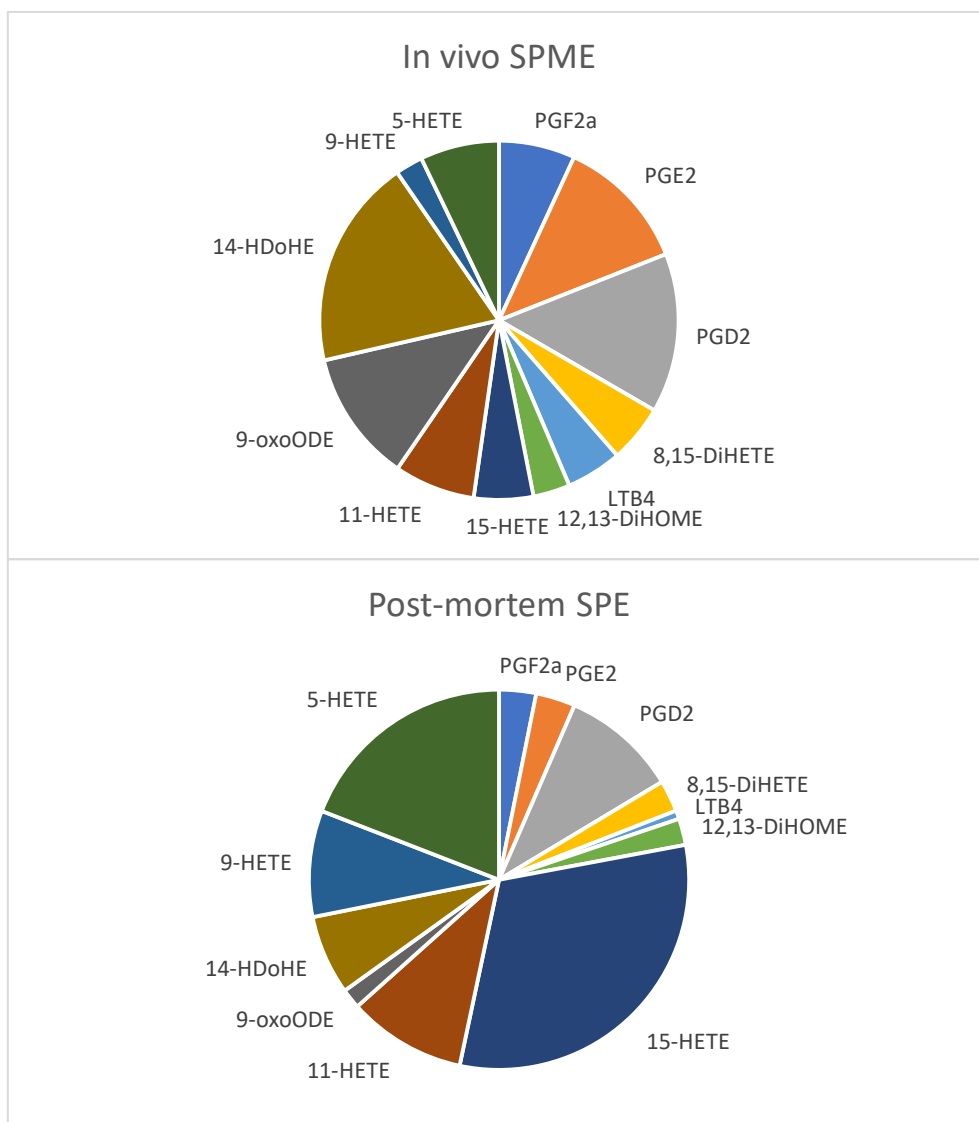


Figure 3.4 Comparison of the distribution (% by amount) of oxylipins detected by *in vivo* SPME and post-mortem SPE extraction of oxylipins in brain. The precursors, AA, EPA and DHA represent 98.3% of all species quantified using *in vivo* SPME and 99.6% of all species quantified using post-mortem SPE so they are omitted for clarity

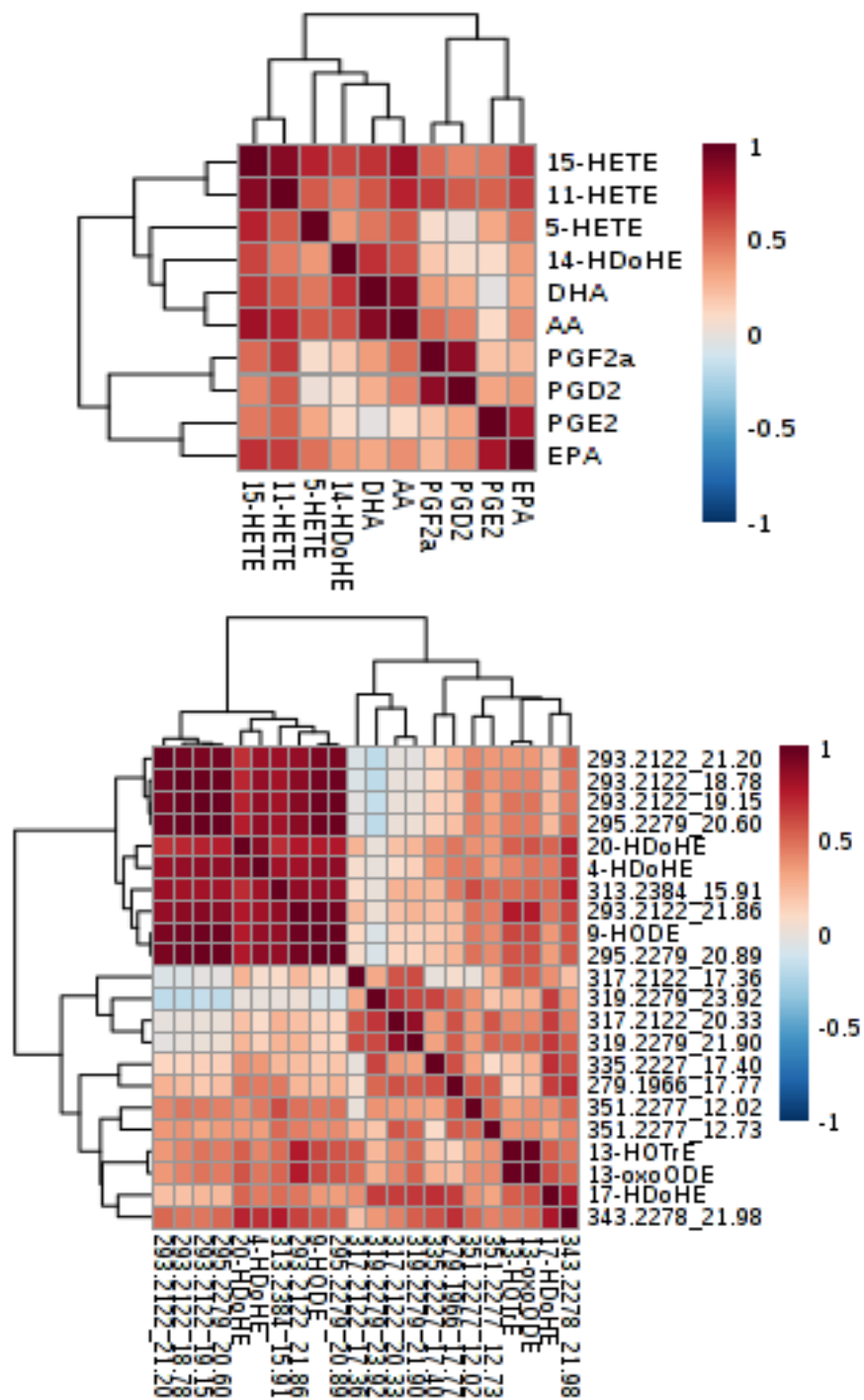


Figure 3.5 Hierarchical clustering and correlation analysis of oxylipins measured in this study (a) known and quantified oxylipins with levels >LOQ in more than 50% of samples using measured oxylipin concentration (ng/mL) and (b) unknown and subsequently identified oxylipins with levels >LOQ in more than 5 samples using peak areas.

3.2.3 Characterization of unknown oxylipins observed using *in vivo* SPME

In addition to the 20 identified oxylipins, 32 unknown oxylipins (that were not presented in target list) were also detected using *in vivo* SPME as summarized in Table 3.1. In a subsequent experiment the identification of six of these oxylipins was confirmed using authentic standards as shown in Table 3.1 This included the identification of three additional HDoHEs: 4-, 17- and 20-HDoHE. This brings our results in excellent agreement with Jouvene *et al.*⁴⁶ and Derogis *et al.*¹²⁹. Among the 32 unknown oxylipins, 14 of these were also detected in post-mortem SPE samples. The remaining 18 oxylipins possibly represent unstable species that are degraded during traditional sample preparation (e.g. undergo enzymatic degradation) or that may be suppressed during LC-MS analysis of tissue samples if they elute in the regions of high matrix effect. To date, we have successfully confirmed the identity of one of the oxylipins unique to *in vivo* SPME – 13-HOTrE. To the best of our knowledge 13-HOTrE has not been detected in the hippocampus before although it was observed in brain stem in one recent study.¹²⁷ 13-HOTrE is derived from α -linolenic acid and is proposed to have the anti-inflammatory role.¹³⁰ Future studies will focus on the extensive characterization of the remaining unknown oxylipins.

Figure 3.5 shows the correlation analysis of all oxylipins detected by *in vivo* SPME. The correlation analysis of unknown oxylipins is particularly interesting as it shows clear pathway and precursor trends. For example, C₂₀H₃₂O₃ oxylipins show poor correlation to C18- and C22-derived oxylipins, and high correlation and clustering to each other. Similarly, C₁₈H₃₀O₃ shows high correlation to other C18-derived oxylipins and some members of HDoHE subclass (4- and 20-, but not 17-) indicating they may be derived via the same pathways.

Table 3.1 Summary of all unknown oxylipins detected using *in vivo* SPME. The identification of six of these oxylipins was performed in a subsequent experiment and is shown in brackets for the relevant oxylipin. The oxylipins indicated in green were also observed in post-mortem SPE samples. The oxylipins indicated in black were observed only using *in vivo* SPME and show that traditional post-mortem analysis does not accurately capture oxylipin profiles in brain.

m/z of unknown oxylipin	Retention time (min) and identification shown in red	Molecular Formula
351.2177	10.37, 12.02, 12.73	C ₂₀ H ₃₂ O ₅
317.2122	14.68, 15.10, 16.62, 17.36, 18.28, 18.56, 19.07, 20.33	C ₂₀ H ₃₀ O ₃
313.2384	15.91, 16.46	C ₁₈ H ₃₄ O ₄
335.2227	17.4	C ₂₀ H ₃₂ O ₄
319.2279	21.9, 23.92	C ₂₀ H ₃₂ O ₃
293.2122	18.54, 18.78, 18.91 (13-HOTrE), 19.15, 21.20, 21.56 (13-oxoODE), 21.86	C ₁₈ H ₃₀ O ₃
343.2278	21.22 (20-HDoHE), 21.82 (17-HDoHE), 21.98, 21.53 (4-HDoHE), 24.31	C ₂₂ H ₃₂ O ₃
295.2279	20.6, 20.89, 21.03 (9-HODE)	C ₁₈ H ₃₂ O ₃
279.1966	17.77	C ₁₇ H ₂₈ O ₃

In conclusion, to the best of our knowledge, the measurement of up to 52 oxylipins in the current study represents the largest panel of oxylipins ever measured in brain *in vivo* under normal baseline physiological conditions. Our results clearly show that *in vivo* SPME can be a powerful approach to study oxylipin biology in more detail and to capture accurately their concentrations *in vivo* with the unprecedented degree of temporal and spatial resolution. Since *in vivo* SPME uses the same set-up as microdialysis, this technology can be easily implemented to the existing well-accepted workflows in order to obtain much richer oxylipin profiles than can be obtained using MD. Although not discussed in this work, a single *in vivo* sampling is sufficient to obtain full untargeted metabolomic profile in addition to the quantitative oxylipin analysis shown in the current study. *In vivo* SPME provides the new tool to evaluate temporal and circadian intra-animal variability in oxylipin concentrations. As shown in this study for the hippocampus, intra-animal variability is much lower than inter-animal variability, and this novel tool allows the monitoring of specific pathway activation in individual animals.

3.3 Experimental

This study was performed on 15 adult male Sprague Dawley rats (220-250g, Charles River). Animals were stereotactically implanted with bilateral guides (MAB 4.15.IC, Scipro, Sanborn, NY) into the hippocampus (anteroposterior -5.0 mm, mediolateral 4.6 mm, and dorsoventral -2.5 mm relative to bregma) one week prior to the experiments.¹³¹ Eight rats were intraperitoneally (IP) injected with fluoxetine (Tocris Bioscience) at 10 mg/kg of body weight, representing an acute drug dose. The remaining rats were dosed with the vehicle only (saline solution) as a control group. *In vivo* SPME was performed on all rats before dosing, and then 30 min after IP injection using biocompatible mixed-mode probes (C18 with benzenesulfonic acid, 4 mm, 45 μ m thickness, 200 μ m diameter, support matrix – polyacrylonitrile, Millipore Sigma). Briefly, the probes were first pre-conditioned prior to use for a minimum of 30 min in acetonitrile/water (1:1 v/v). *In vivo* sampling was performed for 15.0 min. After extraction, fibers were first cleaned with a Kimwipe to remove mechanically any attached tissue residuals. The fibres were then vortexed in ultrapure water for 10 secs and immediately placed in -20°C freezer. At the end of the sampling day, fibers were transferred on dry ice to Concordia University and stored in -80°C freezer until LC-MS analysis. Fibres were desorbed using 80 μ L of desorption solvent (ACN/MeOH/H₂O, 40/40/20) which was spiked with the following deuterated internal standards: L-Phenylalanine-d₅, Cholic acid-d₄, L-Glutamic acid-d₅, Melatonin-d₄, Serotonin-d₄ at the concentration of 160 ng/mL (for metabolomics analysis) and 11 β -PGF₂ α -d₄, LTB₄-d₄, 15-HETE-d₈, (\pm)8(9)-EET-d₁₁, and arachidonic acid-d₈ at the concentration of 3.6 ng/mL (for oxylipin analysis). Desorption was performed for 1 hour at 450 rpm at room temperature. 50 μ L of desorption solvent was then diluted with 30 μ L of water, vortexed and analyzed by negative ESI LC-MS using the optimized C18 LC oxylipin profiling method on 1290 UHPLC coupled to 6550 iFunnel QTOF instrument (Agilent Technologies, Santa Clara, CA, US). More detailed information on LC-MS, data processing, post-mortem SPE extraction, oxylipin identification and statistical data analysis is provided in the Supporting Information. In addition to the study samples, extraction blanks were also prepared on the sampling day by subjecting three SPME fibers to all the steps of SPME procedure except sampling of the animal. Non-optimal SPME set-up for oxylipins was used and additional improvements could be achieved by increasing injection volume, modifying extraction time and/or using HLB versus mixed-mode coating that was used in current *in vivo* experiment (Supplementary Figure S21).

4 Conclusions and future work

4.1 Conclusions

The developed LC-MS method can measure 62 oxylipins including representatives of the following classes: PGs, LTs, DiHOMEs, DiHETs, DiHETEs, HOTrEs, HODEs, oxoODEs, oxoETEs, HEDEs, EpETEs, HEPEs, HETEs, HDoHEs, EETs and 7 deuterated standards in solvent in high-resolution MS scan mode in 40 min. The sensitivity of the method was partially improved by promoting more efficient ionization using 0.02% (v/v) acetic acid as a mobile phase additive instead of 0.02% (v/v) formic acid 10 mM ammonium acetate. LLOQ in solvent for majority of standards was 0.1 ng/ml and LLOQ range in solvent was 0.1-0.8 ng/ml. Long LC separation allowed to resolve the majority of isomeric oxylipins, which is critical for successfully coupling the method to HRMS scan mode whereby parent ions without fragmentation are measured. During method development, three types of stationary phases were assessed: C-18 UHPLC, core-shell C-18 HPLC, T-3 UHPLC and PFP HPLC. Among these, C-18 UHPLC showed the best separation. However, several pairs of isomeric oxylipins were still not resolved chromatographically: 12-HETE/8-HETE; 10,17-DiHDHA/MaR-1; and 11-HEDE/15-HEDE. For all of these pairs, MS/MS fragmentation was developed and unique fragments were found for each oxylipin. However, the use of MS/MS for quantitation also impacted the LLOQs for these analytes except for 12-HETE/8-HETE where the same LLOQ (0.1 ng/ml) as for parent ion was observed. For other pairs LLOQ drop of intensity was that does not allow their separate quantitation. Also, three pairs: 15-HEPE/11-HEPE, 16-HDoHE/17-HDoHE, 11,12-EpETE/8,9-EpETE elute with a separation of less than 0.2 mins and MS/MS fragmentation was required for their quantitation.

During the development of the sample preparation method different parameters such as the type of SPE sorbent, the composition of elution solvent, and elution solvent volume were assessed and optimized to achieve maximum recovery and minimize the matrix effect. HLB and C-18 SPE showed comparable results in terms of recovery of oxylipins. However, C-18 was chosen for further method development as it can decrease the complexity of the matrix better by not retaining polar compounds. The final optimized method demonstrated recovery $\geq 50\%$ for the majority of oxylipins in solvent, with an average recovery of 82% and a recovery range of 50-109%. Only seven standards demonstrated recovery $< 50\%$: EPA, DHA, AA, AA-d8, LTD4, LTE4 and LTE4-d5 and were excluded from calculation of average recovery. In general, more hydrophilic oxylipins showed higher recovery than more hydrophobic. This can be explained by increased nonspecific

adsorption losses that occur when small amount of analytes (e.g. 0.4 ng) were loaded on the cartridge. This was confirmed by the analysis of flow-through and washed fractions, where no oxylipins were detected. The loading of the higher amount of analytes on SPE or the loading of spiked plasma showed much higher recoveries, which is also consistent with a higher-degree of non-specific losses in standards with very low concentrations of oxylipins. In all of these cases, the recoveries of more hydrophobic and more hydrophilic oxylipin standards were comparable and the average recovery in plasma, for example, was 83% ranging from 70 to 97%. The worst method performance in terms of recovery was found for cystenyl leukotrienes. For example, LTE4, LTE4-d5 and LTD4 showed 0% recovery when 0.4 ng/cartridge was tested in the recovery experiment. However, increasing the number of loaded analytes or analyzing spiked plasma instead of standard solutions can increase the recovery of these leukotrienes up to 70%. This can be achieved by loading an excess level of LTE4-d5 or similar internal standard to irreversible bind to any active spots within the sorbent/ This can be used for problematic matrices where losses of leukotrienes are noticeable. Another important finding for leukotrienes was that the acidification of elution solvent noticeably increased their recovery. However, if leukotrienes are not of interest for a given application, pure methanol can be used for elution of the remaining oxylipins and provides slightly higher recoveries than acidified methanol.

Due to the expected low abundance of oxylipins in biological matrices, the analytical method for their analysis requires the preconcentration step. During method development, it was found that the preconcentration step could cause severe losses of analytes and very poor method precision, so several parameters were optimized to decrease these losses. First of all, a speedvac evaporator was chosen for further development because it showed higher recovery rates and better precision than nitrogen evaporation. The addition of the small volume of 30% glycerol prior to loading the sample into the evaporation tube further reduced losses during this critical step. Due to its high boiling point glycerol can not be evaporated in the speedvac, so after the complete evaporation of the other solvent glycerol remains on the bottom of the tube thus preventing interaction of oxylipins with the walls of the tube. This glycerol plug containing the oxylipin analytes can then be easily dissolved in methanol for further analysis. Also, it was found that the more hydrophobic oxylipins are prone to adsorptive losses in polypropylene tubes, so all manipulations, especially the evaporation/reconstitution steps must be performed in glass vessels.

The developed method was applied to plasma samples and it was found that protein precipitation of plasma samples before loading on SPE is the critical step that could lead to the severe oxylipin losses and thus to the underestimation of real oxylipin levels in plasma. We compared TCA protein precipitation of the plasma before loading with direct loading of plasma on SPE. We found that levels of many of oxylipins were much higher without precipitation and in many cases chromatographic peaks were even saturated. So it was concluded that direct loading of plasma samples on SPE is a preferred method for oxylipins analysis. However, direct loading caused changes in the final method. First of all, due to the appearance of the precipitate in samples after the reconstitution step, the additional centrifugation step was added before injection of the sample into the LC-MS system. Wide range of oxylipin concentrations measured in individual and pooled human plasma, for that reason it was decided to use two injections for each sample during analysis. The first injection is of 2.5x pre-concentrated sample obtained after reconstitution and centrifugation, in order to quantify the less abundant oxylipins. The second injection corresponds to 40x diluted plasma in order to measure the more abundant oxylipins that have saturated peaks in the pre-concentrated samples. The analysis of individual plasma samples also demonstrated high inter-individual variability of oxylipin levels. Similar variability was previously demonstrated in other studies^{85,90} and it was suggested that it can be caused by pharmacological and/or nutritional intervention. However, the exact mechanism is not clear. In our case, the variability was much higher than it was previously demonstrated but a very small cohort of individual samples was analyzed, and further experiments are needed to obtain more evidence of inter-individual variability. Also, high levels of some of oxylipins (e.g. 9-HETE) were demonstrated for the first time to the best of our knowledge, and do not match the values currently reported in the HMDB for this oxylipin. The measured levels of this oxylipin in our samples were further verified using standard addition method which confirmed our initial results. To ensure that these higher than expected levels, were not due to possible co-elution of another isobaric species, different LC gradients for the analysis of these spiked samples were also applied and further confirmed the accuracy of our measurement. However, the same experiments also showed that several oxylipins were misidentified using regular gradient and exhibited retention time shift comparatively to their authentic standards, when very shallow gradients were used, e.g. PGE2 and PGD2. So, these oxylipins were excluded from the list of identified compounds and it was concluded that to ensure the correct identification of oxylipins, a shallower gradient should be applied.

Another issue encountered in plasma experiment was the existence of interference peaks that have the same mass as oxylipins in our panel and cannot be resolved chromatographically. Shallower gradient was not able to resolve them requiring further LC development for this matrix. Thus, among the 38 identified oxylipins in plasma only 25 were successfully quantitated, the remaining 13 oxylipins had interferences that precluded correct quantification. For correct quantification use, proper calibration curve is required. However, due to high variability of endogenous level of oxylipins in plasma it is not a trivial task. An optimal calibration curve should take into account all possible losses of analytes during sample preparation step and possible matrix effect. So the ideal calibration curve should be built in the same matrix as analysed samples and should pass all sample preparation steps as analysed samples. We figured out that the calibration curve built in plasma is expensive and its preparation is time consuming. For that reasons SPE calibration curve built in solvent was determined as the best choice for our method. This type of curve does not consider the matrix effect, however in our case we quantitated 17 out of 25 oxylipins in diluted samples where the matrix effect was minimal and for other 8 oxylipins measured the matrix effect allowed to evaluate bias in their analysis.

The developed method was applied for *in vitro* analysis of oxylipins in rat brain tissue, for that, only one additional step with brain tissue homogenization was added to the developed method. This final method for brain tissue allowed for the identification of 43 oxylipins and the quantification of 41 of them. The concentration range of oxylipins in the brain was narrower than in the plasma, and allowed for the quantitation of all oxylipins of interest in one sample without dilution. These results were compared to the analysis of *in vivo* SPME rat brain extracts. Using *in vivo* SPME, 20 oxylipins were identified and 32 unknown peaks with oxylipin *m/z* were detected. Six of them were subsequently successfully identified using authentic standards. To the best of our knowledge, this is the largest oxylipin panel ever detected *in vivo* from the brain tissue of living animals. This experiment showed that *in vivo* SPME can be a powerful approach for *in vivo* studies of oxylipins in brain. The comparison of oxylipin profiles of *in vivo* SPME versus SPE showed significant differences between the two methods. Using post-mortem SPE, HETEs were the predominant oxylipins while for *in vivo* samples PGE₂, PGD₂, 14-HDoHE and 9-oxoODE were the most abundant oxylipin species determined, not including precursors PUFAs. 13-HOTrE was measured only in *in vivo* samples, whereas 20-HETE and 16-HETE were determined only in *in vitro* samples. To the best our knowledge, 13-HOTrE was not identified in brain tissue before.

Also, among 32 unknown peaks only 14 were found in *in vitro* samples as well while 18 were unique for *in vivo*. This gives us additional evidence that *in vitro* and *in vivo* analysis of oxylipins yield different oxylipin profiles, possibly due to post-mortem formation or the degradation of unstable oxylipins during *in vitro* sample preparation. In order to obtain accurate profile of oxylipins *in vivo* analysis should be used.

4.2 Future work

Currently, 26 putative metabolites with oxylipin *m/z* remain unknown in *in vivo* SPME brain samples. Thus, their further identification using *m/z*, RT, MS/MS fragmentation and comparison to authentic standards is required. Furthermore, the brains from the animals that were used for *in vivo* extraction were collected and must be analyzed using *in vitro* post-mortem SPE and SPME methods in order to further compare the oxylipin coverage of *in vivo* and *in vitro* samples on the same brain specimens. This *in vitro* analysis will be performed for the exactly the same brain region that was used for *in vivo* SPME sampling. This will provide more in-depth evidence about the oxylipin profile differences observed using both types of analyses.

The comparison of the method performance between solvent and plasma matrix showed many interferences by additional oxylipins present in biological matrices. Thus, further chromatographic separation and/or use of MS/MS in the future can increase the number of oxylipins that can be accurately quantified in human plasma.

For further comparison of speedvac and nitrogen evaporator, additional experiments with 30 replicates have to be performed to obtain good estimate of standard deviation.

Developed profiling LC-HRMS in combination with *in vivo* SPME could become a powerful analytical instrument for profiling of oxylipins in brain. This methodology could be used for further investigation of oxylipins pathways and functions in the brain, drug development and determination of biomarkers of different physiological and pathological conditions.

References

- (1) Corey, E. J.; Niwa, H.; Falck, J. R.; Mioskowski, C.; Arai, Y.; Marfat, A. Recent Studies on the Chemical Synthesis of Eicosanoids. *Adv. Prostaglandin Thromboxane Res.* **1980**, *6*, 19–25.
- (2) Smith, W. L. The Eicosanoids and Their Biochemical Mechanisms of Action. *Biochem. J.* **1989**, *259* (2), 315–324.
- (3) Strassburg, K.; Huijbrechts, A. M. L.; Kortekaas, K. A.; Lindeman, J. H.; Pedersen, T. L.; Dane, A.; Berger, R.; Brenkman, A.; Hankemeier, T.; van Duynhoven, J.; et al. Quantitative Profiling of Oxylipins through Comprehensive LC-MS/MS Analysis: Application in Cardiac Surgery. *Anal. Bioanal. Chem.* **2012**, *404* (5), 1413–1426.
- (4) Wasternack, C.; Feussner, I. The Oxylipin Pathways: Biochemistry and Function. *Annu. Rev. Plant Biol.* **2018**, *69* (1), 363–386.
- (5) Griffiths, G. Biosynthesis and Analysis of Plant Oxylipins. *Free Radic. Res.* **2015**, *49* (5), 565–582.
- (6) LIPID MAPS Lipidomics Gateway <https://www.lipidmaps.org/> (accessed Jan 15, 2019).
- (7) Smith, W. L.; Murphy, R. C. The Eicosanoids. In *Biochemistry of Lipids, Lipoproteins and Membranes*; Elsevier, 2016; pp 259–296.
- (8) Buczynski, M. W.; Dumlao, D. S.; Dennis, E. A. *Thematic Review Series: Proteomics*. An Integrated Omics Analysis of Eicosanoid Biology. *J. Lipid Res.* **2009**, *50* (6), 1015–1038.
- (9) Lone, A. M.; Taskén, K. Proinflammatory and Immunoregulatory Roles of Eicosanoids in T Cells. *Front. Immunol.* **2013**, *4*.
- (10) Vasquez, A. M.; Mouchlis, V. D.; Dennis, E. A. Review of Four Major Distinct Types of Human Phospholipase A2. *Adv. Biol. Regul.* **2018**, *67*, 212–218.
- (11) Dennis, E. A.; Cao, J.; Hsu, Y.-H.; Magrioti, V.; Kokotos, G. Phospholipase A₂ Enzymes: Physical Structure, Biological Function, Disease Implication, Chemical Inhibition, and Therapeutic Intervention. *Chem. Rev.* **2011**, *111* (10), 6130–6185.
- (12) Murakami, M.; Taketomi, Y.; Sato, H.; Yamamoto, K. Secreted Phospholipase A2 Revisited. *J. Biochem. (Tokyo)* **2011**, *150* (3), 233–255.
- (13) Evans, J. H.; Gerber, S. H.; Murray, D.; Leslie, C. C. The Calcium Binding Loops of the Cytosolic Phospholipase A2 C2 Domain Specify Targeting to Golgi and ER in Live Cells. *Mol. Biol. Cell* **2004**, *15* (1), 371–383.
- (14) Murphy, R. C.; Barkley, R. M.; Zemski Berry, K.; Hankin, J.; Harrison, K.; Johnson, C.; Krank, J.; McAnoy, A.; Uhlson, C.; Zarini, S. Electrospray Ionization and Tandem Mass Spectrometry of Eicosanoids. *Anal. Biochem.* **2005**, *346* (1), 1–42.
- (15) Smith, W. L.; Urade, Y.; Jakobsson, P.-J. Enzymes of the Cyclooxygenase Pathways of Prostanoid Biosynthesis. *Chem. Rev.* **2011**, *111* (10), 5821–5865.
- (16) Smith, W. L. Nutritionally Essential Fatty Acids and Biologically Indispensable Cyclooxygenases. *Trends Biochem. Sci.* **2008**, *33* (1), 27–37.
- (17) Hirata, T.; Narumiya, S. Prostanoid Receptors. *Chem. Rev.* **2011**, *111* (10), 6209–6230.
- (18) Figueiredo-Pereira, M. E.; Rockwell, P.; Schmidt-Glenewinkel, T.; Serrano, P. Neuroinflammation and J2 Prostaglandins: Linking Impairment of the Ubiquitin-Proteasome Pathway and Mitochondria to Neurodegeneration. *Front. Mol. Neurosci.* **2015**, *7*.
- (19) Ricciotti, E.; FitzGerald, G. A. Prostaglandins and Inflammation. *Arterioscler. Thromb. Vasc. Biol.* **2011**, *31* (5), 986–1000.
- (20) Tai, H.-H.; Ensor, C. M.; Tong, M.; Zhou, H.; Yan, F. Prostaglandin Catabolizing Enzymes. *Prostaglandins Other Lipid Mediat.* **2002**, *68–69*, 483–493.
- (21) Haeggström, J. Z.; Funk, C. D. Lipoxygenase and Leukotriene Pathways: Biochemistry, Biology, and Roles in Disease. *Chem. Rev.* **2011**, *111* (10), 5866–5898.
- (22) Nakamura, M.; Shimizu, T. Leukotriene Receptors. *Chem. Rev.* **2011**, *111* (10), 6231–6298.

- (23) Milne, G. L.; Yin, H.; Morrow, J. D. Human Biochemistry of the Isoprostane Pathway. *J. Biol. Chem.* **2008**, *283* (23), 15533–15537.
- (24) Tassoni, D. T.; Kaur, G.; Weisinger, R. S.; Sinclair, A. J. The Role of Eicosanoids in the Brain. *Asia Pac. J. Clin. Nutr.* **2008**, *17* (S1), 220–228.
- (25) Wong, A.; Sagar, D. R.; Ortori, C. A.; Kendall, D. A.; Chapman, V.; Barrett, D. A. Simultaneous Tissue Profiling of Eicosanoid and Endocannabinoid Lipid Families in a Rat Model of Osteoarthritis. *J. Lipid Res.* **2014**, *55* (9), 1902–1913.
- (26) Yue, H.; Jansen, S. A.; Strauss, K. I.; Borenstein, M. R.; Barbe, M. F.; Rossi, L. J.; Murphy, E. A Liquid Chromatography/Mass Spectrometric Method for Simultaneous Analysis of Arachidonic Acid and Its Endogenous Eicosanoid Metabolites Prostaglandins, Dihydroxyeicosatrienoic Acids, Hydroxyeicosatetraenoic Acids, and Epoxyeicosatrienoic Acids in Rat Brain Tissue. *J. Pharm. Biomed. Anal.* **2007**, *43* (3), 1122–1134.
- (27) Brose, S. A.; Baker, A. G.; Golovko, M. Y. A Fast One-Step Extraction and UPLC–MS/MS Analysis for E2/D2 Series Prostaglandins and Isoprostanes. *Lipids* **2013**, *48* (4), 411–419.
- (28) Shaik, J. S. B.; Miller, T. M.; Graham, S. H.; Manole, M. D.; Poloyac, S. M. Rapid and Simultaneous Quantitation of Prostanoids by UPLC–MS/MS in Rat Brain. *J. Chromatogr. B* **2014**, *945–946*, 207–216.
- (29) Phillis, J. W.; Horrocks, L. A.; Farooqui, A. A. Cyclooxygenases, Lipoxygenases, and Epoxygenases in CNS: Their Role and Involvement in Neurological Disorders. *Brain Res. Rev.* **2006**, *52* (2), 201–243.
- (30) Taha, A. Y.; Gao, F.; Ramadan, E.; Cheon, Y.; Rapoport, S. I.; Kim, H.-W. Upregulated Expression of Brain Enzymatic Markers of Arachidonic and Docosahexaenoic Acid Metabolism in a Rat Model of the Metabolic Syndrome. *BMC Neurosci.* **2012**, *13* (1), 131.
- (31) Yokota, K.; Tonai, T.; Horie, K.; Shono, F.; Yamamoto, S. Enzyme Immunoassay of Prostanoids in Human Blood and Urine. *Adv. Prostaglandin. Thromboxane. Leukot. Res.* **1985**, *15*, 33–34.
- (32) Tsikas, D. Quantitative Analysis of Eicosanoids in Biological Samples by LC–MS/MS: Mission Accomplished? *J. Chromatogr. B* **2016**, *1012–1013*, 211–214.
- (33) Tsikas, D.; Zoerner, A. A. Analysis of Eicosanoids by LC-MS/MS and GC-MS/MS: A Historical Retrospect and a Discussion. *J. Chromatogr. B* **2014**, *964*, 79–88.
- (34) Blewett, A. J.; Varma, D.; Gilles, T.; Libonati, J. R.; Jansen, S. A. Development and Validation of a High-Performance Liquid Chromatography-Electrospray Mass Spectrometry Method for the Simultaneous Determination of 23 Eicosanoids. *J. Pharm. Biomed. Anal.* **2008**, *46* (4), 653–662.
- (35) Masoodi, M.; Nicolaou, A. Lipidomic Analysis of Twenty-Seven Prostanoids and Isoprostanes by Liquid Chromatography/Electrospray Tandem Mass Spectrometry. *Rapid Commun. Mass Spectrom.* **2006**, *20* (20), 3023–3029.
- (36) Puppolo, M.; Varma, D.; Jansen, S. A. A Review of Analytical Methods for Eicosanoids in Brain Tissue. *J. Chromatogr. B* **2014**, *964*, 50–64.
- (37) Powell, W. S. Extraction of Eicosanoids from Biological Fluids, Cells, and Tissues. *Methods Mol. Biol. Clifton NJ* **1999**, *120*, 11–24.
- (38) Urban, M.; Enot, D. P.; Dallmann, G.; Körner, L.; Forcher, V.; Enoch, P.; Koal, T.; Keller, M.; Deigner, H.-P. Complexity and Pitfalls of Mass Spectrometry-Based Targeted Metabolomics in Brain Research. *Anal. Biochem.* **2010**, *406* (2), 124–131.
- (39) Dorow, J.; Becker, S.; Kortz, L.; Thiery, J.; Hauschildt, S.; Ceglarek, U. Preanalytical Investigation of Polyunsaturated Fatty Acids and Eicosanoids in Human Plasma by Liquid Chromatography–Tandem Mass Spectrometry. *Biopreservation Biobanking* **2016**, *14* (2), 107–113.
- (40) Miller, T. M.; Donnelly, M. K.; Crago, E. A.; Roman, D. M.; Sherwood, P. R.; Horowitz, M. B.; Poloyac, S. M. Rapid, Simultaneous Quantitation of Mono and Dioxygenated Metabolites of Arachidonic Acid in Human CSF and Rat Brain. *J. Chromatogr. B* **2009**, *877* (31), 3991–4000.

- (41) Liu, H.; Li, W.; Ahmad, M.; Rose, M. E.; Miller, T. M.; Yu, M.; Chen, J.; Pascoe, J. L.; Poloyac, S. M.; Hickey, R. W.; et al. Increased Generation of Cyclopentenone Prostaglandins after Brain Ischemia and Their Role in Aggregation of Ubiquitinated Proteins in Neurons. *Neurotox. Res.* **2013**, *24* (2), 191–204.
- (42) Furman, R.; Lee, J. V.; Axelsen, P. H. Analysis of Eicosanoid Oxidation Products in Alzheimer Brain by LC-MS with Uniformly ¹³C-Labeled Internal Standards. *Free Radic. Biol. Med.* **2018**, *118*, 108–118.
- (43) Golovko, M. Y.; Murphy, E. J. An Improved LC-MS/MS Procedure for Brain Prostanoid Analysis Using Brain Fixation with Head-Focused Microwave Irradiation and Liquid-Liquid Extraction. *J. Lipid Res.* **2008**, *49* (4), 893–902.
- (44) Masoodi, M.; Mir, A. A.; Petasis, N. A.; Serhan, C. N.; Nicolaou, A. Simultaneous Lipidomic Analysis of Three Families of Bioactive Lipid Mediators Leukotrienes, Resolvins, Protectins and Related Hydroxy-Fatty Acids by Liquid Chromatography/Electrospray Ionisation Tandem Mass Spectrometry. *Rapid Commun. Mass Spectrom.* **2008**, *22* (2), 75–83.
- (45) Strauss, K. I.; Gruzdev, A.; Zeldin, D. C. Altered Behavioral Phenotypes in Soluble Epoxide Hydrolase Knockout Mice: Effects of Traumatic Brain Injury. *Prostaglandins Other Lipid Mediat.* **2013**, *104–105*, 18–24.
- (46) Jouvène, C.; Fourmaux, B.; Géoïen, A.; Balas, L.; Durand, T.; Lagarde, M.; Létisse, M.; Guichardant, M. Ultra-Performance Liquid Chromatography-Mass Spectrometry Analysis of Free and Esterified Oxygenated Derivatives from Docosahexaenoic Acid in Rat Brain. *Lipids* **2018**, *53* (1), 103–116.
- (47) Folch, J.; Lees, M.; Sloane Stanley, G. H. A Simple Method for the Isolation and Purification of Total Lipides from Animal Tissues. *J. Biol. Chem.* **1957**, *226* (1), 497–509.
- (48) Bligh, E. G.; Dyer, W. J. A Rapid Method of Total Lipid Extraction and Purification. *Can. J. Biochem. Physiol.* **1959**, *37* (8), 911–917.
- (49) Tajima, Y.; Ishikawa, M.; Maekawa, K.; Murayama, M.; Senoo, Y.; Nishimaki-Mogami, T.; Nakanishi, H.; Ikeda, K.; Arita, M.; Taguchi, R.; et al. Lipidomic Analysis of Brain Tissues and Plasma in a Mouse Model Expressing Mutated Human Amyloid Precursor Protein/Tau for Alzheimer's Disease. *Lipids Health Dis.* **2013**, *12* (1), 68.
- (50) Saunders, R. D.; Horrocks, L. A. Simultaneous Extraction and Preparation for High-Performance Liquid Chromatography of Prostaglandins and Phospholipids. *Anal. Biochem.* **1984**, *143* (1), 71–75.
- (51) Lucci, P.; Pacetti, D.; Núñez, O.; Frega, N. G. Current Trends in Sample Treatment Techniques for Environmental and Food Analysis. *Chromatogr. - Most Versatile Method Chem. Anal.* **2012**.
- (52) Farias, S. E.; Basselin, M.; Chang, L.; Heidenreich, K. A.; Rapoport, S. I.; Murphy, R. C. Formation of Eicosanoids, E₂/D₂ Isoprostanes, and Docosanoids Following Decapitation-Induced Ischemia, Measured in High-Energy-Microwaved Rat Brain. *J. Lipid Res.* **2008**, *49* (9), 1990–2000.
- (53) Ostermann, A. I.; Willenberg, I.; Schebb, N. H. Comparison of Sample Preparation Methods for the Quantitative Analysis of Eicosanoids and Other Oxylipins in Plasma by Means of LC-MS/MS. *Anal. Bioanal. Chem.* **2015**, *407* (5), 1403–1414.
- (54) Ouyang, G.; Vuckovic, D.; Pawliszyn, J. Nondestructive Sampling of Living Systems Using *in Vivo* Solid-Phase Microextraction. *Chem. Rev.* **2011**, *111* (4), 2784–2814.
- (55) Miyazawa, M.; Kimura, M.; Yabe, Y.; Tsukamoto, D.; Sakamoto, M.; Horibe, I.; Okuno, Y. Use of Solid Phase Microextraction (SPME) for Profiling the Volatile Metabolites Produced by *Glomerella Cingulata*. *J. Oleo Sci.* **2008**, *57* (11), 585–590.
- (56) Loi, R. X.; Solar, M. C.; Weidenhamer, J. D. Solid-Phase Microextraction Method for *in Vivo* Measurement of Allelochemical Uptake. *J. Chem. Ecol.* **2008**, *34* (1), 70–75.

- (57) Félix, A.-E.; Genestier, G.; Malosse, C.; Calatayud, P.-A.; Le Rü, B.; Silvain, J.-F.; Frérot, B. Variability in Pheromone Communication among Different Haplotype Populations of *Busseola Fusca*. *J. Chem. Ecol.* **2009**, *35* (5), 618–623.
- (58) Vuckovic, D.; de Lannoy, I.; Gien, B.; Shirey, R. E.; Sidisky, L. M.; Dutta, S.; Pawliszyn, J. In Vivo Solid-Phase Microextraction: Capturing the Elusive Portion of Metabolome. *Angew. Chem. Int. Ed.* **2011**, *50* (23), 5344–5348.
- (59) Cudjoe, E.; Bojko, B.; de Lannoy, I.; Saldivia, V.; Pawliszyn, J. Solid-Phase Microextraction: A Complementary In Vivo Sampling Method to Microdialysis. *Angew. Chem. Int. Ed.* **2013**, *52* (46), 12124–12126.
- (60) Winshwe, T.; Mitsushima, D.; Nakajima, D.; Ahmed, S.; Yamamoto, S.; Tsukahara, S.; Kakeyama, M.; Goto, S.; Fujimaki, H. Toluene Induces Rapid and Reversible Rise of Hippocampal Glutamate and Taurine Neurotransmitter Levels in Mice. *Toxicol. Lett.* **2007**, *168* (1), 75–82.
- (61) Bessonneau, V.; Zhan, Y.; De Lannoy, I. A. M.; Saldivia, V.; Pawliszyn, J. In Vivo Solid-Phase Microextraction Liquid Chromatography–Tandem Mass Spectrometry for Monitoring Blood Eicosanoids Time Profile after Lipopolysaccharide-Induced Inflammation in Sprague-Dawley Rats. *J. Chromatogr. A* **2015**, *1424*, 134–138.
- (62) Kazakevich, Y. HPLC Theory. In *HPLC for Pharmaceutical Scientists*; Kazakevich, Y., LoBrutto, R., Eds.; John Wiley & Sons, Inc.: Hoboken, NJ, USA, 2006; pp 25–74.
- (63) Thakare, R.; Chhonker, Y. S.; Gautam, N.; Nelson, A.; Casaburi, R.; Criner, G.; Dransfield, M. T.; Make, B.; Schmid, K. K.; Rennard, S. I.; et al. Simultaneous LC-MS/MS Analysis of Eicosanoids and Related Metabolites in Human Serum, Sputum and BALF. *Biomed. Chromatogr.* **2018**, *32* (3), e4102.
- (64) Li, Y.; Lin, N.; Xu, J.; Lu, Y.; Chen, S.; Pan, C.; Wang, C.; Xu, M.; Zhou, B.; Xu, R.; et al. Measurement of Serum and Hepatic Eicosanoids by Liquid Chromatography Tandem-Mass Spectrometry (LC-MS/MS) in a Mouse Model of Hepatocellular Carcinoma (HCC) with Delivery of c-Met and Activated β -Catenin by Hepatocyte Hydrodynamic Injection. *Med. Sci. Monit. Int. Med. J. Exp. Clin. Res.* **2018**, *24*, 1670–1679.
- (65) Gouveia-Figueira, S.; Karimpour, M.; Bosson, J. A.; Blomberg, A.; Unosson, J.; Sehlstedt, M.; Pourazar, J.; Sandström, T.; Behndig, A. F.; Nording, M. L. Mass Spectrometry Profiling Reveals Altered Plasma Levels of Monohydroxy Fatty Acids and Related Lipids in Healthy Humans after Controlled Exposure to Biodiesel Exhaust. *Anal. Chim. Acta* **2018**, *1018*, 62–69.
- (66) Peng, L.; Sun, B.; Liu, M.; Huang, J.; Liu, Y.; Xie, Z.; He, J.; Chen, L.; Wang, D.; Zhu, Y.; et al. Plasma Metabolic Profile Reveals PGF 2α Protecting against Non-Proliferative Diabetic Retinopathy in Patients with Type 2 Diabetes. *Biochem. Biophys. Res. Commun.* **2018**, *496* (4), 1276–1283.
- (67) Ecker, J. Profiling Eicosanoids and Phospholipids Using LC-MS/MS: Principles and Recent Applications: Liquid Chromatography. *J. Sep. Sci.* **2012**, *35* (10–11), 1227–1235.
- (68) Kortz, L.; Dorow, J.; Becker, S.; Thiery, J.; Ceglarek, U. Fast Liquid Chromatography–Quadrupole Linear Ion Trap-Mass Spectrometry Analysis of Polyunsaturated Fatty Acids and Eicosanoids in Human Plasma. *J. Chromatogr. B* **2013**, *927*, 209–213.
- (69) Qu, W.; Bradbury, J. A.; Tsao, C.-C.; Maronpot, R.; Harry, G. J.; Parker, C. E.; Davis, L. S.; Breyer, M. D.; Waalkes, M. P.; Falck, J. R.; et al. Cytochrome P450 CYP2J9, a New Mouse Arachidonic Acid ω -1 Hydroxylase Predominantly Expressed in Brain. *J. Biol. Chem.* **2001**, *276* (27), 25467–25479.
- (70) Brose, S. A.; Thuen, B. T.; Golovko, M. Y. LC/MS/MS Method for Analysis of E $_2$ Series Prostaglandins and Isoprostanes. *J. Lipid Res.* **2011**, *52* (4), 850–859.
- (71) Neilson, A. P.; Ren, J.; Hong, Y. H.; Sen, A.; Smith, W. L.; Brenner, D. E.; Djuric, Z. Effect of Fish Oil on Levels of R- and S-Enantiomers of 5-, 12-, and 15 Hydroxyeicosatetraenoic Acids in Mouse Colonic Mucosa. *Nutr. Cancer* **2012**, *64* (1), 163–172.

- (72) Kiss, L.; Bier, J.; Röder, Y.; Weissmann, N.; Grimminger, F.; Seeger, W. Direct and Simultaneous Profiling of Epoxyeicosatrienoic Acid Enantiomers by Capillary Tandem Column Chiral-Phase Liquid Chromatography with Dual Online Photodiode Array and Tandem Mass Spectrometric Detection. *Anal. Bioanal. Chem.* **2008**, *392* (4), 717–726.
- (73) Mesaros, C.; Lee, S. H.; Blair, I. A. Analysis of Epoxyeicosatrienoic Acids by Chiral Liquid Chromatography/Electron Capture Atmospheric Pressure Chemical Ionization Mass Spectrometry Using [¹³C]-Analog Internal Standards. *Rapid Commun. Mass Spectrom. RCM* **2010**, *24* (22), 3237–3247.
- (74) Kumari A. Ubhayasekera, S. J.; Acharya, S. R.; Bergquist, J. A Novel, Fast and Sensitive Supercritical Fluid Chromatography-Tandem Mass Spectrometry (SFC-MS/MS) Method for Analysis of Arachidonic Acid Metabolites. *The Analyst* **2018**, *143* (15), 3661–3669.
- (75) Ando, A.; Satomi, Y. A Simple and Highly Sensitive Quantitation of Eicosanoids in Biological Samples Using Nano-Flow Liquid Chromatography/Mass Spectrometry. *Anal. Sci.* **2018**, *34* (2), 177–182.
- (76) Petta, T.; Moraes, L. A. B.; Faccioli, L. H. Versatility of Tandem Mass Spectrometry for Focused Analysis of Oxylipids: Focused Analysis of Oxylipids. *J. Mass Spectrom.* **2015**, *50* (7), 879–890.
- (77) Wang, N.; Zhao, X.; Wang, W.; Peng, Y.; Bi, K.; Dai, R. Targeted Profiling of Arachidonic Acid and Eicosanoids in Rat Tissue by UFLC-MS/MS: Application to Identify Potential Markers for Rheumatoid Arthritis. *Talanta* **2017**, *162*, 479–487.
- (78) Sanak, M.; Gielicz, A.; Nagraba, K.; Kaszuba, M.; Kumik, J.; Szczeklik, A. Targeted Eicosanoids Lipidomics of Exhaled Breath Condensate in Healthy Subjects. *J. Chromatogr. B Analyt. Technol. Biomed. Life. Sci.* **2010**, *878* (21), 1796–1800.
- (79) Davis, C. M.; Liu, X.; Alkayed, N. J. Cytochrome P450 Eicosanoids in Cerebrovascular Function and Disease. *Pharmacol. Ther.* **2017**, *179*, 31–46.
- (80) Imig, J. D. Epoxyeicosatrienoic Acids, 20-Hydroxyeicosatetraenoic Acid, and Renal Microvascular Function. *Prostaglandins Other Lipid Mediat.* **2013**, *104–105*, 2–7.
- (81) Zhang, Y.; Wang, M.-Y.; Huang, Q.-Y.; Zhu, M.-Z.; Ren, J.; Cao, X.; Xiong, W.-C.; Xiao, X.-D.; Zhu, X.-H. An Improved Ultra-High Performance Liquid Chromatography-Tandem Mass Spectrometry Method for Simultaneous Quantitation of Cytochrome P450 Metabolites of Arachidonic Acid in Human Plasma. *J. Chromatogr. A* **2018**, *1563*, 144–153.
- (82) Miller, T. M.; Poloyac, S. M.; Anderson, K. B.; Waddell, B. L.; Messamore, E.; Yao, J. K. A Rapid UPLC-MS/MS Assay for Eicosanoids in Human Plasma: Application to Evaluate Niacin Responsivity. *Prostaglandins Leukot. Essent. Fatty Acids* **2018**, *136*, 153–159.
- (83) Wang, N.; Dai, R.; Wang, W.; Peng, Y.; Zhao, X.; Bi, K. Simultaneous Profiling of Eicosanoid Metabolome in Plasma by UPLC-MS/MS Method: Application to Identify Potential Makers for Rheumatoid Arthritis. *Talanta* **2016**, *161*, 157–164.
- (84) Watrous, J. D.; Niiranen, T. J.; Lagerborg, K. A.; Henglin, M.; Xu, Y.-J.; Rong, J.; Sharma, S.; Vasan, R. S.; Larson, M. G.; Armando, A.; et al. Directed Non-Targeted Mass Spectrometry and Chemical Networking for Discovery of Eicosanoids and Related Oxylipins. *Cell Chem. Biol.* **2019**.
- (85) Willenberg, I.; Ostermann, A. I.; Schebb, N. H. Targeted Metabolomics of the Arachidonic Acid Cascade: Current State and Challenges of LC-MS Analysis of Oxylipins. *Anal. Bioanal. Chem.* **2015**, *407* (10), 2675–2683.
- (86) Berkecz, R.; Lása, M.; Holčapek, M. Analysis of Oxylipins in Human Plasma: Comparison of Ultrahigh-Performance Liquid Chromatography and Ultrahigh-Performance Supercritical Fluid Chromatography Coupled to Mass Spectrometry. *J. Chromatogr. A* **2017**, *1511*, 107–121.
- (87) Lubin, A.; Geerinckx, S.; Bajic, S.; Cabooter, D.; Augustijns, P.; Cuyckens, F.; Vreeken, R. J. Enhanced Performance for the Analysis of Prostaglandins and Thromboxanes by Liquid Chromatography-

- Tandem Mass Spectrometry Using a New Atmospheric Pressure Ionization Source. *J. Chromatogr. A* **2016**, *1440*, 260–265.
- (88) Ban, G.-Y.; Cho, K.; Kim, S.-H.; Yoon, M. K.; Kim, J.-H.; Lee, H. Y.; Shin, Y. S.; Ye, Y.-M.; Cho, J.-Y.; Park, H.-S. Metabolomic Analysis Identifies Potential Diagnostic Biomarkers for Aspirin-Exacerbated Respiratory Disease. *Clin. Exp. Allergy* **2017**, *47* (1), 37–47.
- (89) Mazaleuskaya, L. L.; Salamatipour, A.; Sarantopoulou, D.; Weng, L.; FitzGerald, G. A.; Blair, I. A.; Mesaros, C. Analysis of HETEs in Human Whole Blood by Chiral UHPLC-ECAPCI/HRMS. *J. Lipid Res.* **2018**, *59* (3), 564–575.
- (90) Yasumoto, A.; Tokuoka, S. M.; Kita, Y.; Shimizu, T.; Yatomi, Y. Multiplex Quantitative Analysis of Eicosanoid Mediators in Human Plasma and Serum: Possible Introduction into Clinical Testing. *J. Chromatogr. B* **2017**, *1068–1069*, 98–104.
- (91) Wang, Y.; Armando, A. M.; Quehenberger, O.; Yan, C.; Dennis, E. A. Comprehensive Ultra-Performance Liquid Chromatographic Separation and Mass Spectrometric Analysis of Eicosanoid Metabolites in Human Samples. *J. Chromatogr. A* **2014**, *1359*, 60–69.
- (92) Matuszewski, B. K.; Constanzer, M. L.; Chavez-Eng, C. M. Strategies for the Assessment of Matrix Effect in Quantitative Bioanalytical Methods Based on HPLC–MS/MS. *Anal. Chem.* **2003**, *75* (13), 3019–3030.
- (93) Kortz, L.; Dorow, J.; Ceglarek, U. Liquid Chromatography–Tandem Mass Spectrometry for the Analysis of Eicosanoids and Related Lipids in Human Biological Matrices: A Review. *J. Chromatogr. B* **2014**, *964*, 1–11.
- (94) Astarita, G.; Kendall, A. C.; Dennis, E. A.; Nicolaou, A. Targeted Lipidomic Strategies for Oxygenated Metabolites of Polyunsaturated Fatty Acids. *Biochim. Biophys. Acta BBA - Mol. Cell Biol. Lipids* **2015**, *1851* (4), 456–468.
- (95) Rago, B.; Fu, C. Development of a High-Throughput Ultra Performance Liquid Chromatography–Mass Spectrometry Assay to Profile 18 Eicosanoids as Exploratory Biomarkers for Atherosclerotic Diseases. *J. Chromatogr. B* **2013**, *936*, 25–32.
- (96) Deems, R.; Buczynski, M. W.; Bowers-Gentry, R.; Harkewicz, R.; Dennis, E. A. Detection and Quantitation of Eicosanoids via High Performance Liquid Chromatography-Electrospray Ionization-Mass Spectrometry. *Methods Enzymol.* **2007**, *432*, 59–82.
- (97) Yang, J.; Schmelzer, K.; Georgi, K.; Hammock, B. D. Quantitative Profiling Method for Oxylipin Metabolome by Liquid Chromatography Electrospray Ionization Tandem Mass Spectrometry. *Anal. Chem.* **2009**, *81* (19), 8085–8093.
- (98) Galvão, A. F.; Petta, T.; Flamand, N.; Bollela, V. R.; Silva, C. L.; Jarduli, L. R.; Malmegrim, K. C. R.; Simões, B. P.; de Moraes, L. A. B.; Faccioli, L. H. Plasma Eicosanoid Profiles Determined by High-Performance Liquid Chromatography Coupled with Tandem Mass Spectrometry in Stimulated Peripheral Blood from Healthy Individuals and Sick Cell Anemia Patients in Treatment. *Anal. Bioanal. Chem.* **2016**, *408* (13), 3613–3623.
- (99) Souverain, S.; Rudaz, S.; Veuthey, J.-L. Protein Precipitation for the Analysis of a Drug Cocktail in Plasma by LC–ESI–MS. *J. Pharm. Biomed. Anal.* **2004**, *35* (4), 913–920.
- (100) Polson, C.; Sarkar, P.; Inledon, B.; Raguvaran, V.; Grant, R. Optimization of Protein Precipitation Based upon Effectiveness of Protein Removal and Ionization Effect in Liquid Chromatography–Tandem Mass Spectrometry. *J. Chromatogr. B* **2003**, *785* (2), 263–275.
- (101) Zhang, X.; Yang, N.; Ai, D.; Zhu, Y. Systematic Metabolomic Analysis of Eicosanoids after Omega-3 Polyunsaturated Fatty Acid Supplementation by a Highly Specific Liquid Chromatography–Tandem Mass Spectrometry-Based Method. *J. Proteome Res.* **2015**, *14* (4), 1843–1853.
- (102) Human Metabolome Database <http://www.hmdb.ca/> (accessed Nov 15, 2018).
- (103) Monnin, C.; Ramrup, P.; Daigle-Young, C.; Vuckovic, D. Improving Negative Liquid Chromatography/Electrospray Ionization Mass Spectrometry Lipidomic Analysis of Human Plasma

- Using Acetic Acid as a Mobile-Phase Additive. *Rapid Commun. Mass Spectrom.* **2018**, 32 (3), 201–211.
- (104) Suhr, A. C.; Bruegel, M.; Maier, B.; Holdt, L. M.; Kleinhempel, A.; Teupser, D.; Grimm, S. H.; Vogeser, M. Ferromagnetic Particles as a Rapid and Robust Sample Preparation for the Absolute Quantification of Seven Eicosanoids in Human Plasma by UHPLC–MS/MS. *J. Chromatogr. B* **2016**, 1022, 173–182.
- (105) Hu, T.; Tie, C.; Wang, Z.; Zhang, J.-L. Highly Sensitive and Specific Derivatization Strategy to Profile and Quantitate Eicosanoids by UPLC-MS/MS. *Anal. Chim. Acta* **2017**, 950, 108–118.
- (106) Liu, X.; Davis, C. M.; Alkayed, N. J. P450 Eicosanoids and Reactive Oxygen Species Interplay in Brain Injury and Neuroprotection. *Antioxid. Redox Signal.* **2018**, 28(10), 987-1007
- (107) Aronoff, D. M.; Romanovsky, A. A. Eicosanoids in Non-Febrile Thermoregulation. *Prog. Brain Res.* **2007**, 162, 15–25.
- (108) Hayaishi, O. Invited Review: Molecular Genetic Studies on Sleep-Wake Regulation, with Special Emphasis on the Prostaglandin D2 System. *J. Appl. Physiol.* **2002**, 92 (2), 863–868.
- (109) Chen, C.; Bazan, N. G. Lipid Signaling: Sleep, Synaptic Plasticity, and Neuroprotection. *Prostaglandins Other Lipid Mediat.* **2005**, 77 (1–4), 65–76.
- (110) Ito, S.; Okuda-Ashitaka, E.; Minami, T. Central and Peripheral Roles of Prostaglandins in Pain and Their Interactions with Novel Neuropeptides Nociceptin and Nocistatin. *Neurosci. Res.* **2001**, 41 (4), 299–332.
- (111) Shishehbor, M. H.; Zhang, R.; Medina, H.; Brennan, M.-L.; Brennan, D. M.; Ellis, S. G.; Topol, E. J.; Hazen, S. L. Systemic Elevations of Free Radical Oxidation Products of Arachidonic Acid Are Associated with Angiographic Evidence of Coronary Artery Disease. *Free Radic. Biol. Med.* **2006**, 41 (11), 1678–1683.
- (112) Tam, V. C.; Quehenberger, O.; Oshansky, C. M.; Suen, R.; Armando, A. M.; Treuting, P. M.; Thomas, P. G.; Dennis, E. A.; Aderem, A. Lipidomic Profiling of Influenza Infection Identifies Mediators That Induce and Resolve Inflammation. *Cell* **2013**, 154 (1), 213–227.
- (113) Sugimoto, M. A.; Sousa, L. P.; Pinho, V.; Perretti, M.; Teixeira, M. M. Resolution of Inflammation: What Controls Its Onset? *Front. Immunol.* **2016**, 7, 160.
- (114) Trépanier, M.-O.; Eiden, M.; Morin-Rivron, D.; Bazinet, R. P.; Masoodi, M. High-Resolution Lipidomics Coupled with Rapid Fixation Reveals Novel Ischemia-Induced Signaling in the Rat Neurolipidome. *J. Neurochem.* **2017**, 140 (5), 766–775. <https://doi.org/10.1111/jnc.13934>.
- (115) Golovko, M. Y.; Murphy, E. J. Brain Prostaglandin Formation Is Increased by α -Synuclein Gene-Ablation during Global Ischemia. *Neurosci. Lett.* **2008**, 432 (3), 243–247.
- (116) Sun, L.; Stenzen, J. A. Improving Microdialysis Extraction Efficiency of Lipophilic Eicosanoids. *J. Pharm. Biomed. Anal.* **2003**, 33 (5), 1059–1071.
- (117) Alfredson, H.; Thorsen, K.; Lorentzon, R. In Situ Microdialysis in Tendon Tissue: High Levels of Glutamate, but Not Prostaglandin E2 in Chronic Achilles Tendon Pain. *Knee Surg. Sports Traumatol. Arthrosc. Off. J. ESSKA* **1999**, 7 (6), 378–381.
- (118) Karamouzis, M.; Karamouzis, I.; Vamvakoudis, E.; Ampatzidis, G.; Christoulas, K.; Angelopoulou, N.; Mandroukas, K. The Response of Muscle Interstitial Prostaglandin E(2)(PGE(2)), Prostacyclin I(2)(PGI(2)) and Thromboxane A(2)(TXA(2)) Levels during Incremental Dynamic Exercise in Humans Determined by in Vivo Microdialysis. *Prostaglandins Leukot. Essent. Fatty Acids* **2001**, 64 (4–5), 259–263.
- (119) Łazarewicz, J. W.; Salińska, E.; Stafiej, A.; Ziembowicz, A.; Ziemińska, E. NMDA Receptors and Nitric Oxide Regulate Prostaglandin D2 Synthesis in the Rabbit Hippocampus in Vivo. *Acta Neurobiol. Exp. (Warsz.)* **2000**, 60 (4), 427–435.
- (120) Pepicelli, O.; Fedele, E.; Berardi, M.; Raiteri, M.; Levi, G.; Greco, A.; Ajmone-Cat, M. A.; Minghetti, L. Cyclo-Oxygenase-1 and -2 Differently Contribute to Prostaglandin E2 Synthesis and Lipid

- Peroxidation after in Vivo Activation of N-Methyl-D-Aspartate Receptors in Rat Hippocampus. *J. Neurochem.* **2005**, *93* (6), 1561–1567.
- (121) Kondo, F.; Tachi, M.; Gosho, M.; Fukayama, M.; Yoshikawa, K.; Okada, S. Changes in Hypothalamic Neurotransmitter and Prostanoid Levels in Response to NMDA, CRF, and GLP-1 Stimulation. *Anal. Bioanal. Chem.* **2015**, *407* (18), 5261–5272.
- (122) Clausen, F.; Marklund, N.; Lewén, A.; Enblad, P.; Basu, S.; Hillered, L. Interstitial F2-Isoprostane 8-Iso-PGF2 α As a Biomarker of Oxidative Stress after Severe Human Traumatic Brain Injury. *J. Neurotrauma* **2011**, *29* (5), 766–775.
- (123) Vuckovic, D.; Risticvic, S.; Pawliszyn, J. In Vivo Solid-Phase Microextraction in Metabolomics: Opportunities for the Direct Investigation of Biological Systems. *Angew. Chem. Int. Ed.* **2011**, *50* (25), 5618–5628.
- (124) Chong, J.; Xia, J. MetaboAnalystR: An R Package for Flexible and Reproducible Analysis of Metabolomics Data. *Bioinforma. Oxf. Engl.* **2018**, *34* (24), 4313–4314.
- (125) Chong, J.; Soufan, O.; Li, C.; Caraus, I.; Li, S.; Bourque, G.; Wishart, D. S.; Xia, J. MetaboAnalyst 4.0: Towards More Transparent and Integrative Metabolomics Analysis. *Nucleic Acids Res.* **2018**, *46* (W1), W486–W494.
- (126) Yuan, Z.-X.; Rapoport, S. I. Transient Postnatal Fluoxetine Decreases Brain Concentrations of 20-HETE and 15-Epi-LXA4, Arachidonic Acid Metabolites in Adult Mice. *Prostaglandins Leukot. Essent. Fatty Acids* **2015**, *101*, 9–14.
- (127) Hennebelle, M.; Zhang, Z.; Metherel, A. H.; Kitson, A. P.; Otoki, Y.; Richardson, C. E.; Yang, J.; Lee, K. S. S.; Hammock, B. D.; Zhang, L.; et al. Linoleic Acid Participates in the Response to Ischemic Brain Injury through Oxidized Metabolites That Regulate Neurotransmission. *Sci. Rep.* **2017**, *7* (1).
- (128) Crago, E. A.; Thampatty, B. P.; Sherwood, P. R.; Kuo, C.-W. J.; Bender, C.; Balzer, J.; Horowitz, M.; Poloyac, S. M. Cerebrospinal Fluid 20-HETE Is Associated with Delayed Cerebral Ischemia and Poor Outcomes after Aneurysmal Subarachnoid Hemorrhage. *Stroke* **2011**, *42* (7), 1872–1877.
- (129) Derogis, P. B. M. C.; Freitas, F. P.; Marques, A. S. F.; Cunha, D.; Appolinário, P. P.; de Paula, F.; Lourenço, T. C.; Murgu, M.; Di Mascio, P.; Medeiros, M. H. G.; et al. The Development of a Specific and Sensitive LC-MS-Based Method for the Detection and Quantification of Hydroperoxy- and Hydroxydocosahexaenoic Acids as a Tool for Lipidomic Analysis. *PLoS ONE* **2013**, *8* (10), e77561.
- (130) Devassy, J. G.; Leng, S.; Gabbs, M.; Monirujjaman, M.; Aukema, H. M. Omega-3 Polyunsaturated Fatty Acids and Oxylipins in Neuroinflammation and Management of Alzheimer Disease. *Adv. Nutr. Bethesda Md* **2016**, *7* (5), 905–916.
- (131) Volle, J.; Bregman, T.; Scott, B.; Diwan, M.; Raymond, R.; Fletcher, P. J.; Nobrega, J. N.; Hamani, C. Deep Brain Stimulation and Fluoxetine Exert Different Long-Term Changes in the Serotonergic System. *Neuropharmacology* **2018**, *135*, 63–72.

Appendix A: Supplementary information for Chapters 2 and 3

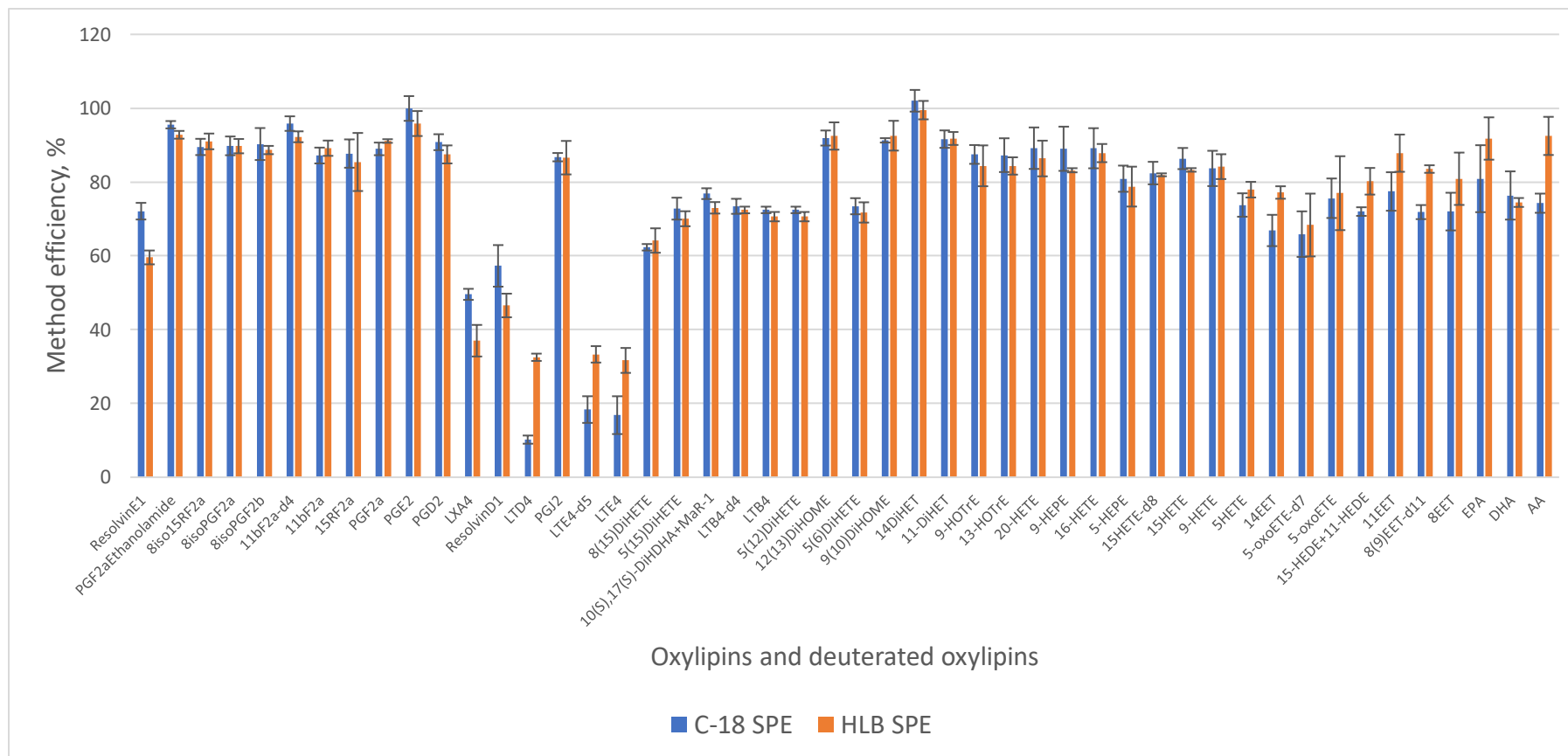


Figure S1 Comparison of method efficiency of HLB and C-18 SPE for the analysis of 3.125 ng/mL oxylipin standard without pre-concentration factor ($n=3$). Hydrophilic-lipophilic-balanced sorbent (Oasis HLB) (3 cc, 60 mg, average particle diameter 29.2 μm , Waters, Massachusetts, USA) and C-18 (Strata Phenomenex 200mg) SPE was performed as follows: (i) conditioning with 1 ml 100% MeOH and 1 ml 20% MeOH, (ii) loading 500 μl of 3.125 ng/ml mix of (61) standards in 20% MeOH, (iii) washing with 1 ml of 20% MeOH, (iv) elution with 1 ml of 99% MeOH +1% Hac in glass tube containing 20 μl 30% Glycerol in MeOH, (v) evaporation in speedvac followed by reconstitution in 500 μl MeOH and injection into LC-MS. The method efficiency was calculated using the following formula Method efficiency % = $A_{\text{spe}}/A_{\text{std}} * 100\%$, where A_{spe} is the average peak area of standard after SPE extraction and A_{std} is the peak area of the standard of the same concentration in solvent that did not undergo SPE. Error bars = $\pm\text{SD}$

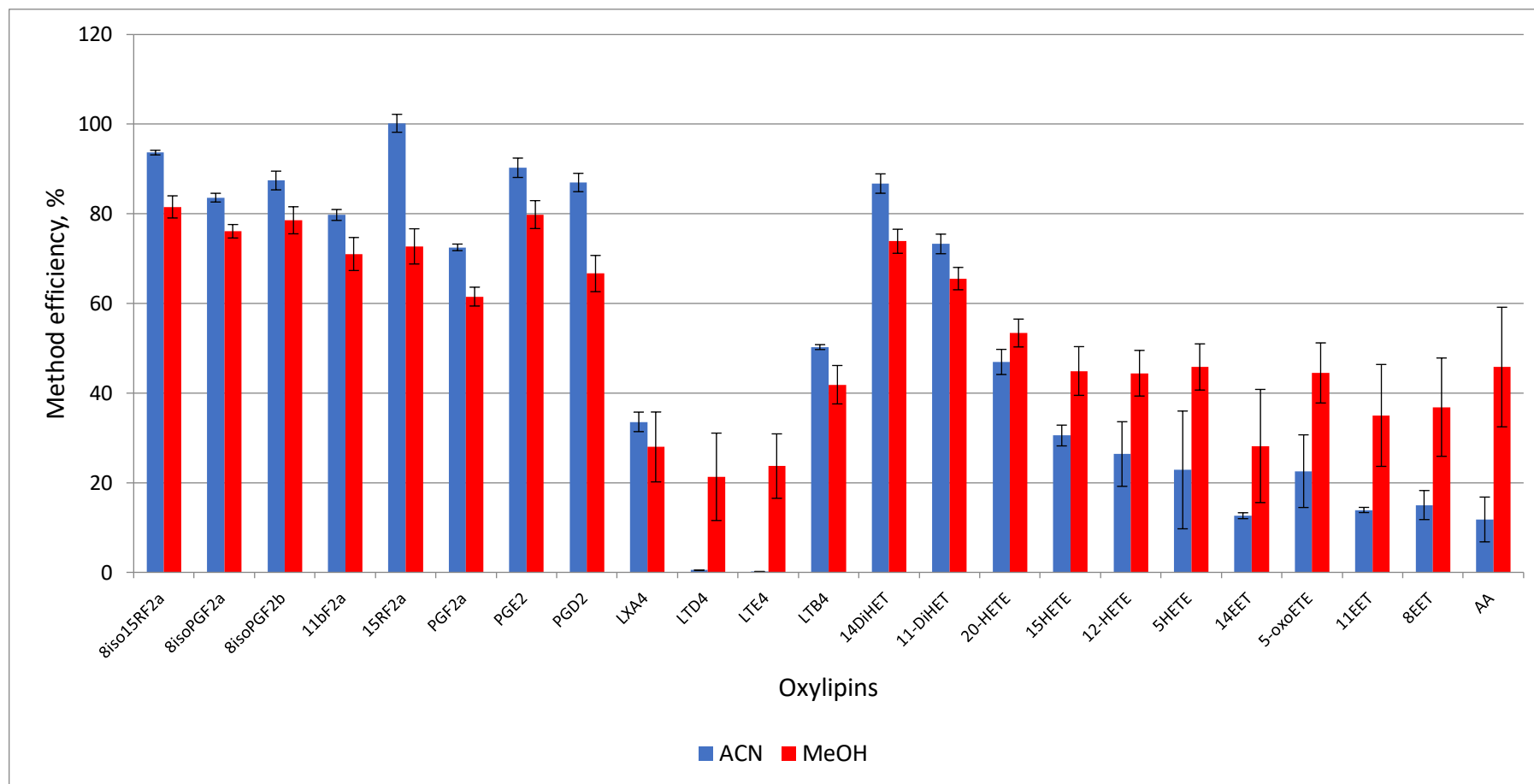


Figure S2 Comparison of ACN and MeOH as elution solvent for C-18 SPE. C-18 (Strata Phenomenex 200 mg) SPE were performed at steps (i)-(iii) as at Figure S1, (iv) elution was performed with 1 ml of 100% MeOH (n=3) or 100% ACN (n=3) in glass tubes and (v) transfer 100 μ l of eluent to HPLC glass inserts for LC-MS analysis. Method efficiency was calculated as in Figure S1. PGs, LXA₄, LTB₄ and DiHETs showed 10-20% higher recovery with ACN elution, however more hydrophobic HETEs, EETs and AA showed in most cases two times higher recovery with MeOH elution, also LTE₄ and LTD₄ where eluted only with MeOH. In the follow-up experiment additional elution with 1 ml of ethyl acetate was performed after elution with MeOH. The eluents were collected in separate glass tubes, evaporated in speedvac to dryness, reconstituted and injected into LC-MS. Oxylipins were not detected in EtAc eluent. So, MeOH was chosen as elution solvent for the final method.

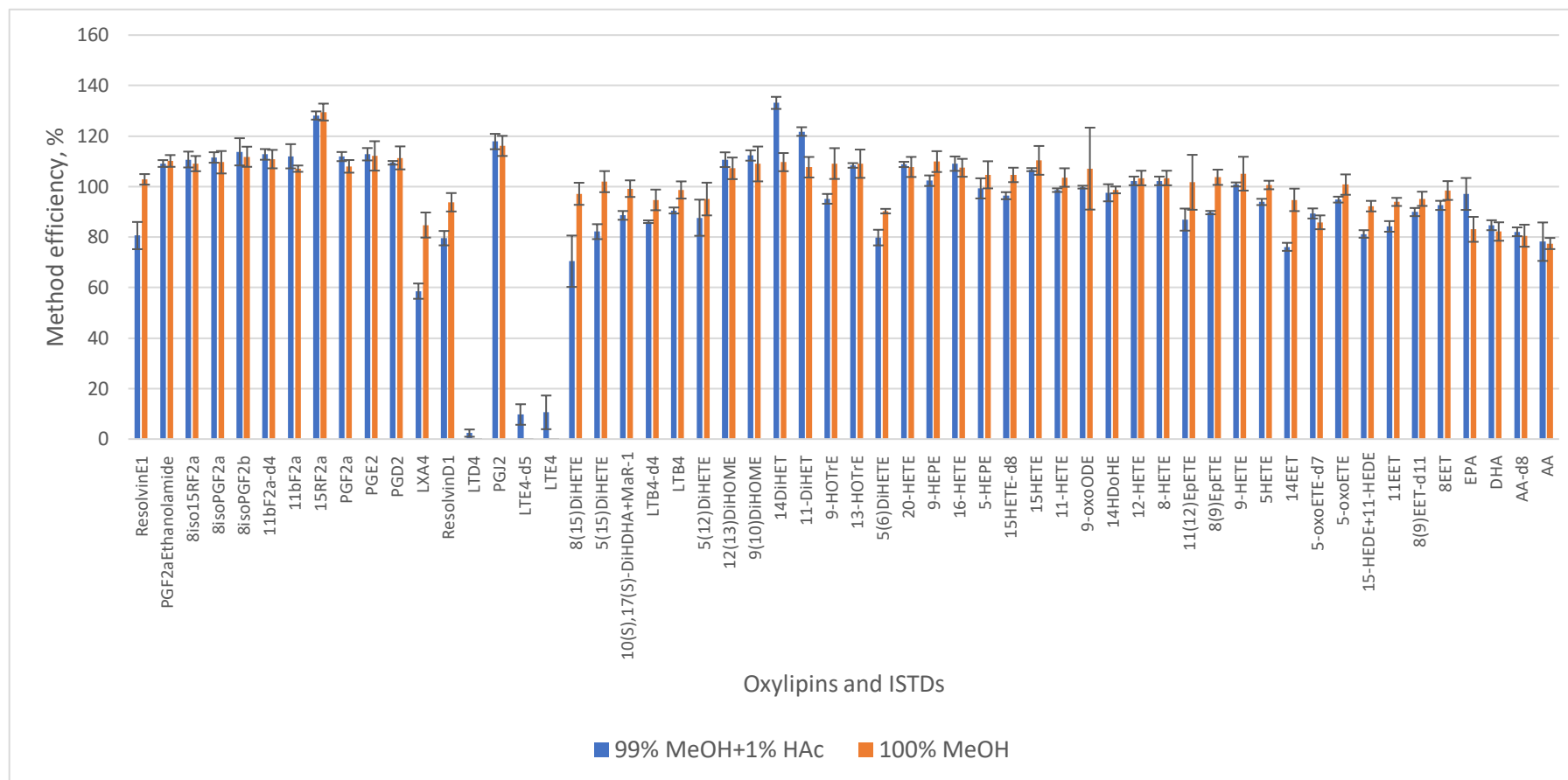


Figure S3 Comparison of method efficiency with and without acid in elution solvent. C-18 (Strata Phenomenex 200mg) SPE were performed at steps (i)-(iii) as at Figure S1, (iii) elution was performed with 100% MeOH and 99% MeOH with 1% HAc (n=3 replicates for each condition). After elution samples were evaporated in speedvac and reconstituted in 100 µl of 100% MeOH. Method efficiency was calculated as in Figure S1. It was assumed that acidification of elution solvent helps to keep oxylipins in protonated form that prevents secondary interaction of oxylipins with silica of stationary phase during elution. Experiment showed that elution with acetic acid in solvent gives slightly higher method efficiency for one oxylipins and slightly lower for others, however presence of acid in solvent is critical for recovery of LTE₄ and LTD₄. Elution with 1% and 4% acetic acid showed comparable recoveries (data not shown) so it was decided to use lower concentration of acetic acid in final method. Methanol volume was further optimized and 1ml was determined as optimal elution volume.

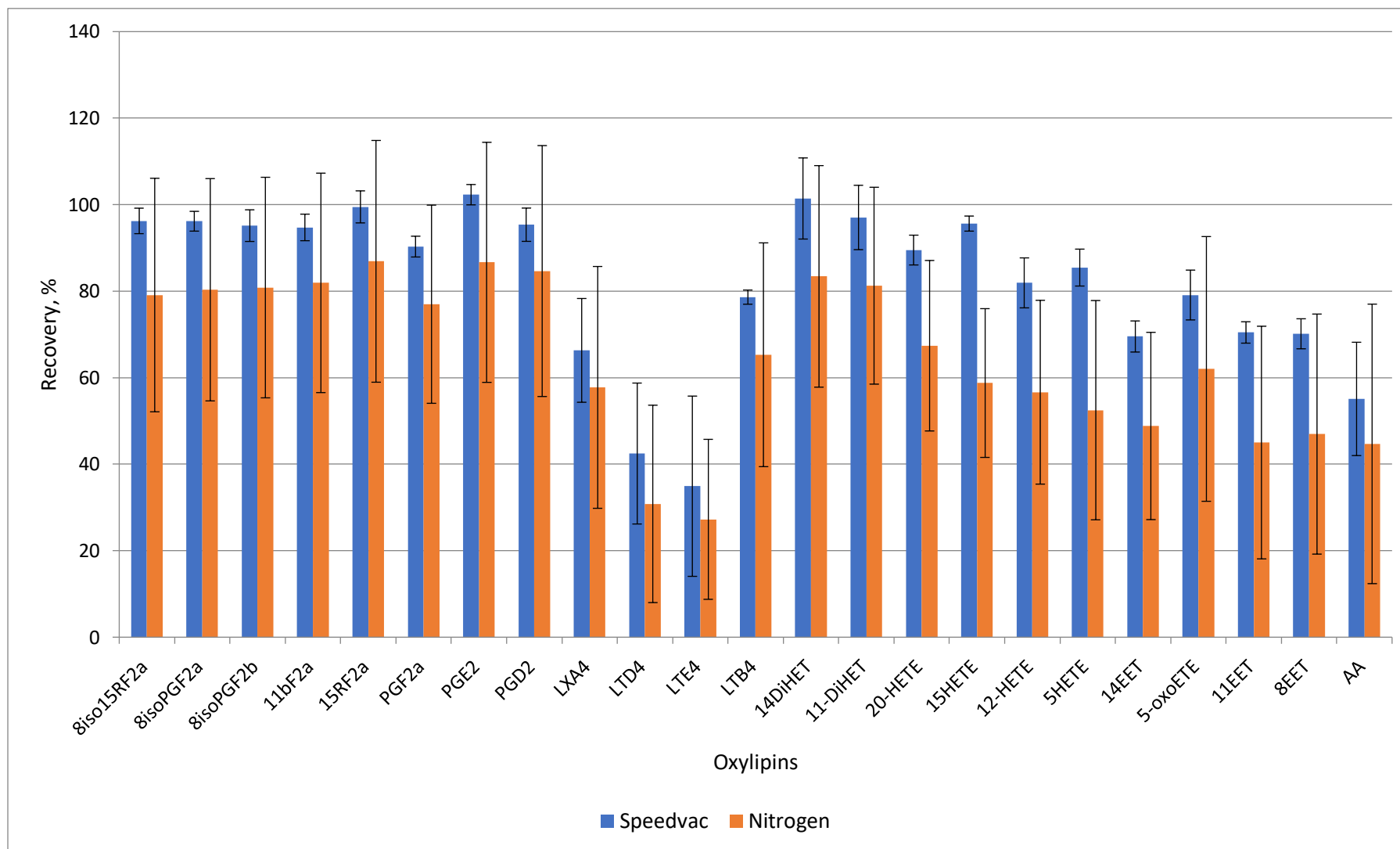


Figure S4 Comparison of speedvac and nitrogen evaporation. 100 μ l of 20 ng/ml of oxylipin standards were added to glass amber round bottom tubes and evaporated in speedvac (n=3 replicates) and 100 μ l were added to glass LC vial and evaporated under stream of nitrogen. After evaporation all samples were reconstituted in 100 μ l MeOH and injected into LC-MS. Recovery was calculated as method efficiency in Figure S1.

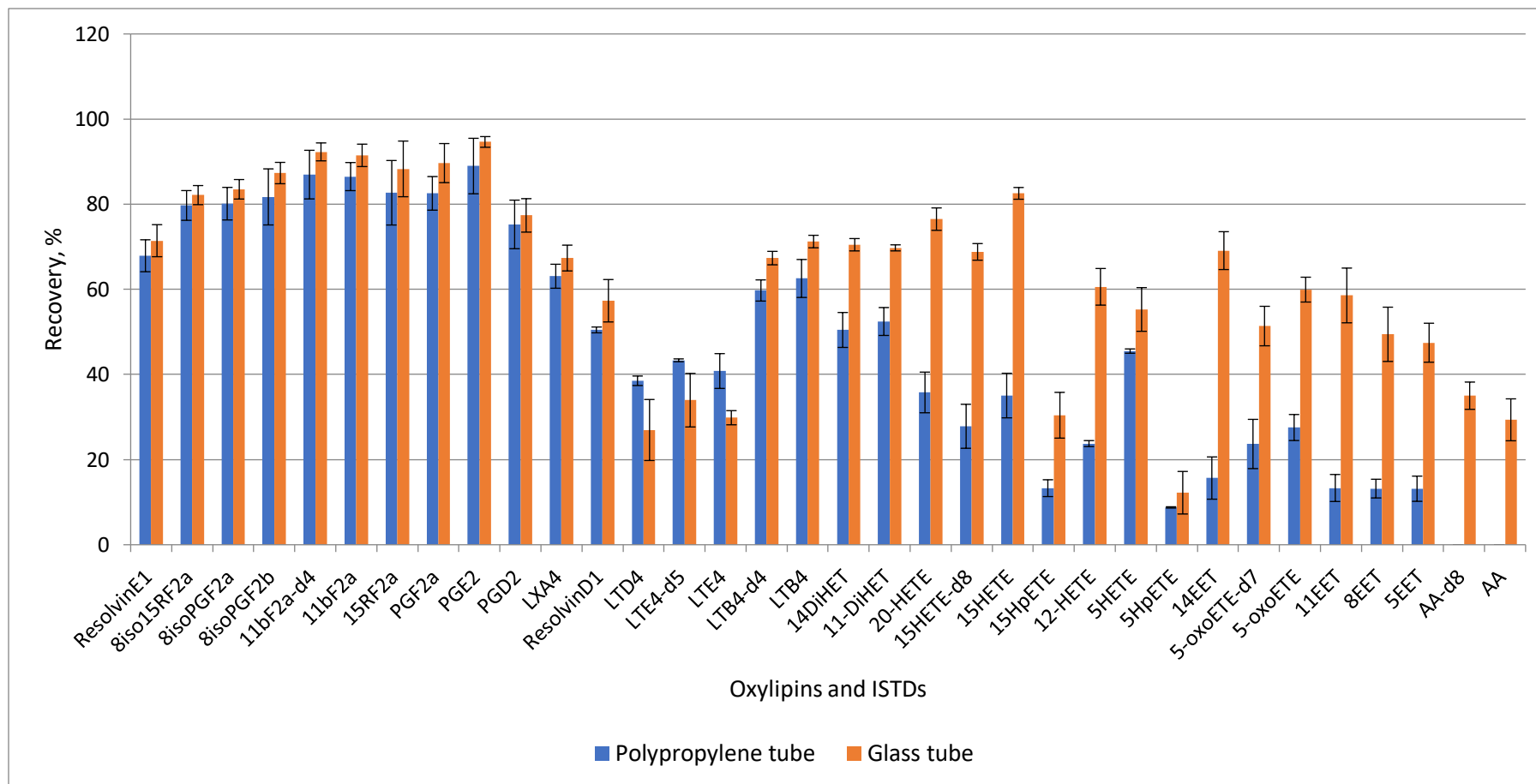


Figure S5 Comparison of glass and polypropylene tubes. 100 μ l of 5 ng/ml of oxylipin mix were added to glass amber round bottom tubes (n=3) and to polypropylene Eppendorf tubes (n=3) and evaporated in speedvac. After evaporation all samples were reconstituted in 100 μ l MeOH and injected into LC-MS. Recovery was calculated as method efficiency in Figure S1. It was assumed that material which tubes for evaporation are made could influence on amount of losses of oxylipins during evaporation. For more hydrophilic PGs, LTB₄ and DiHETs recovery was slightly higher in glass tubes, for leukotriens D₄ and E₄ recovery was slightly higher in plastic tubes but for more hydrophobic HETEs and EETs recovery in glass tubes was 2-5 times higher than in plastic, most hydrophobic AA was not observed at all after evaporation in plastic tubes. That can be explained by that more hydrophobic oxylipins have stronger interactions with hydrophobic polypropylene. Despite glass tubes have less interactions with oxylipins during evaporation 20-60% losses are observed.

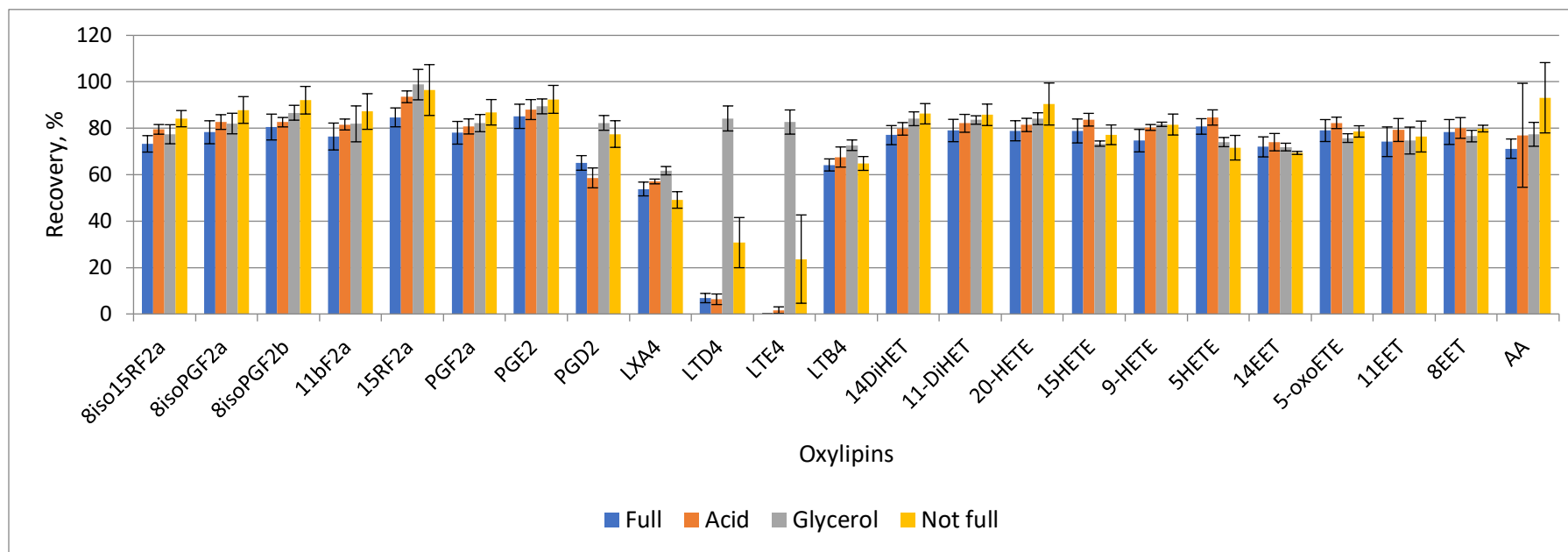


Figure S6 Optimization of speedvac evaporation 100 μ l of 20 ng/ml of oxylipin standards were added to six 1 ml glass amber round bottom tubes that were not pretreated with anything, 100 μ l were added to three glass tubes that were washed with concentrated acetic acid, 100 μ l were added to three glass tubes where 6 μ l of 30% glycerol in MeOH were added. Samples in three tubes that were without any treatments were evaporated to 2 μ l on the bottom of the tube, other nine samples were evaporated to dryness (in case of samples with glycerol after evaporation of solvent 2 μ l of the glycerol left on the bottom of the tube). After evaporation all samples were reconstituted in 100% MeOH and injected into LC-MS. Recovery was calculated as in Figure S1. The second way is to treat wall of the glass tubes with concentrated acid before loading the samples into the tube. Glass tubes may have negatively charged silica groups on their surface and these groups can be protonated by acid. The third way is addition 30% glycerol in methanol at the bottom of the tube before loading of the sample. The idea is that after full evaporation of solvent only small known amount of glycerol that cannot be evaporated at these conditions will be on the bottom of the tube and all oxylipins from the solvent will stick to this glycerol and during reconstitution glycerol will be dissolved in solvent and oxylipins as well. Comparison of these ways of evaporation in speedvac showed following trend for most oxylipins recovery was slightly growing from full evaporation and no treatment-treatment with acid-addition of glycerol-not full evaporation. Exception was observed only leukotriens D₄ and E₄ that showed 85% recovery in tubes with addition of glycerol comparatively to 30% recovery in tubes where not full evaporation was performed. So for the final sample preparation method addition of 20 μ l of 30% MeOH before loading of the sample to the 1 ml glass tube for evaporation in speedvac (volume was increased from initial 6 μ l because of wide diameter of the bottom of the tube, 2 μ l of glycerol is not enough to cover full bottom).

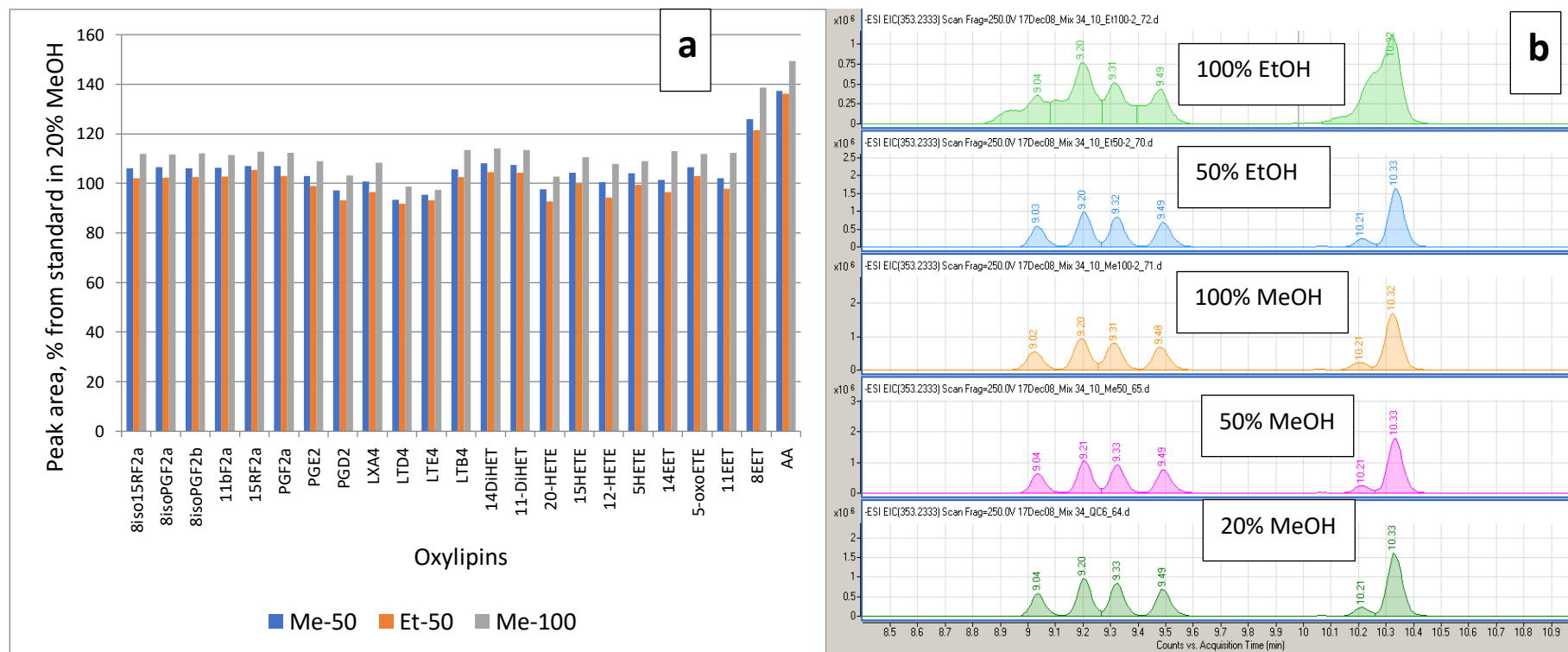


Figure S7 Assessment of reconstitution/injection solvent. (a) Peak area of standards injected in 50 and 100% MeOH and 50% EtOH relatively to standard injected in 20% MeOH. (b) EICs at m/z 353.2333 for standards injected in different solvents. Reconstitution after evaporation is important step as well because recovery of oxylipins strongly depends on efficiency of reconstitution. However, to obtain highest enrichment we have to use as lower volume of reconstitution as possible and at the same time this volume should be enough to reconstitute and remove all analytes without additional losses. At initial method reconstitution was performed in two steps: addition of 20 μ l of 100% MeOH to reconstitute majority of oxylipins on the bottom of the tube and then addition 80 μ l of water to be able to wash walls of the tube and to decrease level of organic phase to 20% because in initial method samples before injection should have been in 20% organic. However, 100 μ l is high volume that does not allow preconcentration e.g. 100 μ l samples. Possibility of injection of oxylipins in other percentages of organic phase was assessed. It was found that injection of oxylipins in 50% and 100% of MeOH does not influence in peak area, peak shape and RT, so it was decided to inject samples from 100% MeOH. And this is allowing to decrease volume of reconstitution solvent and optimal volume was found (data not shown). In final method reconstitution performed by addition of 40 μ l of 100% MeOH with subsequent vortexing. Using of this volume show good reproducibility, high recovery and allows at least two injections of sample (injection volume in the method is 10 μ l) and allows preconcentration of even small volume samples (100 μ l).

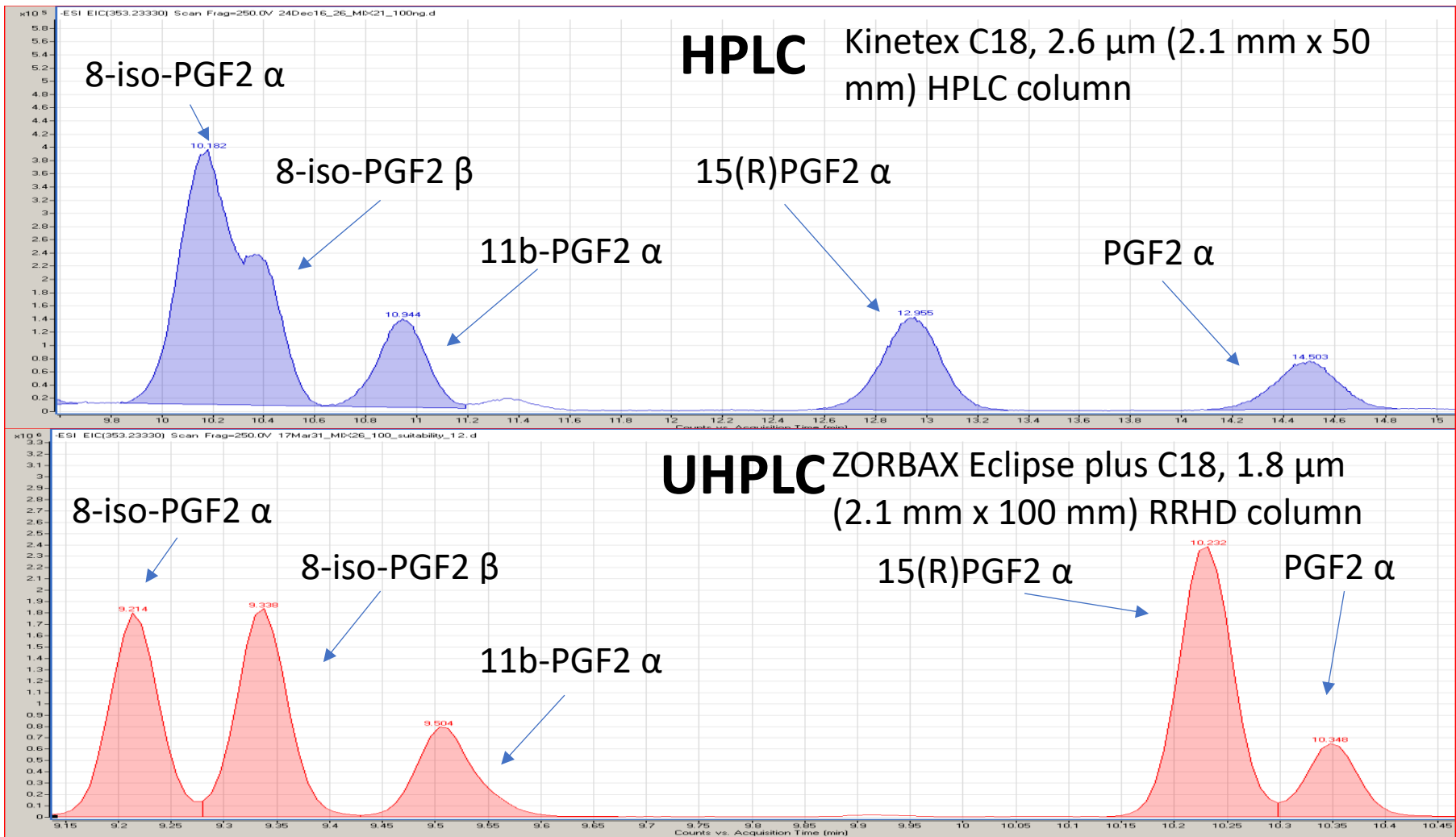


Figure S8 EICs of 100 ng/ml oxylipin standard showing the separation of PGF₂a isomers on Zorbax UHPLC and Kinetex core-shell HPLC columns.

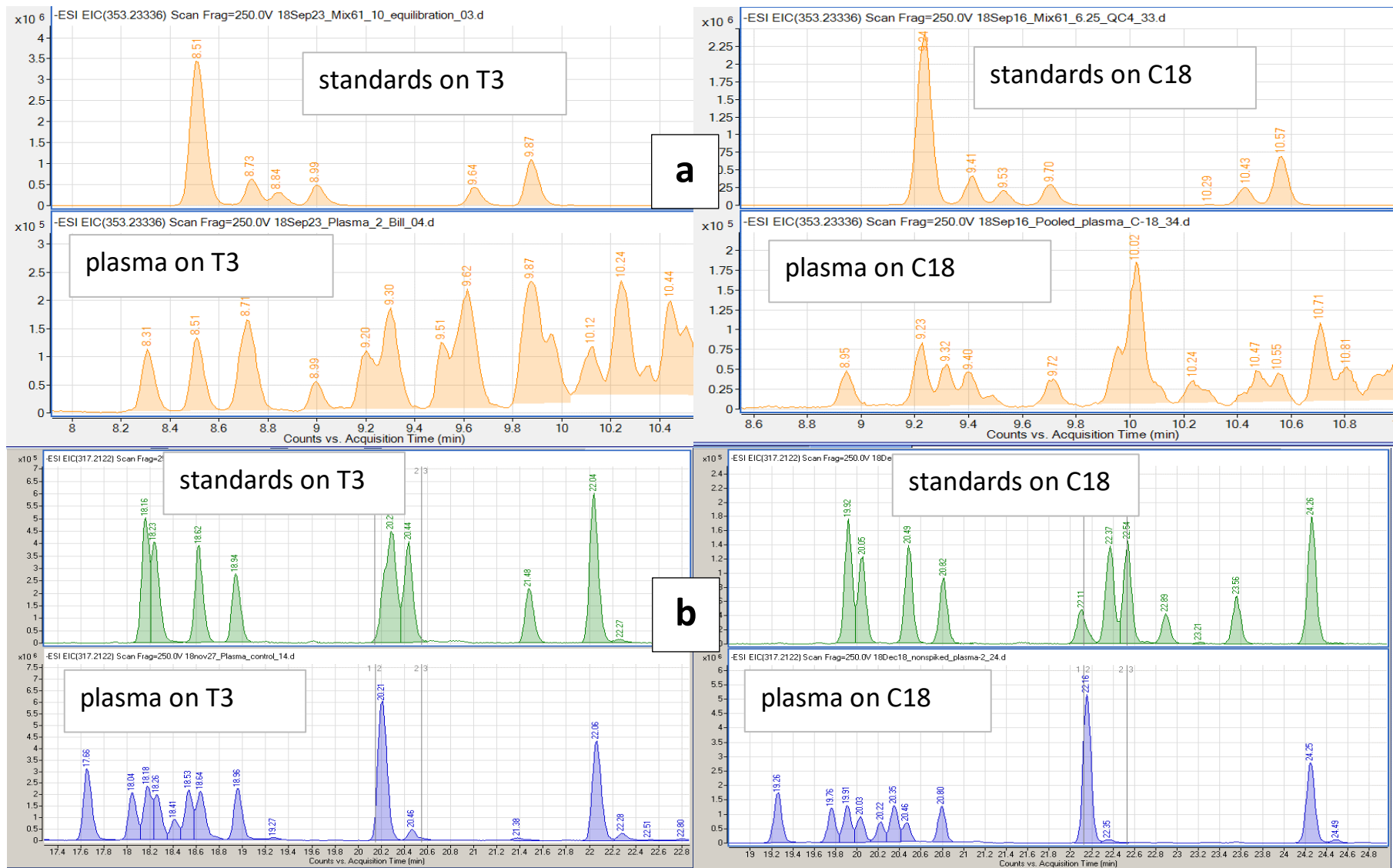


Figure S9 EICs at (a) m/z 353.2333 (b) m/z 317.2122 showed chromatographic separation of oxylipin isomers performed by T3 and Zorbax UHPLC columns. T3 showed better separation for more hydrophilic 353.2333 while Zorbax was better for 317.2122.

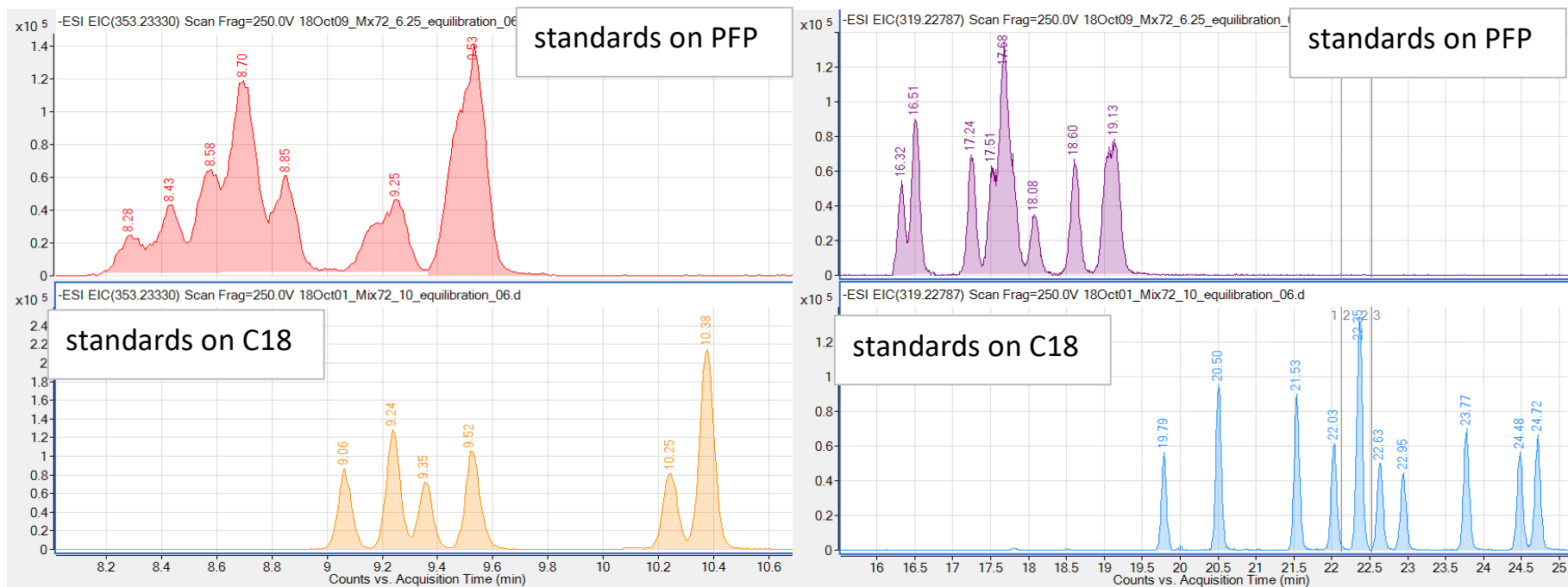


Figure S10 EICs at (a) m/z 353.2333 (b) m/z 319.2179 showed chromatographic separation of oxylipin isomers performed by PFP and Zorbax UHPLC columns.

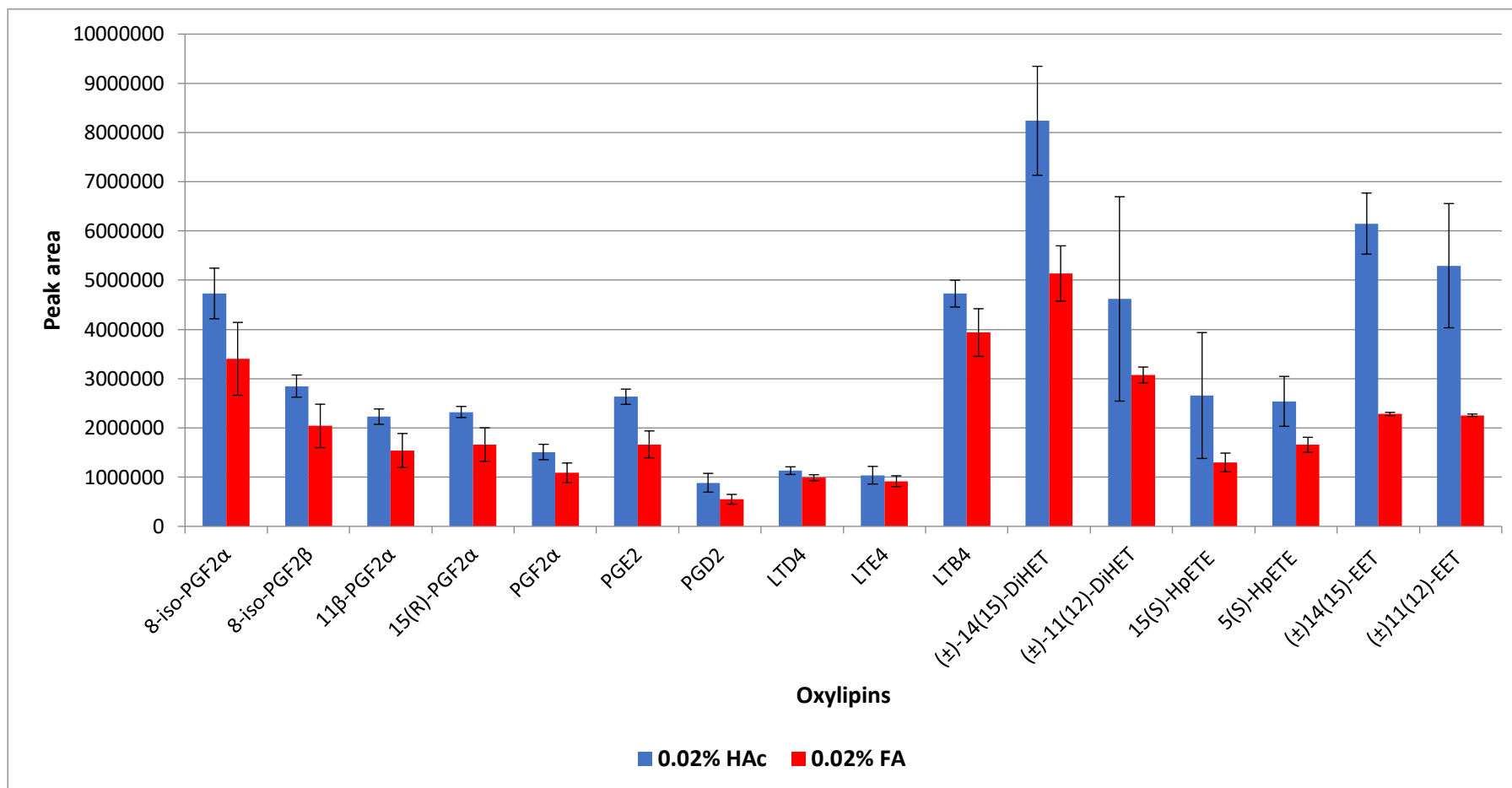


Figure S11 Comparison of 0.02% HAc (v/v) and 0.02% FA as mobile phase additives for the analysis of 200 ng/ml oxylipin standard (n=3). 0.02% HAc increased peak areas of all oxylipins by 10-40% versus FA.

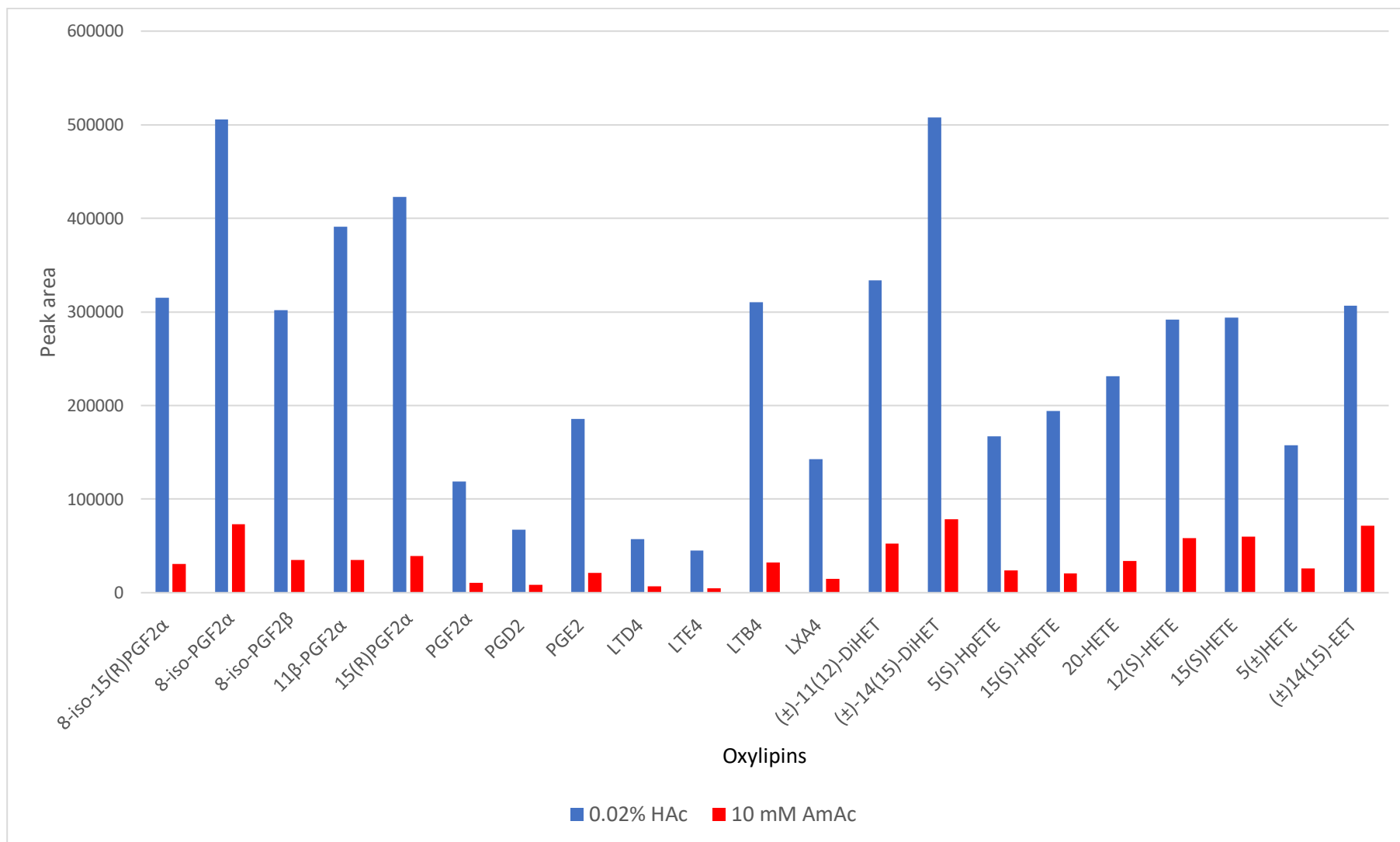


Figure S12 Comparison of 0.02% HAc and 10 mM AmAc as mobile phase additive for the analysis of 6.25 ng/ml oxylipin standard. The use of 0.02% HAc improves signal intensity on average 8x and provides better peak shapes for this application.

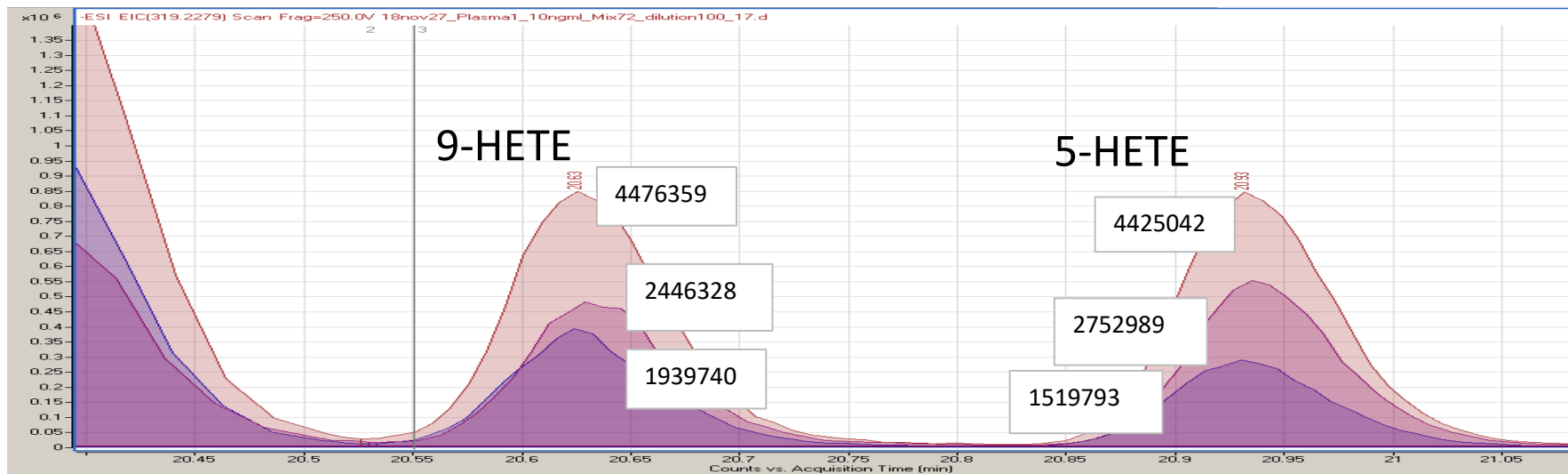


Figure S13 EIC at m/z 319.22787 showed doubled peak area (pink) of 9-HETE and 5-HETE resulted in sum of endogenous (purple) and spiked standard (red) levels (10 ng/ml). Peak areas for each level are placed on chromatogram.

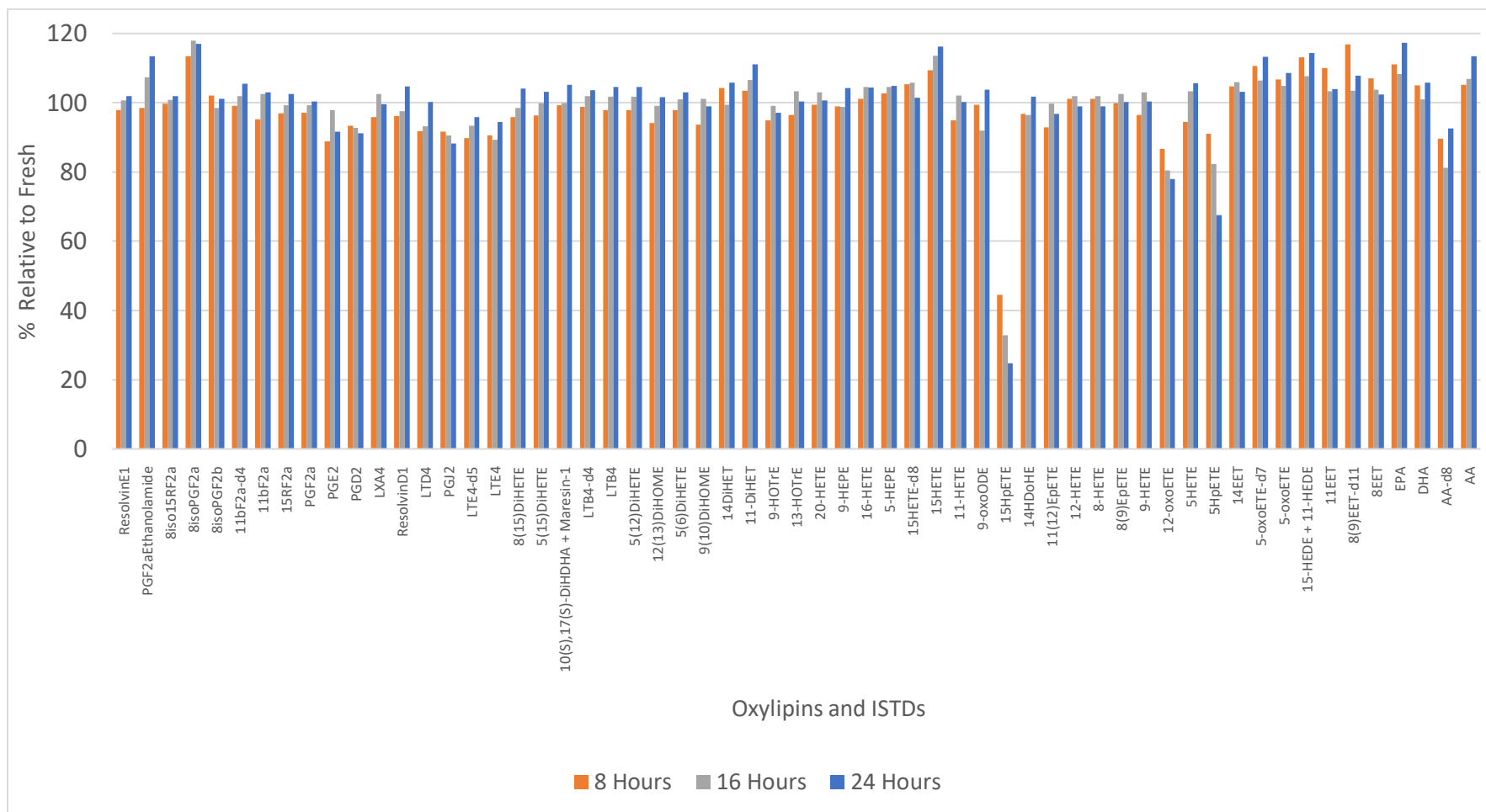


Figure S14 Evaluation of autosampler stability of oxylipin during 24 hours at concentration 1 ng/ml. 100µl of 1 ng/ml mix of oxylipins were added to glass inserts in glass LC vials (n=3). Vials were placed in 54-well autosampler tray at 40C and every sample was injected every 6 hours (fresh, 6, 12, 18, 24 hours). Stability was evaluated by comparison of peak areas of the standards in 6,12,18,24 hours samples with peak areas of standards in freshly prepared sample. 15-HpETE showed drastic drop of intensity up to 75%, also 5-HpETE and 12-oxoETE showed drop of intensity over 20%, for that reason these oxylipins were excluded from quantitative analysis, however they still be monitoring during analysis.

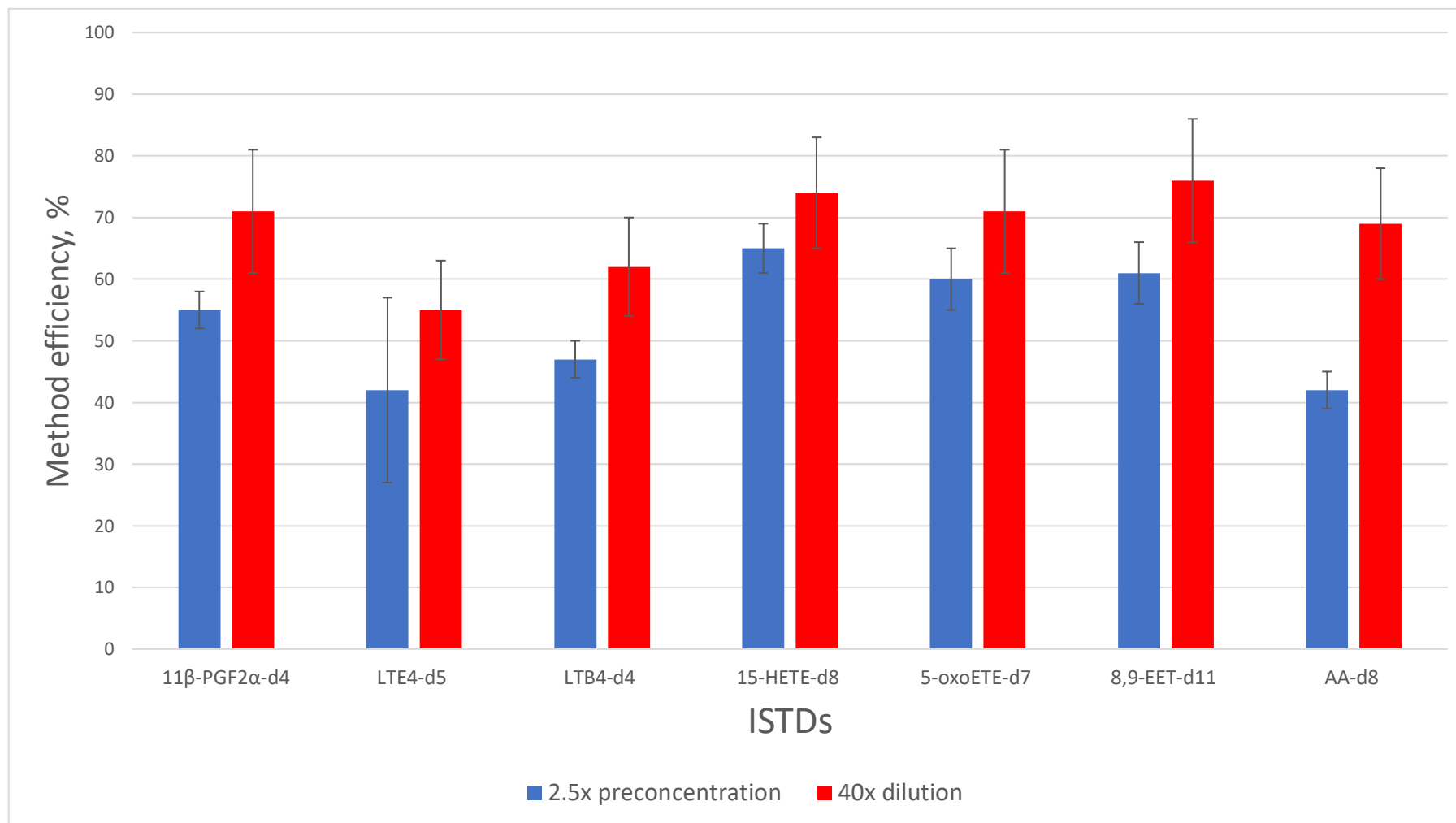


Figure S15 Evaluation of method efficiency for method of extraction of oxylipins from plasma. Recovery% = $\frac{A_{pre}}{A_{sol}} \times 100\%$, where red colour is used for 2.5x pre-concentrated samples, there pre-extraction spike was performed at 4 ng/ml mix of standards and measured against 10ng/ml mix of standards in solvent. For more abundant oxylipins (highlighted in blue) pre-extraction spike was performed at 40 ng/ml mix of 18 most abundant standards and ISTDs and measured against 10ng/ml mix of standards in solvent. The results show mean values (n=6), error bars show mean values of SD for each standard.

Table S1 List of standards analyzed by the method. Oxylipins that were detected in plasma are highlighted in green. In “Detection in plasma comment” column four types of detection quality were determined: DQ-detected and quantified; D- detected but accurate quantitation is not possible due to the reason specified in brackets; ND-P – not detected in plasma samples tested in this study, however, 10 ng/ml pre-spiked standard gives good quality peak, so potentially endogenous level of this oxylipin could be measured accurately if its concentration in a study sample is higher than LLOQ. ND – not detected and could not be accurately quantitated in pre-spiked plasma standards. The reasons for problems with quantitation include: (i) interference – interfering peak present in plasma co-elutes with analyte peak and results in inaccurate quantitation or obscures the peak of interest in case of large difference in concentrations between analyte and interference; (ii) shift – denotes that although the peak can be detected using regular gradient employed in final method (and matches retention time of standard), further investigation using a shallower gradient with extremely long chromatographic method indicates that the analyte was in fact misidentified as it shows a retention time that no longer corresponds to authentic standard; (iii) unstable - means that the analyte does not show adequate autosampler stability either due to degradation or non-specific adsorption and correct quantitation is impossible unless labelled standard for that analyte is used; (iv) matrix effect - significant matrix effect is observed in plasma and adversely impacts quantitation; and (v) too high concentration of AA does not allow its accurate quantitation using the final extraction method and proposed low and high calibration ranges. The “Most abundant” column A shows the most abundant oxylipins in plasma that were used in Mix 18 and Mix 25

Oxylipin name	Abbreviation	Formula	m/z of [M-H] ⁻	RT (min)	Detection in plasma comment	Most abundant
Resolvin E1	RvE1	C ₂₀ H ₃₀ O ₅	349.20204	7.53	ND-P	
Prostaglandin F2 α ethanolamide	PGF2 α -EA	C ₂₂ H ₃₉ NO ₅	396.27556	7.85	ND-P	
8-iso-15(R)-Prostaglandin F2 α	8-iso-15(R)-PGF2 α	C ₂₀ H ₃₄ O ₅	353.23336	9.06	DC	
8-iso-Prostaglandin F2 α	8-iso-PGF2 α	C ₂₀ H ₃₄ O ₅	353.23336	9.23	D (interference)	
8-iso-Prostaglandin F2 β	8-iso-PGF2 β	C ₂₀ H ₃₄ O ₅	353.23336	9.35	ND-P	
11 β -Prostaglandin F2 α	11 β -PGF2 α	C ₂₀ H ₃₄ O ₅	353.23336	9.51	ND (shift)	
15(R)-Prostaglandin F2 α	15(R)-PGF2 α	C ₂₀ H ₃₄ O ₅	353.23336	10.24	ND (interference)	
Prostaglandin F2 α	PGF2 α	C ₂₀ H ₃₄ O ₅	353.23336	10.36	ND (shift)	
Prostaglandin E2	PGE2	C ₂₀ H ₃₂ O ₅	351.2177	10.63	ND (interference)	
Prostaglandin D2	PGD2	C ₂₀ H ₃₂ O ₅	351.2177	11.09	ND (interference + shift)	
Lipoxin A4	LXA4	C ₂₀ H ₃₂ O ₅	351.2177	12.16	ND (interference + shift)	
Resolvin D1	RvD1	C ₂₂ H ₃₂ O ₅	375.2177	12.3	D (interference)	
Leukotriene D4	LTD4	C ₂₅ H ₄₀ N ₂ O ₆ S	495.25344	12.7	ND-P	

13,14-dihydro-15-keto-Prostaglandin D2	13,14-dihydro-15-keto-PGD2	C ₂₀ H ₃₂ O ₅	351.2177	13	ND (interference)	
8-iso-Prostaglandin A1	8-iso-PGA1	C ₂₀ H ₃₂ O ₄	335.2228	13.68	ND (interference)	
Prostaglandin J2	PGJ2	C ₂₀ H ₃₀ O ₄	333.20714	13.94	ND (interference)	
Leukotriene E4	LTE4	C ₂₃ H ₃₇ NO ₅ S	438.23198	14.16	ND-P	
8,15-dihydroxy-5Z,9E,11Z,13E-eicosatetraenoic acid	8,15-DiHETE	C ₂₀ H ₃₂ O ₄	335.2228	15.35	ND (interference)	
5,15-dihydroxy-6E,8Z,10Z,13E-eicosatetraenoic acid	5,15-DiHETE	C ₂₀ H ₃₂ O ₄	335.2228	15.72	DC	A
10,17-dihydroxy-4Z,7Z,11E,13Z,15E,19Z-docosahexaenoic acid	10,17-DiHDHA	C ₂₂ H ₃₂ O ₄	359.2228	16.17	DC, Unresolved, MS/MS must be used for quantitation	
Maresin 1	MaR-1	C ₂₂ H ₃₂ O ₄	359.2228	16.17		
Leukotriene B4	LTB4	C ₂₀ H ₃₂ O ₄	335.2228	16.17	ND (interference)	
12,13-dihydroxy-9Z-octadecenoic acid	12,13-DiHOME	C ₁₈ H ₃₄ O ₄	313.23842	16.71	DC	
5,12-dihydroxy-6E,8Z,10E,14Z-eicosatetraenoic acid	5,12-DiHETE	C ₂₀ H ₃₂ O ₄	335.2228	16.71	DC	A
9,10-dihydroxy-12Z-octadecenoic acid	9,10-DiHOME	C ₁₈ H ₃₄ O ₄	313.23842	17.16	DC	
14,15-dihydroxy-5Z,8Z,11Z-eicosatrienoic acid	14,15-DiHET	C ₂₀ H ₃₄ O ₄	337.23842	17.84	D (interference)	
11,12-dihydroxy-5Z,8Z,14Z-eicosatrienoic acid	11,12-DiHET	C ₂₀ H ₃₄ O ₄	337.23842	18.53	ND-P	
9-hydroxy-10E,12Z,15Z-octadecatrienoic acid	9-HOTrE	C ₁₈ H ₃₀ O ₃	293.21221	18.91	D (matrix effect)	
13-hydroxy-9Z,11E,15Z-octadecatrienoic acid	13-HOTrE	C ₁₈ H ₃₀ O ₃	293.21221	19.15	DC	
15-deoxy-Δ12,14 Prostaglandin J2	15-deoxy-Δ12,14 PGJ2	C ₂₀ H ₂₈ O ₃	315.19658	19.35	ND-P	
5,6-dihydroxy-7E,9E,11Z,14Z-eicosatetraenoic acid	5,6-DiHETE	C ₂₀ H ₃₂ O ₄	335.2228	19.61	D (interference)	
20-hydroxy-5Z,8Z,11Z,14Z-eicosatetraenoic acid	20-HETE	C ₂₀ H ₃₂ O ₃	319.22786	19.82	ND-P	
15-hydroxy-5Z,8Z,11Z,13E,17Z-eicosapentaenoic acid	15-HEPE	C ₂₀ H ₃₀ O ₃	317.21221	19.85	D (interference)	
11-hydroxy-5Z,8Z,12E,14Z,17Z-eicosapentaenoic acid	11-HEPE	C ₂₀ H ₃₀ O ₃	317.21221	19.97	D (interference)	
9-hydroxy-5Z,7E,11Z,14Z,17Z-eicosapentaenoic acid	9-HEPE	C ₂₀ H ₃₀ O ₃	317.21221	20.45	D (interference)	
16-hydroxy-5Z,8Z,11Z,14Z-eicosatetraenoic acid	16-HETE	C ₂₀ H ₃₂ O ₃	319.22786	20.63	ND (interference)	
5-hydroxy-6E,8Z,11Z,14Z,17Z-eicosapentaenoic acid	5-HEPE	C ₂₀ H ₃₀ O ₃	317.21221	20.77	DC	A
9-hydroxy-10E,12Z-octadecadienoic acid	9-HODE	C ₁₈ H ₃₂ O ₃	295.22786	20.99	DC	A
20-hydroxy Docosahexaenoic Acid	20-HDoHE	C ₂₂ H ₃₂ O ₃	343.22786	21.21	DC	A
13-oxo-9Z,11E-octadecadienoic acid	13-OxoODE	C ₁₈ H ₃₀ O ₃	293.21221	21.51	DC	A

15-hydroxy-5Z,8Z,11Z,13E-eicosatetraenoic acid	15-HETE	C ₂₀ H ₃₂ O ₃	319.22786	21.58	DC	A
16-hydroxy Docosahexaenoic Acid	16-HDoHE	C ₂₂ H ₃₂ O ₃	343.22786	21.69	D, not resolved	
17-hydroxy Docosahexaenoic Acid	17-HDoHE	C ₂₂ H ₃₂ O ₃	343.22786	21.8		
11-hydroxy-5Z,8Z,12E,14Z-eicosatetraenoic acid	11-HETE	C ₂₀ H ₃₂ O ₃	319.22786	22.03	DC	A
9-oxo-10E,12Z-octadecadienoic acid	9-oxoODE	C ₁₈ H ₃₀ O ₃	293.21221	22.04	DC	A
15-hydroperoxy-5Z,8Z,11Z,13E-eicosatetraenoic acid	15-HpETE	C ₂₀ H ₃₂ O ₄	317.21168	22.09	ND (interference + unstable)	
14-hydroxy Docosahexaenoic Acid	14-HDoHE	C ₂₂ H ₃₂ O ₃	343.22786	22.21	DC	A
11,12-Epoxyeicosatetraenoic Acid	11,12-EpETE	C ₂₀ H ₃₀ O ₃	317.21221	22.32	ND (shift + interference)	
12-hydroxy-5Z,8Z,10E,14Z-eicosatetraenoic acid	12-HETE	C ₂₀ H ₃₂ O ₃	319.22786	22.41	DC, unresolved MS/MS is required for quantitation	A
8-hydroxy-5Z,9E,11Z,14Z-eicosatetraenoic acid	8-HETE	C ₂₀ H ₃₂ O ₃	319.22786	22.41		A
8,9-Epoxyeicosatetraenoic Acid	8,9-EpETE	C ₂₀ H ₃₀ O ₃	317.21221	22.48	ND (shift + interference)	
9-hydroxy-5Z,7E,11Z,14Z-eicosatetraenoic acid	9-HETE	C ₂₀ H ₃₂ O ₃	319.22786	22.68	DC	A
12-oxo-5Z,8Z,10E,14Z-eicosatetraenoic acid	12-OxoETE	C ₂₀ H ₃₀ O ₃	317.21221	22.85	D (unstable)	
5-hydroxy-6E,8Z,11Z,14Z-eicosatetraenoic acid	5-HETE	C ₂₀ H ₃₂ O ₃	319.22786	22.99	DC	A
5-hydroperoxy-6E,8Z,11Z,14Z-eicosatetraenoic acid	5-HpETE	C ₂₀ H ₃₂ O ₄	317.21168	23.56	D (unstable)	
4-hydroxy Docosahexaenoic Acid	4-HDoHE	C ₂₂ H ₃₂ O ₃	343.22786	23.49	DC	A
14,15-epoxy-5Z,8Z,11Z-eicosatrienoic acid	14,15-EET	C ₂₀ H ₃₂ O ₃	319.22786	23.84	DC	
5-oxo-6E,8Z,11Z,14Z-eicosatetraenoic acid	5-oxoETE	C ₂₀ H ₃₀ O ₃	317.21221	24.27	DC	A
11-hydroxy-12E,14Z-eicosadienoic acid	11-HEDE	C ₂₀ H ₃₆ O ₃	323.25917	24.75	DC, Unresolved, MS/MS is required for quantitation	
15-hydroxy-11Z,13E-eicosadienoic acid	15-HEDE	C ₂₀ H ₃₆ O ₃	323.25917	24.75		
11,12-epoxy-5Z,8Z,14Z-eicosatrienoic acid	11,12-EET	C ₂₀ H ₃₂ O ₃	319.22786	24.56	ND (shift)	
8,9-epoxy-5Z,11Z,14Z-eicosatrienoic acid	8,9-EET	C ₂₀ H ₃₂ O ₃	319.22786	24.79	ND (shift+interference)	
Eicosapentaenoic Acid	EPA	C ₂₀ H ₃₀ O ₂	301.21730	27.26	DC	A
Docosahexaenoic Acid	DHA	C ₂₂ H ₃₂ O ₂	327.23296	29.01	DC	A
Arachidonic acid	AA	C ₂₀ H ₃₂ O ₂	303.23296	29.43	D (too high concentration)	

Table S2 List of internal standards used in the method

Oxylipin name	Abbreviation	Formula	m/z of [M-H] ⁻	RT (min)
11β-Prostaglandin F2α-d4	11β-PGF2α-d4	C ₂₀ H ₃₀ D ₄ O ₅	357.25844	9.47
Leukotriene E4-d5	LTE4-d5	C ₂₃ H ₃₂ D ₅ NO ₅ S	443.26335	14.1
Leukotriene B4-d4	LTB4-d4	C ₂₀ H ₂₈ D ₄ O ₄	339.24788	16.09
Techin	15-HETE-d8	C ₂₀ H ₂₄ D ₈ O ₃	327.27809	21.4
5-oxo-6E,8Z,11Z,14Z-eicosatetraenoic-6,8,9,11,12,14,15-d7 acid	5-oxoETE-d7	C ₂₀ H ₂₃ D ₇ O ₃	324.25615	24.1
(±)8(9)-epoxy-5Z,8Z,14Z-eicosatrienoic-16,16,17,17,18,18,19,19,20,20,20 acid	8,9-EET-d11	C ₂₀ H ₂₁ D ₁₁ O ₃	330.29692	24.48
5Z,8Z,11Z,14Z-eicosatetraenoic-16,16,17,17,18,18,19,19,20,20,20-d11 acid	AA-d8	C ₂₀ H ₂₁ D ₁₁ O ₂	311.28316	29.22

Table S3 LogP values for oxylipins from list of standards reported by different sources. Table is arranged in terms of elution order on C-18 UHPLC column

№	Oxylipin	LogP			
		Experimental ¹	ALOGPS ¹	ChemAxon ¹	ACD ²
1	RvE1	NA	4.24	NA	NA
2	PGF2 α Ethanolamide	NA	2.09	1.34	NA
3	8-iso-15(R)-PGF2 α	NA	NA	NA	2.14
4	8-iso-PGF2 α	2.183	3.11	2.61	NA
5	8-iso-PGF2 β	NA	3.11	2.61	NA
6	11 β -PGF2 α	NA	3.11	2.61	NA
7	15(R)-PGF2 α	NA	NA	NA	2.14
8	PGF2 α	4.39	3.11	2.61	NA
9	PGE2	2.82	3.31	3.23	NA
10	PGD2	NA	3.12	3.23	NA
11	LXA4	NA	4.61	3.05	NA
12	RvD1	NA	4.66	3.12	NA
13	LTD4	NA	1.17	0.76	NA
14	13,14-dihydro-15-keto-PGD2	NA	3.52	3.64	NA
15	8-isoPGA1	NA	4.21	4.74	NA
16	PGJ2	NA	4.1	4.38	NA
17	LTE4	NA	1.57	2.02	NA
18	8,15-DiHETE	NA	5.37	4.13	NA
19	5,15-DiHETE	NA	5.33	4.13	NA
20	10,17-DiHDHA+Maresin 1	NA	NA	NA	3.81
21	LTB4	NA	5.46	4.13	NA
22	12,13-DiHOME	NA	5.2	4.32	NA
23	5,12-DiHETE	NA	NA	NA	4.06
24	9,10-DiHOME	NA	5.18	4.32	NA
25	14,15-DiHET	NA	5.28	4.49	NA

26	11,12-DiHET	NA	5.41	4.49	NA
27	9-HOTrE	NA	NA	NA	4.81
28	13-HOTrE	NA	5.39	4.38	NA
29	15-deoxy- Δ 12,14 PGJ2	3.983	5.39	5.46	NA
30	5,6-DiHETE	NA	NA	NA	3.62
31	20-HETE	NA	5.87	5.15	NA
32	15-HEPE	NA	5.55	4.99	NA
33	11-HEPE	NA	5.53	4.99	NA
34	9-HEPE	NA	5.54	4.99	NA
35	16-HETE	NA	5.77	5.36	NA
36	5-HEPE	NA	5.54	4.99	NA
37	9-HODE	NA	5.88	5.19	NA
38	20-HDoHE	NA	6.01	5.52	NA
39	15-HETE	4.405	5.82	5.36	NA
40	9-OxoODE	NA	5.62	5.6	NA
41	16-HDoHE	NA	5.95	5.52	NA
42	17-HDoHE	NA	5.96	5.52	NA
43	13-oxoODE	NA	5.66	5.6	NA
44	11-HETE	4.056	5.85	5.36	NA
45	15-HpETE	5.86	5.86	5.81	NA
46	14-HDoHE	NA	5.92	5.14	NA
47	11,12-EpETE	NA	NA	NA	5.85
48	12-HETE	NA	5.86	5.36	NA
49	8-HETE	NA	5.86	5.37	NA
50	8,9-EpETE	NA	NA	NA	5.62
51	9-HETE	NA	5.88	5.36	NA
52	12-OxoETE	NA	5.79	5.77	NA
53	5-HETE	NA	5.88	5.36	NA
54	5-HpETE	NA	5.92	5.81	NA

55	4-HDoHE	NA	6.01	5.52	NA
56	14,15-EET	NA	6.23	5.65	NA
57	5-oxoETE	NA	5.85	5.77	NA
58	11-HEDE + 15-HEDE	NA	NA	NA	6.39
59	11,12-EET	NA	6.25	5.65	NA
60	8,9-EET	NA	6.25	5.65	NA
61	Eicosapentaenoic Acid (EPA)	NA	6.53	6.23	NA
62	Docosahexaenoic Acid (DHA)	6.73	6.83	6.75	NA
63	Arachidonic acid (AA)	6.98	6.8	6.59	NA

1. Human metabolome data base (HMDB), accessed 20.11.2018

2. www.chemspider.com, accessed 20.11.2018

Supplementary Methods (Chapter 3)

Materials

LC-MS grade solvents and mobile phase additives were purchased from Fisher Scientific (Ottawa, ON, Canada). L-Phenylalanine-d₅, Cholic acid-d₄, L-Glutamic acid-d₅, Melatonin-d₄ standards were purchased from CDN isotopes, Pointe-Claire, Quebec, Canada. Serotonin-d₄ hydrochloride standard was purchased from Toronto Research Chemicals (Toronto, ON, Canada). All oxylipin standards were purchased directly from Cayman Chemicals (Ann Arbor, MI, US) or their Canadian distributor Cedarlane Labs (Burlington, ON, Canada).

Overall experiment schematic

The same samples that were used for oxylipin analysis, were also used for untargeted metabolomics using both reversed-phase and HILIC as shown in Supplementary Figure S16. The latter two analyses are not further discussed in this manuscript, but it is important to emphasize two key points. Firstly, from a single in vivo SPME sampling sufficient material can be obtained to perform three analyses (oxylipin profiling and quantitation, analysis of polar metabolome and analysis of intermediate metabolome), thus providing very rich information profiles for all sampling time points. Secondly, the choice of mixed-mode coating was dictated by the need to analyze polar metabolome. If only oxylipin analysis is of interest, commercial biocompatible C18 coatings provide slightly better extraction efficiency and possibly oxylipin coverage (Supplementary Figure S21).

SPE brain procedure

10 tissue samples were weighed (approx. 20 mg), immersed in liquid nitrogen and then disrupted with a Bessman tissue pulverizer. Tissue pellet was transferred to 1.5 ml Eppendorf tube where 200 µl of 99% MeOH + 1% FA were added. Tissue was then homogenized with mechanical tissue grinder (Fisher Scientific). Ten homogenized tissue samples were mixed together, vortexed and divided into ten samples of 200 µl each. Five samples were spiked with 10 µl of 10 ng/ml IS working standard, remaining 5 samples were not spiked. All samples were centrifuged at 15 000 g for 10 min at 40C. 100 µl of supernatant were transferred to separate tubes and nonspiked samples were now spiked

with 8.3 μl of 10 ng/ml of IS working standard. All 10 samples were then subjected to SPE procedure performed on C-18 (Strata Phenomenex 200 mg): (i) conditioning with 1 ml of MeOH and 1 ml of 20% MeOH, (ii) loading 100 μl (or 108.3 μl in case of post-spiked samples) of sample, (iii) washing with 1 ml of 20% MeOH, and (iv) elution with 1 ml of 99% MeOH with 1% HAc into a 5 ml culture glass tube. After elution, all eluent was transferred to 1 ml glass amber round-bottom tube contained pre-dispensed 20 μl of 30% glycerol in MeOH and evaporated in speedvac to dryness (6 μl of glycerol on the bottom of the tube). After evaporation, the samples were reconstituted with 40 μl of MeOH with vortexing. Finally, 20 μl was transferred to a new HPLC glass insert for LC-MS analysis.

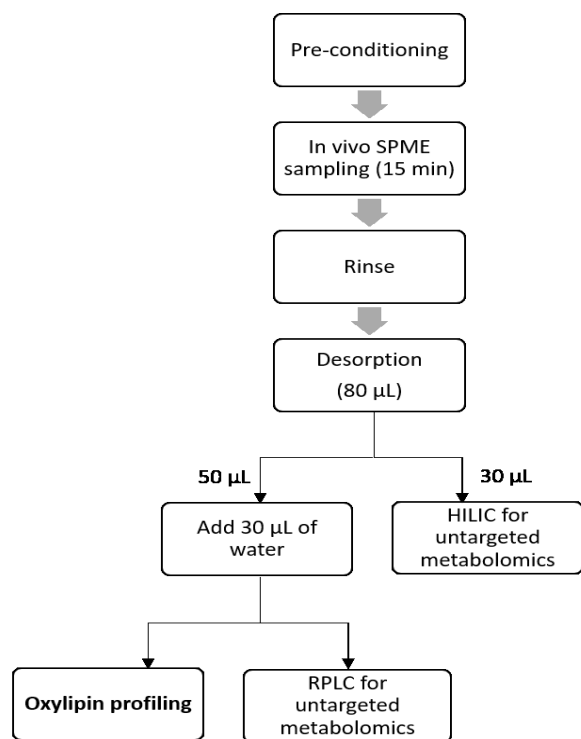


Figure S16 Overall experimental design showing that both oxylipin quantitative profiling and full untargeted metabolomics profiles can be obtained from single sampling

LC-MS for oxylipin analysis

The separation of analytes was performed on ZORBAX Eclipse plus C18, 1.8 μm (2.1 mm x 100 mm) Rapid Resolution High Definition (RRHD) column (Agilent) protected by a guard column (2.1 mm x 5 mm; Agilent) made of the same packing material. Temperature of column was 50°C. Mobile phase flow rate was 0.4 ml/min. Mobile phase A consisted of 0.02% acetic acid in LC-MS grade water while mobile phase B was composed of 0.02% acetic acid, 10% 2-propanol and 90% acetonitrile (v/v). Initial mobile phase composition was 95% A : 5% B, and was held for 1.0 min. Then, %B was increased to 20% over 0.1 min, followed by a linear gradient from 20% to 80% over 29.9 min. Finally, %B was increased to 95% over 0.1 min, and held for 3.9 min. The column was then re-equilibrated to initial conditions of 95% A for 5 min prior to next injection. Total run time per sample was 40 min. Injection volume was 10 μl . Following MS parameters were set: capillary voltage 3500 V, nozzle voltage 500 V, drying gas temperature 250°C and sheath gas temperature 275°C. Experiment was divided into four time segments: 0-22.3 min MS, 22.2-22.5 MS/MS with collision energy 20 V, 22.5-30 min MS, 30-40 min LC stream goes to the waste. Internal mass calibration was performed using Dual AJS ESI ion source using calibrant masses 119.03632 (purine) and 980.01638 (HP-0921 acetate adduct) from Agilent mass reference solution. LC-MS data acquisition was performed using MassHunter software version B.07.00 (Agilent). The concentrations of oxylipins in SPME extracts were determined using standard calibration curve prepared to match the final composition of SPME samples. Working oxylipin standard was first prepared at 312.5 ng/mL in MeOH from individual oxylipin stock standards. From this working standard, seven calibration points were obtained at final concentrations of 6.25, 3.125, 1.563, 0.78125, 0.3906, 0.1953, and 0.0977 ng/mL prepared in final SPME sample solvent composition (ACN/MeOH/H₂O, 25/25/50) using serial dilution. All samples were run in randomized order after conditioning of LC-MS system and running calibration curve

Data processing

Targeted data processing was performed using Agilent Masshunter software (TOF Qualitative Analysis B.07.00 and TOF Quantitative Analysis B.07.00) using 30 ppm extraction window. Deprotonated ion [M-H]⁻ was the most intense ion for most of oxylipins and was used for all data processing. The calculation of oxylipin final concentrations was performed using 1/x weighted solvent calibration curves. The

determination of 12-HETE and 8-HETE was performed using MS/MS using product ions: m/z 179.1 and 155.07 respectively. Supplementary Tables summarize formulas, m/z and retention times of all oxylipins for which (i) authentic standards were available and were fully quantitated if present in sample (Supplementary Table S1), (ii) internal standards (Supplementary Table S2) or (iii) authentic standards which were purchased to confirm the identifications of several unknown oxylipins after initial study.

Table S4 Authentic standards that were used in experiment for both identification and quantitation of oxylipins in brain

Full name	Abbreviation	Formula	[M-H]- m/z	RT (min)	LLOQ (ng/ml)
ResolvinE1	RvE1	C ₂₀ H ₃₀ O ₅	349.2020	7.53	0.1
Prostaglandin F2 α ethanolamide	PGF2 α -EA	C ₂₂ H ₃₉ NO ₅	396.2756	7.85	0.1
8-iso-15(R)-Prostaglandin F2 α	8-iso-15(R)-PGF2 α	C ₂₀ H ₃₄ O ₅	353.2334	9.06	0.1
8-iso-Prostaglandin F2 α	8-iso-PGF2 α	C ₂₀ H ₃₄ O ₅	353.2334	9.23	0.1
8-iso-Prostaglandin F2 β	8-iso-PGF2 β	C ₂₀ H ₃₄ O ₅	353.2334	9.35	0.1
11 β -Prostaglandin F2 α	11 β -PGF2 α	C ₂₀ H ₃₄ O ₅	353.2334	9.51	0.1
15(R)-Prostaglandin F2 α	15(R)-PGF2 α	C ₂₀ H ₃₄ O ₅	353.2334	10.24	0.1
Prostaglandin F2 α	PGF2 α	C ₂₀ H ₃₄ O ₅	353.2334	10.36	0.1
Prostaglandin E2	PGE2	C ₂₀ H ₃₂ O ₅	351.2177	10.63	0.1
Prostaglandin D2	PGD2	C ₂₀ H ₃₂ O ₅	351.2177	11.09	0.1
Lipoxin A4	LXA4	C ₂₀ H ₃₂ O ₅	351.2177	12.16	0.2
ResolvinD1	RvD1	C ₂₂ H ₃₂ O ₅	375.2177	12.30	0.1
Leukotriene D4	LTD4	C ₂₅ H ₄₀ N ₂ O ₆ S	495.2534	12.70	0.1
Prostaglandin J2	PGJ2	C ₂₀ H ₃₀ O ₄	333.2071	13.94	0.2
Leukotriene E4	LTE4	C ₂₃ H ₃₇ NO ₅ S	438.2320	14.16	0.1
8,15-dihydroxy-5Z,9E,11Z,13E-eicosatetraenoic acid	8,15-DiHETE	C ₂₀ H ₃₂ O ₄	335.2228	15.35	0.1
5,15-dihydroxy-6E,8Z,10Z,13E-eicosatetraenoic acid	5,15-DiHETE	C ₂₀ H ₃₂ O ₄	335.2228	15.72	0.1

10,17-dihydroxy-4Z,7Z,11E,13Z,15E,19Z-docosahexaenoic acid	10,17-DiHDHA	C ₂₂ H ₃₂ O ₄	359.2228	15.91	0.1
Maresin 1	MaR-1	C ₂₂ H ₃₂ O ₄	359.2228	15.96	0.1
Leukotriene B4	LTB4	C ₂₀ H ₃₂ O ₄	335.2228	16.17	0.1
12,13-dihydroxy-9Z-octadecenoic acid	12,13-DiHOME	C ₁₈ H ₃₄ O ₄	313.2384	16.71	0.1
5,12-dihydroxy-6E,8Z,10E,14Z-eicosatetraenoic acid	5,12-DiHETE	C ₂₀ H ₃₂ O ₄	335.2228	16.71	0.1
9,10-dihydroxy-12Z-octadecenoic acid	9,10-DiHOME	C ₁₈ H ₃₄ O ₄	313.2384	17.16	0.1
14,15-dihydroxy-5Z,8Z,11Z-eicosatrienoic acid	14,15-DiHET	C ₂₀ H ₃₄ O ₄	337.2384	17.84	0.1
11,12-dihydroxy-5Z,8Z,14Z-eicosatrienoic acid	11,12-DiHET	C ₂₀ H ₃₄ O ₄	337.2384	18.53	0.1
9-hydroxy-10E,12Z,15Z-octadecatrienoic acid	9-HOTrE	C ₁₈ H ₃₀ O ₃	293.2122	18.91	0.1
13-hydroxy-9Z,11E,15Z-octadecatrienoic acid	13-HOTrE	C ₁₈ H ₃₀ O ₃	293.2122	19.15	0.1
5,6-dihydroxy-7E,9E,11Z,14Z-eicosatetraenoic acid	5,6-DiHETE	C ₂₀ H ₃₂ O ₄	335.2228	19.61	0.1
20-hydroxy-5Z,8Z,11Z,14Z-eicosatetraenoic acid	20-HETE	C ₂₀ H ₃₂ O ₃	319.2279	19.82	0.1
9-hydroxy-5Z,7E,11Z,14Z,17Z-eicosapentaenoic acid	9-HEPE	C ₂₀ H ₃₀ O ₃	317.2122	20.45	0.1
16-hydroxy-5Z,8Z,11Z,14Z-eicosatetraenoic acid	16-HETE	C ₂₀ H ₃₂ O ₃	319.2279	20.63	0.1
5-hydroxy-6E,8Z,11Z,14Z,17Z-eicosapentaenoic acid	5-HEPE	C ₂₀ H ₃₀ O ₃	317.2122	20.77	0.1
15-hydroxy-5Z,8Z,11Z,13E-eicosatetraenoic acid	15-HETE	C ₂₀ H ₃₂ O ₃	319.2279	21.58	0.1
11-hydroxy-5Z,8Z,12E,14Z-eicosatetraenoic acid	11-HETE	C ₂₀ H ₃₂ O ₃	319.2279	22.03	0.1
9-oxo-10E,12Z-octadecadienoic acid	9-OxoODE	C ₁₈ H ₃₀ O ₃	293.2122	22.04	0.1
15-hydroperoxy-5Z,8Z,11Z,13E-eicosatetraenoic acid	15-HpETE	C ₂₀ H ₃₂ O ₄	317.2117	22.09	0.1
14-hydroxy Docosahexaenoic Acid	14-HDoHE	C ₂₂ H ₃₂ O ₃	343.2279	22.21	0.2
11,12-Epoxyeicosatetraenoic Acid	11,12-EpETE	C ₂₀ H ₃₀ O ₃	317.2122	22.32	0.1
12-hydroxy-5Z,8Z,10E,14Z-eicosatetraenoic acid	12-HETE	C ₂₀ H ₃₂ O ₃	319.2278 to 179.1	22.41	0.1
8-hydroxy-5Z,9E,11Z,14Z-eicosatetraenoic acid	8-HETE	C ₂₀ H ₃₂ O ₃	319.2278 to 155.07	22.41	0.1
8,9-Epoxyeicosatetraenoic Acid	8,9-EpETE	C ₂₀ H ₃₀ O ₃	317.2122	22.48	0.1
9-hydroxy-5Z,7E,11Z,14Z-eicosatetraenoic acid	9-HETE	C ₂₀ H ₃₂ O ₃	319.2279	22.68	0.1
12-oxo-5Z,8Z,10E,14Z-eicosatetraenoic acid	12-OxoETE	C ₂₀ H ₃₀ O ₃	317.2122	22.85	0.1

5-hydroxy-6E,8Z,11Z,14Z-eicosatetraenoic acid	5-HETE	C ₂₀ H ₃₂ O ₃	319.2279	22.99	0.1
5-hydroperoxy-6E,8Z,11Z,14Z-eicosatetraenoic acid	5-HpETE	C ₂₀ H ₃₂ O ₄	317.2117	23.56	0.1
14(15)-epoxy-5Z,8Z,11Z-eicosatrienoic acid	14(15)-EET	C ₂₀ H ₃₂ O ₃	319.2279	23.84	0.1
5-oxo-6E,8Z,11Z,14Z-eicosatetraenoic acid	5-oxoETE	C ₂₀ H ₃₀ O ₃	317.2122	24.27	0.1
11-hydroxy-12E,14Z-eicosadienoic acid	11-HEDE	C ₂₀ H ₃₆ O ₃	323.2592	24.40	0.1
15-hydroxy-11Z,13E-eicosadienoic acid	15-HEDE	C ₂₀ H ₃₆ O ₃	323.2592	24.40	0.1
11(12)-epoxy-5Z,8Z,14Z-eicosatrienoic acid	11(12)-EET	C ₂₀ H ₃₂ O ₃	319.2279	24.56	0.1
8(9)-epoxy-5Z,11Z,14Z-eicosatrienoic acid	8(9)-EET	C ₂₀ H ₃₂ O ₃	319.2279	24.79	0.1
Eicosapentaenoic Acid	EPA	C ₂₀ H ₃₀ O ₂	301.2173	27.26	0.1
Docosahexaenoic Acid	DHA	C ₂₂ H ₃₂ O ₂	327.2330	29.01	0.1
Arachidonic acid	AA	C ₂₀ H ₃₂ O ₂	303.2330	29.43	0.4

Table S5 Deuterated internal standards that were used in experiment

Full name	Abbreviation	Formula	[M-H] ⁻ m/z	RT (min)	LLOQ (ng/ml)
11β-Prostaglandin F2α-d4	11β-PGF2α-d4	C ₂₀ H ₃₀ D ₄ O ₅	357.2584	9.47	0.1
Leukotriene E4-d5	LTE4-d5	C ₂₃ H ₃₂ D ₅ NO ₅ S	443.2634	14.10	0.1
Leukotriene B4-d4	LTB4-d4	C ₂₀ H ₂₈ D ₄ O ₄	339.2479	16.09	0.1
(5Z,8Z,11Z,13E,15S)-15-Hydroxy(5,6,8,9,11,12,14,15-2H8)-5,8,11,13-icosatetraenoic acid	15(S)-HETE-d8	C ₂₀ H ₂₄ D ₈ O ₃	327.2781	21.40	0.1
5-oxo-6E,8Z,11Z,14Z-eicosatetraenoic-6,8,9,11,12,14,15-d7 acid	5-oxoETE-d7	C ₂₀ H ₂₃ D ₇ O ₃	324.2562	24.10	0.1
8(9)-epoxy-5Z,8Z,14Z-eicosatrienoic-16,16,17,17,18,18,19,19,20,20,20 acid	8(9)-EET-d11	C ₂₀ H ₂₁ D ₁₁ O ₃	330.2969	24.48	0.1
5Z,8Z,11Z,14Z-eicosatetraenoic-16,16,17,17,18,18,19,19,20,20,20-d11 acid	AA-d8	C ₂₀ H ₂₁ D ₁₁ O ₂	311.2832	29.22	0.8

Table S6 Additional standards that were used after experiment for the identification of unknowns

Full name	Abbreviation	Formula	[M-H] ⁻ m/z	RT (min)	LLOQ (ng/ml)
13,14-dihydro-15-keto-Prostaglandin D2	13,14-dihydro-15-keto-PGD2	C ₂₀ H ₃₂ O ₅	351.2177	13.00	0.4
8-iso-Prostaglandin A1	8-iso-PGA1	C ₂₀ H ₃₂ O ₄	335.2228	13.68	0.1
15-deoxy-Δ12,14 Prostaglandin J2	15-deoxy-Δ12,14 PGJ2	C ₂₀ H ₂₈ O ₃	315.1966	19.35	0.4
15-hydroxy-5Z,8Z,11Z,13E,17Z-eicosapentaenoic acid	15-HEPE	C ₂₀ H ₃₀ O ₃	317.2122	19.85	0.1
11-hydroxy-5Z,8Z,12E,14Z,17Z-eicosapentaenoic acid	11-HEPE	C ₂₀ H ₃₀ O ₃	317.2122	19.97	0.2
9-hydroxy-10E,12Z-octadecadienoic acid	9-HODE	C ₁₈ H ₃₂ O ₃	295.2279	20.99	0.2
20-hydroxy Docosahexaenoic Acid	20-HDoHE	C ₂₂ H ₃₂ O ₃	343.2279	21.21	0.2
13-oxo-9Z,11E-octadecadienoic acid	13-oxoODE	C ₁₈ H ₃₀ O ₃	293.2122	21.51	0.1
16-hydroxy Docosahexaenoic Acid	16-HDoHE	C ₂₂ H ₃₂ O ₃	343.2279	21.69	0.4
17-hydroxy Docosahexaenoic Acid	17-HDoHE	C ₂₂ H ₃₂ O ₃	343.2279	21.80	0.4
4-hydroxy Docosahexaenoic Acid	4-HDoHE	C ₂₂ H ₃₂ O ₃	343.2279	23.49	0.4

Table S7 Average concentration (ng/ml or pg/mg brain tissue \pm SD) of oxylipins in pooled brain sample (n=10 technical replicates) extracted by SPE. D-detected, but not quantitated

Oxylipin	Concentration (ng/ml)	Concentration (pg/mg wet tissue)
8-iso-15(R)-PGF2 α	0.36 \pm 0.18	0.72 \pm 0.36
8-iso-PGF2 α	0.25 \pm 0.09	0.5 \pm 0.18
11 β -PGF2 α	0.12 \pm 0.02	0.24 \pm 0.04
PGF2 α	1.08 \pm 0.08	2.16 \pm 0.16
PGE2	1.15 \pm 0.22	2.3 \pm 0.44
PGD2	3.39 \pm 0.83	6.78 \pm 1.66
LXA4	1.53 \pm 1.14	3.06 \pm 2.28
13,14-dihydro-15-keto-PGD2	0.49 \pm 0.27	0.98 \pm 0.54
8,15-DiHETE	0.92 \pm 0.75	1.84 \pm 1.5
5,15-DiHETE	0.37 \pm 0.14	0.74 \pm 0.28
10,17-DiHDHA+MaR-1	0.07 \pm 0.01	0.14 \pm 0.02
LTB4	0.25 \pm 0.16	0.5 \pm 0.32
12,13-DiHOME	0.77 \pm 0.23	1.54 \pm 0.46
5,12-DiHETE	0.37 \pm 0.14	0.74 \pm 0.28
14,15-DiHET	0.28 \pm 0.07	0.56 \pm 0.14
15-deoxy- Δ 12,14 PGJ2	0.47 \pm 0.22	0.94 \pm 0.44
20-HETE	0.37 \pm 0.04	0.74 \pm 0.08
15-HEPE	0.36 \pm 0.34	0.72 \pm 0.68
16-HETE	2.17 \pm 1.09	4.34 \pm 2.18
9-HODE	1.48 \pm 0.3	2.96 \pm 0.6
20-HDoHE	1.94 \pm 0.41	3.88 \pm 0.82
15-HETE	10.72 \pm 3.5	21.44 \pm 7
13-oxoODE	0.68 \pm 0.19	1.36 \pm 0.38

16-HDoHE	1.05±0.27	2.1±0.54
17-HDoHE	1.3±0.23	2.6±0.46
11-HETE	3.45±0.51	6.9±1.02
9-oxoODE	0.58±0.16	1.16±0.32
14-HDoHE	2.32±0.25	4.64±0.5
11,12-EpETE	1.13±0.34	2.26±0.68
12-HETE	D	D
8-HETE	D	D
8,9-EpETE	0.52±0.18	1.04±0.36
9-HETE	3.1±0.5	6.2±1
5-HETE	6.55±2.23	13.1±4.46
4-HDoHE	3.51±0.92	7.02±1.84
14,15-EET	1.59±0.79	3.18±1.58
5-oxoETE	3.87±1.86	7.74±3.72
15-HEDE+11-HEDE	0.12±0.02	0.24±0.04
11,12-EET	2.15±1.05	4.3±2.1
8,9-EET	1.95±1.3	3.9±2.6
EPA	47.7±5.47	95.4±10.94
DHA	1383±46.7	2766±93.4
AA	7561±1617	15122±3234

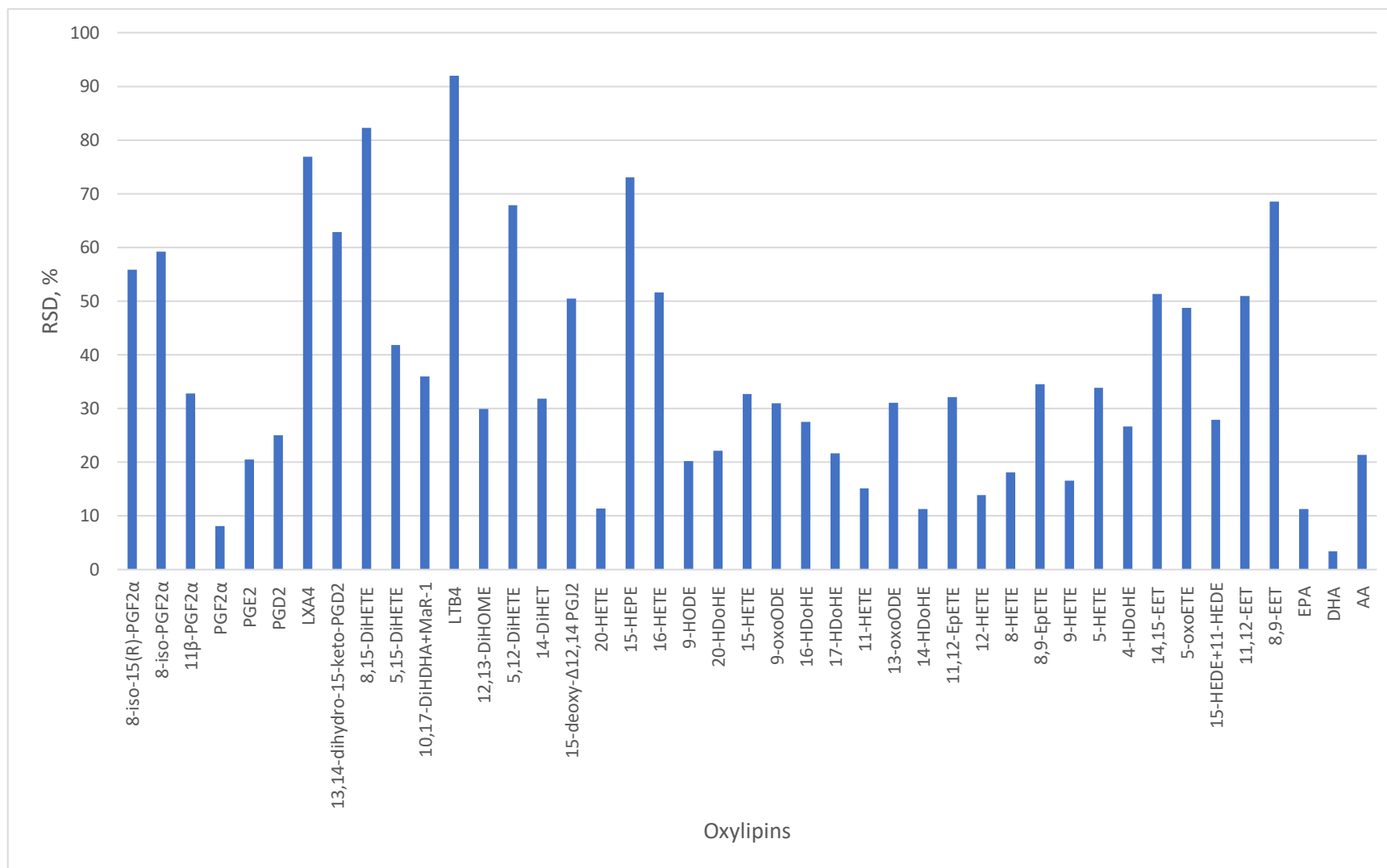


Figure S17 Method precision (%RSD, n=10 technical replicates) of SPE method for the extraction of endogenous oxylipins from pooled brain homogenate

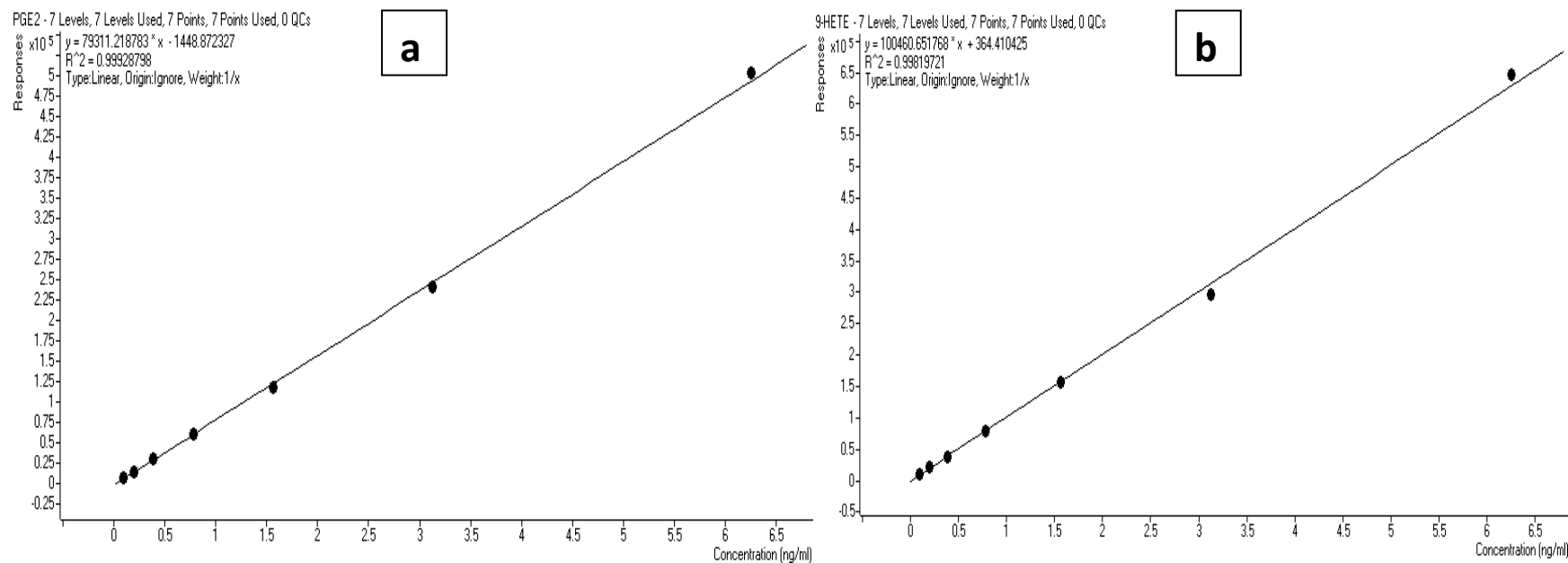


Figure S18 Examples of calibration curves used for quantitation (a) PGE2, (b) 9-HETE in SPME samples. Concentration range 0.098-6.25 ng/ml.

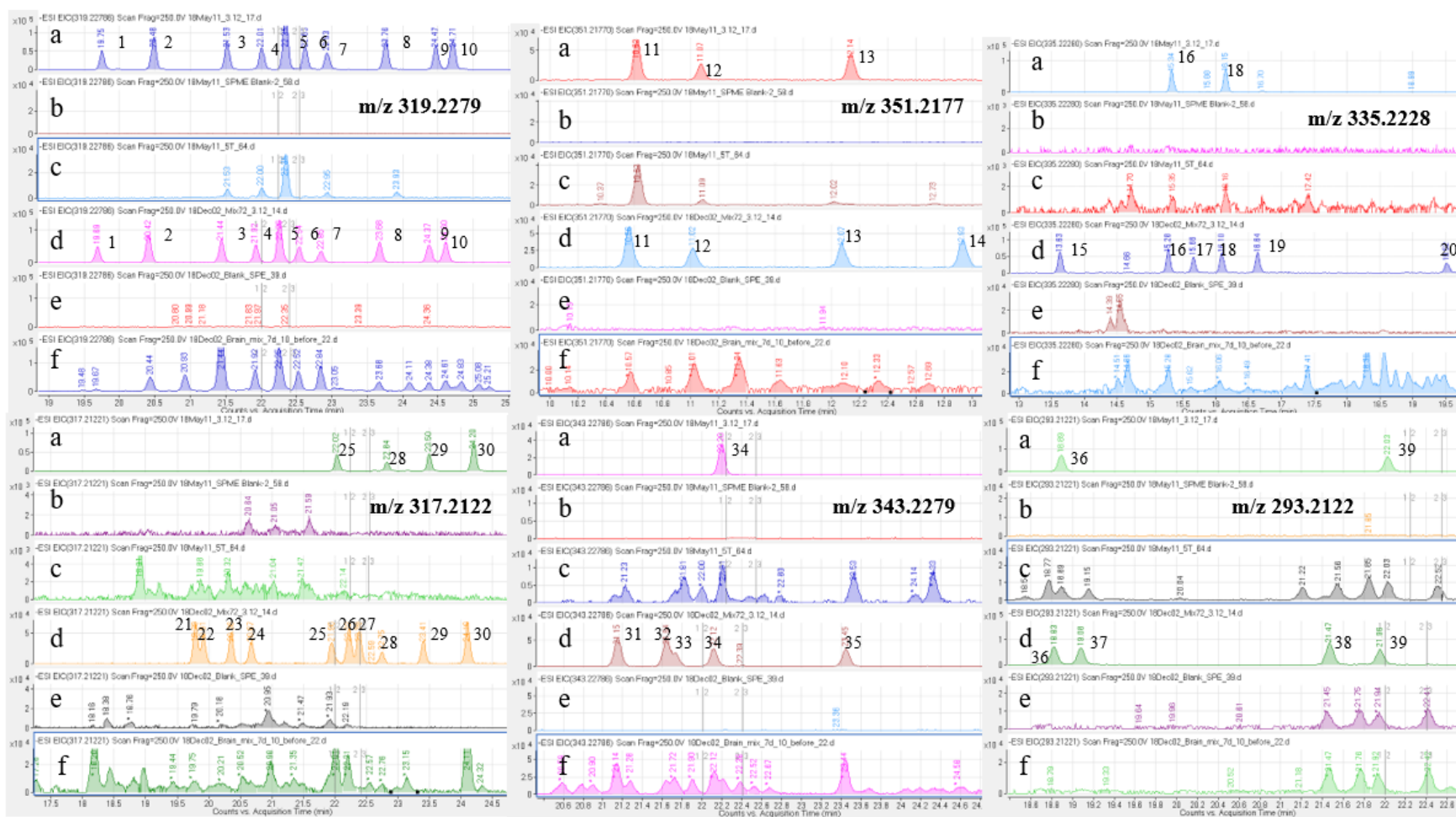


Figure S19 EICs of isomeric oxylipins in (a) oxylipin standard at final concentration of 3.12 ng/mL in MeOH solvent during SPME experiment (b) SPME blank, (c) oxylipins extracted from brain by in vivo SPME, (d) oxylipin standard at final concentration of 3.12 ng/mL in MeOH solvent during SPE experiment (e) SPE blank, (f) oxylipins extracted from brain by SPE. 1)-20)-HETE, 2)-16)-HETE, 3)-15)-HETE, 4)-11)-HETE, 5)-12)-HETE+8)-HETE, 6)-9)-HETE, 7)-5)-HETE, 8)-14,15)-EET, 9)-11,12)-EET, 10)-8,9)-EET, 11)-PGE2, 12)-PGD2, 13)-LXA4, 14)- 13,14)-dihydro-15)-keto-PGD2, 15)- 8)-iso-PGA1, 16)-8,15)-DiHETE, 17)-5,15)-DiHETE, 18)-LTB4, 19)-5,12)-DiHETE, 20)-5,6)-DiHETE, 21)-15)-HEPE, 22)-11)-HEPE, 23)-9)-HEPE, 24)-5)-HEPE, 25)-15)-HpETE, 26)-11,12)-EpETE, 27)-8,9)-EpETE, 28)-12)-oxoETE, 29)-5)-HpETE, 30)-5)-oxoETE, 31)20)-HDoHE, 32)-16)-HDoHE, 33)-17)-HDoHE, 34)-14)-HDoHE, 35)-4)-HDoHE, 36)-9)-HOTrE, 37)-13)-HOTrE, 38)-13)-oxoODE, 39)-9)-oxoODE

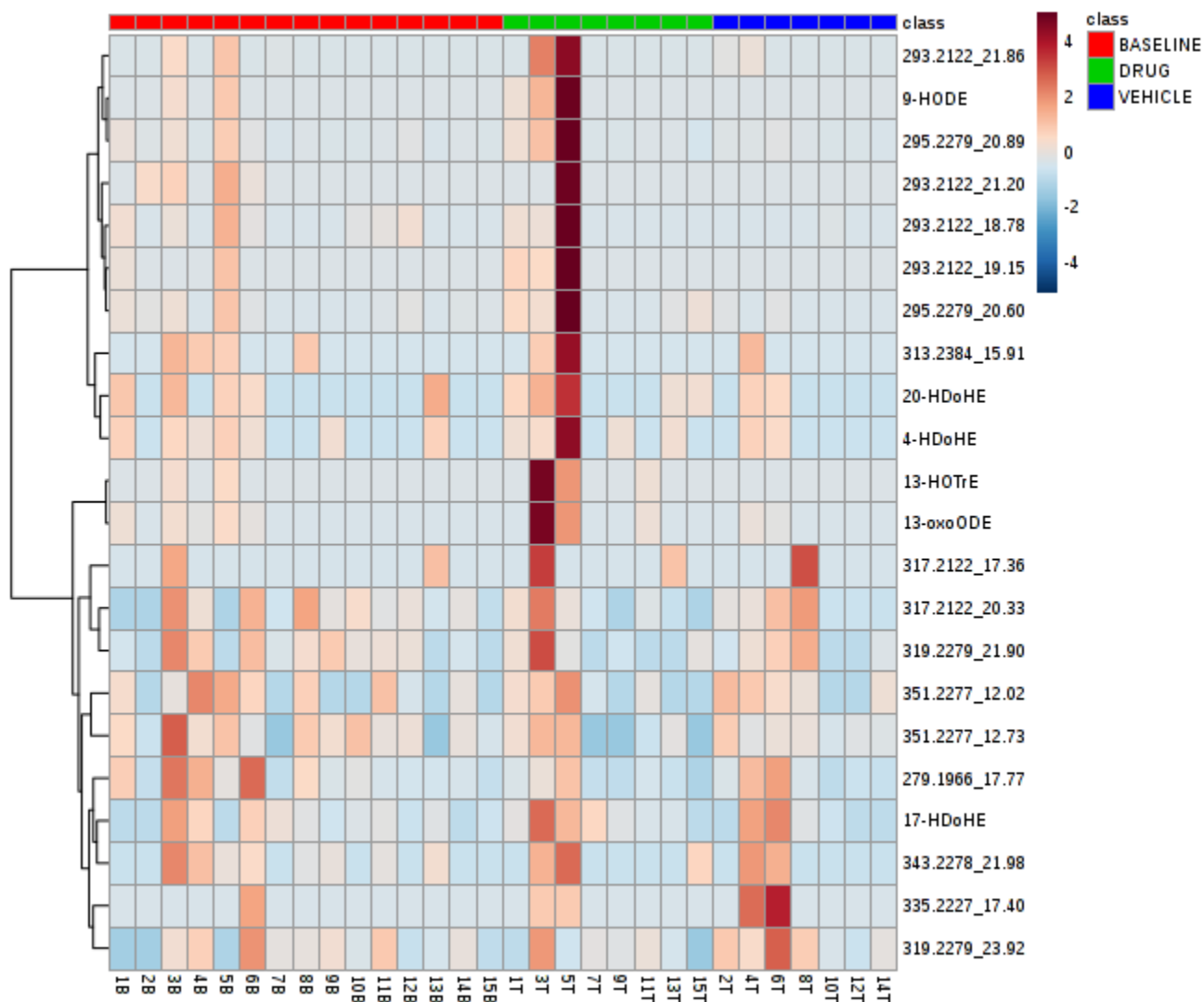


Figure S20 Hierarchical clustering by class (baseline, drug and vehicle) using Euclidian distance of unknown and subsequently identified oxylipins observed by SPME in a minimum of 5 samples. Clustering was performed using peak area using Metaboanalyst 4.0.

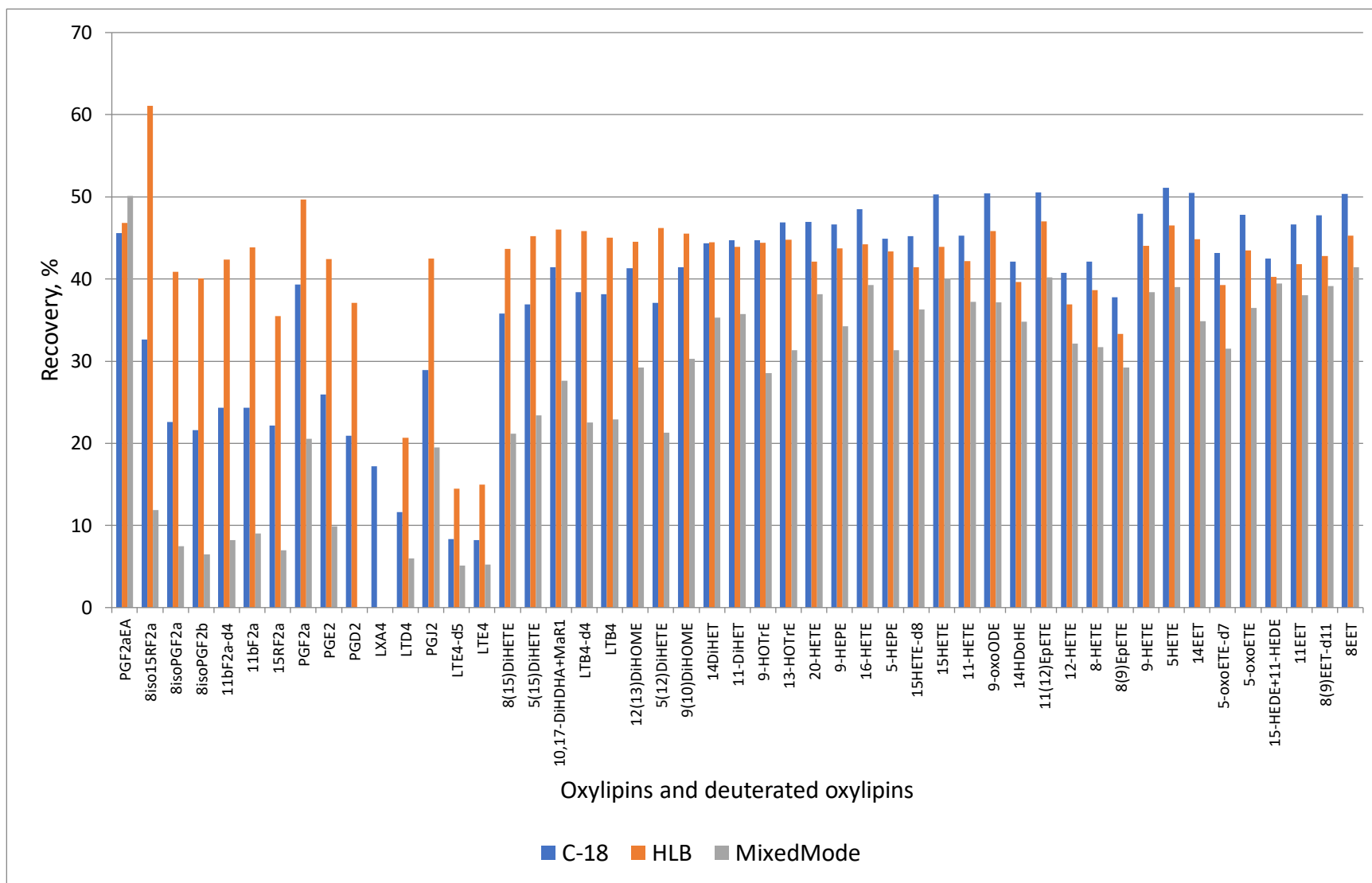


Figure S21 Oxylipin recoveries demonstrated by three types of SPME fiber coating: C-18, HLB and MixedMode. Extraction was performed from methanol 100 ng/ml solution of oxylipins during 12 hours at room temperature. SPME procedure was performed as described in Section 3.3. Extraction time profile of oxylipins was demonstrated by Bessonneau et al.⁶¹